INVESTIGATING MUCOLIPIDOSIS II:

A ROLE FOR PROTEASES IN CARTILAGE PATHOGENESIS

by

AARON CHRISTOPHER PETREY

(Under the Direction of Richard A. Steet)

ABSTRACT

The severe pediatric disorder Mucolipidosis II (ML-II) is characterized by multiple developmental defects including pronounced skeletal, craniofacial, and cartilage abnormalities. ML-II patients have mutations in the gene encoding the catalytic activity of the enzyme GlcNAc-1-phosphotransferase leading to impaired biosynthesis of mannose-6-phosphate (Man-6-P), the key recognition marker for sorting of lysosomal hydrolases to lysosomes. Though the genetic bases for this disorder are now well established, the molecular mechanisms underlying the pathophysiology of individuals with ML-II remain poorly understood. In an effort to investigate the developmental defects of this disease we analyzed the expression level and activity of a number of lysosomal hydrolases using a zebrafish model for ML-II. The present work addresses the role of lysosomal and matrix proteases in the cartilage pathogenesis of ML-II. Several cathepsins and matrix metalloproteinases (MMPs) were found to be present at elevated levels in ML-II. Analysis of cathepsin K, an enzyme

involved in bone and cartilage homeostasis, revealed the enzyme is tightly regulated during early cartilage development in zebrafish. Further studies showed cathepsin K is present at normal levels but subject to enhanced proteolytic activation in ML-II. The pharmacological or genetic suppression of cathepsin K was shown to alleviate several aspects of the craniofacial defects as well as the elevated activities of other proteases. Cathepsin K was found to be a highly Man-6-P modified enzyme capable of functioning at a pH consistent with the extracellular space, and deficient within sorted chondrocytes. By contrast, the related enzyme cathepsin D was poorly Man-6-P modified and present at normal levels in chondrocytes, suggesting cathepsin-specific hypersecretion occurs in zebrafish. Removal of specific N-glycans of cathepsin K and exogenous expression in wild-type embryos revealed that the enzyme is subject to enhanced activation upon loss of Man-6-P modification and is capable of generating cartilage phenotypes analogous to those seen in ML-II. Further studies using a feline model revealed that increased MMP activity is a general feature of ML-II, and is accompanied by the increased expression of proinflammatory cytokines. Collectively, these results indicate that the inappropriate extracellular activity of cathepsin K plays a central role in the cartilage pathogenesis of ML-II.

INDEX WORDS: N-linked glycosylation, mannose 6-phosphate, Mucolipidosis II, lysosomal storage disorder, cathepsin, matrix metalloproteinase

INVESTIGATING MUCOLIPIDOSIS II:

A ROLE FOR PROTEASES IN CARTILAGE PATHOGENESIS

by

AARON CHRISTOPHER PETREY

B.S., University of Georgia 2007

A Dissertation Submitted to the Graduate Faculty of The University of Georgia in Partial Fulfillment of the Requirements for the Degree

DOCTOR OF PHILOSOPHY

ATHENS, GEORGIA

2012

© 2012

Aaron Christopher Petrey

All Rights Reserved

INVESTIGATING MUCOLIPIDOSIS II:

A ROLE FOR PROTEASES IN CARTILAGE PATHOGENESIS

by

AARON CHRISTOPHER PETREY

Major Professor: Richard A. Steet

Committee: Michael Tiemeyer
Lance Wells
Lianchun Wang

Electronic Version Approved:

Maureen Grasso
Dean of the Graduate School
The University of Georgia
December 2012

DEDICATION

This work is dedicated to the memory of my grandparents: Harry and Genevieve Petrey, and Joe and Catherine Green, and also to my family who supported and encouraged my natural curiosity from a young age. I have been exceptionally fortunate to have such a wonderful family. I would have never been able to do this without your love and support. It means more to me than you will ever know.

ACKNOWLEDGEMENTS

There have been so many influential and supportive friends, family members, and colleagues along the way it is an impossible task to list them all. I have to start by thanking Carl Bergmann, who is responsible for training me in the earliest stages of becoming a scientist. Thanks for all you have done through the years, from teaching me the KISS principle, to offering advice and support no matter how busy you were. To Kelley Moremen and Alison Nairn: thank you for training me and being supportive, I learned a lot in my time with you. To my committee members Michael Tiemeyer, Lance Wells, and Lianchun Wang: thank you for all the guidance and stimulating scientific discussion. You have all made several meaningful contributions to my development as a scientist and have been fantastic mentors. I hope we can work together as colleagues in the future.

To the Steet Lab members: I have never had better coworkers. Jarrod, you were the best cubby-mate a dude could ask for. Thanks for all the times I had to help you jump start your car, push your car, or drive you to get gas or parts for your car. Thanks for everything, especially the cubby. To Abigail: WE DID IT. How does it feel to be the first person from our group to graduate? Wait, tell me tomorrow. I wish you all the best. You will make a fantastic double doctor. To Jennifer, the best fish room technician: thank you, thank you, thank you. None of this would have been possible without your hard work. Seriously. Best of luck with graduate school, not that you will need it. To Sanjukta, though we haven't

worked together for as long as the rest of this motley crew, you are also MY hero. To Megan, the baby: there are great things ahead and you are going to go far. Thanks for all the margaritas and don't forget to give science high-fives once I'm gone. When it is your turn, I'll be back to buy you a beer.

To my friends Matt, Sarah, Travis, Rachel, Jeff, and Mike – you guys are the best friends anyone could ask for. Thank you for all your support, listening to me talk about science and why it is the best job on the planet, and sharing in my victories and failures. I could have never made it this far without such an amazing group of friends. Much love and best wishes for you all.

To my friends at the CCRC: you all are responsible for our awesome community. I'm proud to call each of you a friend and colleague. Thanks for all the good scientific talks, the venting about the woes of being a grad student, and the fun nights where we didn't talk about science AT ALL.

To Rich and Heather, thank you both for bringing me into the lab at such an exciting time. It has been a real privilege to work with and learn from you both. Heather, thank you so much for all your help, guidance and training. I'll never forget trying to fix the biofilter while everyone else was out of town and getting covered in slime. Rich: thank you for always having an open door and having time for some of my ridiculous ideas and deep scientific discussions. Both of you have a deep passion and enthusiasm for science and it is contagious. You have helped me become the scientist I am today, thank you.

Lastly, and most importantly, I have to thank my family for everything. Mom and dad, you have always been supportive and encouraging. Thank you for

teaching me that it doesn't matter what I do as long as I put my heart into it. Jefferson: thanks for the ridiculous emails, music, movies, and great discussions – you've helped me maintain my sanity, not a small thing. Jessica: thanks for always being there to talk to and for being the same perpetual ray of sunshine since we were kids. I love you guys!

TABLE OF CONTENTS

Page

ACKNOWLEDGEMENTS v

LIST OF TABLES xi

LIST OF FIGURES xii

CHAPTER

1 LITERATURE REVIEW AND INTRODUCTION 1

An Overview of Glycosylation 1

Discovery of a Sugar-Phosphate as a Common Recognition Marker of Lysosomal Enzymes 8

Machinery of the Mannose-6-Phosphate Trafficking Pathway 10

The Structure and Function of Mannose-6-Phosphate Receptors 15

Defects in the Turnover of Glycans Leads to Disease 22

Clinical Characteristics of Mucolipidosis II 25

Development of Craniofacial Cartilage 29

Cathepsin Proteases are Involved in Many Normal Physiological Processes 31

Matrix Metalloproteinases are Effectors of Development and Physiology 32

Dissertation Overview 35

References 37

2 EXCESSIVE ACTIVITY OF CATHEPSIN K IS ASSOCIATED WITH THE CARTILAGE DEFECTS IN A ZEBRAFISH MODEL FOR MUCOLIPIDOSIS II 65
Abstract 66
Introduction 67
Results 70
Discussion 84
Materials and Methods 89
Acknowledgements 97
References 97
3 ALTERED ACTIVITY AND LOCALIZATION OF CATHEPSIN K UNDERLIES THE CARTILAGE DEFECTS IN A ZEBRAFISH MODEL OF MUCOLIPIDOSIS II 111
Abstract 112
Introduction 113
Results 116
Discussion 125
Materials and Methods 129
References 134
4 EXTRACELLULAR MATRIX DISRUPTION IS MEDIATED BY MATRIX METALLOPROTEINASES IN MUCOLIPIDOSIS II 148
Abstract 149
Introduction 150

Results 152
Discussion 158
Materials and Methods 161
References 164
5 DISCUSSION AND FUTURE PERSPECTIVES 174
The Contribution of Proteases to the Pathophysiology of Mucolipidosis II 174
The Role of Cathepsin K and Type II Collagen in ML-II 178
Future Perspectives – The Role of Other Cathepsins in ML-II 181
Matrix Metalloproteinases and ECM Turnover 183
Future Perspectives – Mechanisms of Elevated Protease Transcription 184
References 188
APPENDICES
A SUPPLEMENTAL FIGURES 194

LIST OF TABLES

Page

Table 1.1: Lysosomal Storage Disorders 63

Table 3.1: Mannose phosphorylation of zebrafish cathepsins 139

Table 3.2: Concanavalin A binding of cathepsin D..... 139

Table 3.3: Concavalin A binding of zebrafish cathepsin K 143

LIST OF FIGURES

Page

Figure 1.1: Biosynthesis and Processing of N-Glycans 59

Figure 1.2: Cultured Skin Fibroblasts from a ML-III alpha/beta patient 60

Figure 1.3: GlcNAc-1-Phosphotransferase Catalyzes the Biosynthesis of Mannose-6-Phosphate 61

Figure 1.4: Domain Structure of the Two Mannose-6-Phosphate Receptors..... 62

Figure 1.5: Clinical Features of Children with ML-II and ML-III 64

Figure 2.1: GFP-positive and –negative cells isolated from *Tg(fli1a*:EGFP) Animals are highly pure and enriched for markers of craniofacial chondrocytes 101

Figure 2.2: Transcript abundance of genes involved in ECM synthesis and Modification is altered in 2 and 3 dpf ML-II morphants 102

Figure 2.3: Cathepsin activity is elevated and sustained in ML-II zebrafish embryos 103

Figure 2.4: Cathepsin expression is enriched in the craniofacial skeleton of zebrafish embryos 104

Figure 2.5: The mature form of cathepsin K is present early and Persists in ML-II Embryos..... 105

Figure 2.6: *In vivo* inhibition of cathepsin K reduces the activities of multiple cathepsins..... 106

Figure 2.7: Inhibition of cathepsin K expression or activity results in correction of the ML-II cartilage morphogenesis defects 107
Figure 2.8: Inhibition of cathepsin K activity reduces type II collagen accumulation in ML-II morphant cartilages 109
Figure 3.1: Enzymatic activity profile of zebrafish cathepsins 138
Figure 3.2: Amino acid alignment of zebrafish cathepsins D and K with their human homologues 140
Figure 3.3: Cathepsins K and L are deficient within isolated chondrocyte cell populations 141
Figure 3.4: Selective hypersecretion in isolated ML-II chondrocytes 142
Figure 3.5: Heterologously expressed zebrafish cathepsin K is secreted into the media of cultured cells 143
Figure 3.6: Loss of Man-6-P modification of cathepsin K corresponds with increased activity 144
Figure 3.7: Cathepsin K and L activity is elevated in zebrafish heads and tails upon loss of Man-6-P 145
Figure 3.8: Overexpression of cathepsin K leads to craniofacial cartilage defects 146
Figure 3.9: Overexpression of catalytically cathepsin K lacking N-glycans does not alter craniofacial cartilage morphology 147
Figure 4.1: MMP activity is increased in ML-II embryos 168
Figure 4.2: MMP activity is elevated in the head and cartilage of ML-II embryos 169

Figure 4.3: MMP-13 is significantly elevated in ML-II 170

Figure 4.4: *In vivo* inhibition of cathepsin K reduces MMP activity in ML-II embryos 170

Figure 4.5: Inhibition of MMP-13 is unable to reduce the activity of cathepsins K and L in ML-II zebrafish 171

Figure 4.6: Matrix Metalloproteinase activity is elevated in a feline ML-II model 172

Figure 4.7: Genes involved in inflammation are elevated in feline lysosomal storage disorders including ML-II 173

Figure 5.1: Schematic representation of implicated pathological mechanisms underlying the disease process in ML-II 192

CHAPTER 1: LITERATURE REVIEW AND INTRODUCTION

An Overview of Glycosylation

Despite billions of years of evolutionary divergence, the surface of diverse organisms ranging from encapsulated viruses, to bacteria, to fungi, up to more complex multi-cellular organisms including plants and animals, is decorated with a rich coat of oligosaccharides or glycans. These glycans play critical and diverse roles both on the exterior and interior of the cell, including protection against pathogens, transmission of signals at the cell-surface, protein stability and resistance to degradation, self vs. non-self identification, molecular scaffolding, and many other functions.

Glycans are divided on a structural basis and can exist as homo- or hetero-polymers of monosaccharides which may be linear or branched, or as glycoconjugates; carbohydrates covalently attached to proteins or lipids. Glycosylation of proteins can be classified as either N-linked, via attachment to the nitrogen of an asparagine residue in an N-glycosidic bond, O-linked where the glycan is typically attached via the hydroxyl of either a serine or threonine residue, or as glycosaminoglycans (GAGs) in which 2-aminosugars are linked in alternating fashion with uronic acids to a core protein. Glycans can also be

attached to lipids forming glycolipids, and GPI anchors. The subsequent discussion will focus on the variety of roles N-glycans play in health and disease.

Biosynthesis and Processing of N-linked Glycans

The cellular biology of N-linked glycosylation spans the cytosol, the endoplasmic reticulum (ER) and the Golgi apparatus [1-3]. Monosaccharides are activated to form nucleotide sugars and then imported from the cytoplasm by the action of nucleotide sugar transporters into the lumen of either the ER or Golgi [4-8]. These nucleotide sugars are donor substrates for highly specific glycosyl transferases responsible for the biosynthesis of glycans. This complex process begins on the cytoplasmic side of the ER with the generation of dolichol-phosphate sugars from nucleotide sugar precursors[4, 5]. The lipid-linked glycan is initiated by the transfer of *N*-acetylglucosamine-1-P to dolichol-P, followed by addition of a second GlcNAc-P and five mannose sugars. The Man5GlcNAc2-P-P-Dol glycan precursor then flips into the lumen of the ER, whereupon the mature N-linked glycan precursor is completed by consecutive addition of four mannose and three glucose sugars (Glc3Man9GlcNAc2-dolicol-PP). The 14-sugar glycan is then co-translationally transferred to the Asn-X-Ser/Thr sequon of nascent polypeptide chains within the lumen of the ER by the action of a membrane-bound multisubunit complex termed oligosaccharyltransferase (OST) [9, 10].

Upon completion of protein translation, trimming of the glucose residues of the N-glycan occurs commensurate with folding of the glycoprotein. Protein

folding chaperones, such as calnexin and calreticulin, within the ER recognize specific sugar linkages and mediate protein folding [11-13]. Two glucosidases remove the glucose during protein folding and re-addition of a single glucose may occur until the protein has either properly folded or is targeted for degradation [12-14]. After folding, the glycoprotein then exits the ER for the *cis*-Golgi and, for most glycoproteins, the oligomannose chain is further processed from a Man8 or Man9 structure to Man5 structure by the action of mannosidases [15-18].

During the trimming of the oligomannose chains of lysosomal enzymes the action of a highly specific sugar-phosphate transferase within the *cis*-Golgi alters the processing and trafficking itinerary of these glycoproteins through the transfer of a sugar-phosphate trafficking marker (Figure 1.1). This mannose 6-phosphate (M6P) marker results in targeting of proteins to the lysosomal compartment and will be discussed in greater detail below [19-22].

For non-lysosomal glycoproteins, the α1–3 linked arm of a N-glycan is modified by the glycosyl transferase GlcNAcT-I in the *medial*-Golgi by addition of a β1-2 linked *N*-acetylglucosamine [23, 24]. Following the action of GlcNAcT-I, the α1-3Man and α1-6Man residues are removed from the α1-6 arm by the action of Golgi mannosidases, generating the acceptor substrate for the transfer of a second *N*-acetylglucosamine by GlcNAcT-II [23, 24]. The resulting oligosaccharide, GlcNAc2Man3GlcNAc2-Asn, is the precursor for all further sequential elaborations to form complex N-glycans [10, 25]. It is possible only a single GlcNAc is added to the precursor resulting in a hybrid structure with

mannose residues attached to the Man α1-6 arm, while the α1-3 antennae initiated by GlcNAcT-I is extended with other monosaccharides forming a hybrid structure [25, 26]. Though significant heterogeneity exists, N-glycans frequently fall into three categories: oligomannose, complex, and hybrid.

Ultimately, it is the balance of interactions and localization of glycosyltransferases, processing glycosidases, and substrate availability distributed throughout the Golgi, which leads to the final outcome of any given N-glycan oligosaccharide.

Biological Functions of N-Glycans

In order to understand biological functions of N-glycans, early studies were aimed at disrupting N-glycosylation through a variety of methods including use of inhibitors of lipid-linked oligosaccharide biosynthesis such as tunicamycin, inhibitors of N-glycan processing such as swainsonine, or generation of mutants lacking glycosylation activity [18, 27, 28]. Glycosylation mutants produce glycans with truncated or abnormal structures and shed light on functional roles of glycans within the context of a living cell. Although glycosylation in many cases is not necessary for survival of isolated cells in culture, it is critical *in vivo* and numerous mutational studies in mice have shown a functional glycosylation pathway is essential for embryogenesis [29].

Deletion of the *Mgat1* gene, which encodes GlcNAcT-1, blocks synthesis of complex and hybrid N-glycans and results in a Man5GlcNAc2 structure at N-glycan. Loss of GlcNAcT-1 activity does not affect the viability or growth of

cultured Lec1 cells, but *in vivo* results in death during embryonic development at stage E9-E10 [29, 30]. Loss of other components of the glycosylation machinery such as heparan sulfate biosynthesis, also result in early embryonic lethality, whereas loss of O-fucosyltransferase results in developmental defects mirroring Notch1 knockout mice [31, 32]. These mutations, which affect entire pathways, are significantly more severe than mutations that affect specific glycan reactions though these alone lead to a spectrum of human disease.

Defective biosynthesis of glycans is the molecular basis underlying a large contingent of human diseases. Impaired biosynthesis or processing of nearly every class of glycan results in human disease and a complete absence of N-glycans is embryonic lethal [29]. These diseases, termed congenital disorders of glycosylation (CDGs) are the result of direct or indirect defects in utilization of sugar precursors, glycan processing, glycosyl transferase activity, or in the proteins that control the distribution of glycosylation enzymes within the cell [33-35]. Clinical and biochemical features are heterogeneous and thus far treatment has proven difficult.

N-Glycan Structures Contain Biological Information

Several studies have shown the importance of N-glycan chains in the proper folding of proteins within the ER. Two proteins within the ER, calnexin and calreticulin, contain carbohydrate recognition domains and function to ensure proper protein folding. If the protein folding and quality control machinery are overwhelmed misfolded proteins can be targeted for degradation. Tunicamycin is

a potent inhibitor of GlcNAc phosphotransferase (GPT), the enzyme responsible for generation of dolichol-PP-GlcNAc required for initiation of N-glycans. In the presence of tunicamycin, cells are unable to initiate N-glycan chains resulting in cellular stress and initiation of unfolded protein response (UPR) [27, 28]. UPR is activated as a result of an accumulation of unfolded and/or misfolded proteins within the ER and functions to halt translation and increase production of molecular chaperones involved in protein folding [36, 37]. In cases where this response is not sufficient to restore the ER to normal function the UPR commits the cell to apoptosis [38].

The cystic fibrosis (CF) transmembrane conductance regulator (CFTR) highlights two important biological roles of N-glycans in protein folding and half-life. Loss of CFTR function at the plasma membrane causes CF, one of the most common genetic diseases in the Caucasian population. The CFTR is a large glycosylated transmembrane chloride ion transporter and has been shown to reach a folded state at ~30-40% frequency [39]. The most common mutation in humans causes deletion of phenylalanine-508 and results in nearly total abolishment of proper protein folding. Wild-type CFTR lacking N-glycans is capable of productive folding at only 5% efficiency, greatly reducing its function at the plasma membrane [40].

Following proper glycoprotein folding, the biological activity of secreted proteins is further influenced by N-glycans. Once at the cell surface N-glycans interact with a number of extracellular factors, including galectins, which directly influence the cell surface half-life for many proteins including receptors and

transporters such as the CFTR and fibroblast growth factor receptor (FGFR) [41]. Impaired complex N-glycosylation of both the CFTR and FGFR leads to a reduction in cell-surface resonance time and an increase in endocytosis and ubiquitin-mediated lysosomal degradation [40, 42]. The folding, half-life, and stability of many glycoproteins are regulated by the presence and degree of N-glycan branched modifications.

From the plasma membrane, the ER, the Golgi apparatus, and even within the cytosol, N-glycans interact with several classes of proteins and it is recognition by these carbohydrate-binding proteins, termed lectins, which mediate many of the biological roles of glycans. Discovered over 100 years ago for their ability to agglutinate erythrocytes, lectins are ubiquitous throughout nature [43, 44]. Most lectins contain carbohydrate-recognition domains that recognize the terminus of specific glycan chains. Though some lectins bind their substrate with a high affinity, many lectins interact with carbohydrates with low affinity (micromolar), but through multivalent interactions between multiple lectins and multiple glycans cumulatively produce a high-avidity binding interaction [45, 46].

Lectin-glycan interactions serve many biological functions, including: leukocyte extravasation and adhesion at the site of injury by selectins, the mannose receptors at the surface of macrophages initiate phagocytosis via binding to pathogens, the Ashwell receptor on the surface of liver cells binds to glycoproteins in which a sialic acid residue has been removed thereby clearing them from circulation, and the mannose-6-phosphate receptors (M6PR) guide

intracellular sorting of proteins out of the secretory pathway and to the lysosome [21, 47-49]. The pituitary glycoprotein hormones lutropin (LH) and thyrotropin (TSH) contain unusual 4-O-sulfated GalNAc residues that play a role in the ovulatory cycle in vertebrates. LH levels must rise and fall in a pulsatile manner, and rapid clearance of LH from circulation depends upon the the sulfated GalNAc. In each of these examples, the interaction between N-glycan and lectin plays an important role in human health and disease.

Discovery of a Sugar-Phosphate as a Common Recognition Marker of Lysosomal Enzymes

The discovery of the M6P trafficking pathway began with early studies of human genetic disorders that shared the commonality of failure to degrade cellular material, which accumulated within the lysosome. Many of these diseases, such as Hurler and Hunter syndromes, were poorly characterized [50]. Neufeld's group undertook a series of cross-correction experiments in which media containing secreted factors from normal cells was added to patient cells. Their studies determined that soluble lysosomal enzymes from normal cells could reverse these storage defects, and it was these enzymes that were deficient in patients with different diseases [20, 51, 52]. In these cases, patients proved to be deficient in a single lysosomal enzyme and these diseases were later termed lysosomal storage disorders (LSDs). Neufeld's experiments revealed that the enzymes secreted into culture existed in two forms: a saturable, "high-uptake"

form that could correct deficient cells, and a “low-uptake” form, unable to correct the storage defects [20, 51].

At roughly the same time, Leroy and Demar described a disorder that similar clinical manifestations to Hurler syndrome, but lacked mucopolysaccharidurıa [53]. Fibroblasts isolated from patients contained large inclusions within the cytoplasm; hence Leroy and Demar termed the disorder “I-cell” disease as shown in Figure 1.2. Analysis of I-cell fibroblasts led to the finding that patients were not deficient in one, but almost all lysosomal enzymes within the cell and unlike the LSDs, I-cell patients synthesized the lysosomal enzymes but secreted them into the media. Secretion studies utilizing I-cells revealed that they were fully capable of incorporating “high-uptake” enzymes secreted by normal cells, but enzymes secreted by I-cells were unable to correct storage defects in Hunter or Hurler syndrome cells and existed as the “low-uptake” form [20]. These studies led to the suggestion that there existed a common lysosomal targeting recognition marker associated with lysosomal enzymes and this marker was impaired in patients with I-cell disease.

Further analysis of fibroblasts from I-cell patients performed by William Sly revealed that addition of mannose-6-phosphate or treatment of lysosomal enzymes with alkaline phosphatase both blocked internalization of “high uptake” enzymes [19]. Kornfeld’s group had defined the general pathway of complex N-glycan biosynthesis and as mannose is abundant on oligomannosyl N-glycans, it was postulated these residues were phosphorylated. Inhibition of N-glycan synthesis by tunicamycin led to failure of lysosomal enzymes to reach the

lysosome and resulted in their secretion into the media of cultured cells. These data suggested that the common recognition marker proposed by Neufeld was a sugar-phosphate, and was soon identified as mannose-6-phosphate on oligomannosyl N-glycans released from lysosomal enzymes [54].

A disorder similar to I-cell disease, but with a more mild clinical presentation was identified and termed pseudo-Hurler polydystrophy [55]. Characterization of fibroblasts from these two I-cell diseases revealed abnormal levels of mucopolysaccharides and sphingolipids, leading to their reclassification, with the more severe case termed Mucolipidosis-II (ML-II) and the milder termed Mucolipidosis-III (ML-III) [56].

The details of this pathway including how newly synthesized lysosomal hydrolases are recognized by GlcNAc-1-phosphotransferase and targeted to the lysosome by the M6PRs are discussed below.

Machinery of the Mannose-6-Phosphate Trafficking Pathway

The M6P trafficking system served as one of the first examples of a biological role for glycans and connected defective glycoprotein biosynthesis to a human disease. As previously mentioned, the activity of a highly specific sugar-phosphate transferase in the *cis*-Golgi leads to the generation of a N-linked glycan containing terminal M6P. This phosphomannosyl biomarker interacts with one of two M6PRs in the terminal Golgi compartments and diverts most lysosomal hydrolases out of the secretory pathway and to the lysosome.

Generation of the M6P moiety is the result of a two-step enzymatic process that begins in the *cis*-Golgi. The enzyme UDP-*N*-acetylglucosamine:lysosomal-enzyme *N*-acetylglucosamine-1-phosphotransferase (GlcNAc-1-phosphotransferase) initiates biosynthesis by transfer of a GlcNAc-1-phosphate in a phosphodiester linkage to the carbon-6 position of α1-2-linked mannose residues on oligomannosyl glycoproteins [57]. A second enzyme, α-*N*-acetylglucosaminyl-1-phosphodiester glycosidase or "uncovering enzyme" (UCE) removes the GlcNAc residue "uncovering" the M6P monoester within the *trans*-Golgi network (TGN) [58-60]. This terminal M6P moiety functions as an essential recognition marker utilized by two high affinity receptors which divert lysosomal proteins from the secretory pathway and deliver them to the lysosome.

Molecular Characteristics of GlcNAc-1-Phosphotransferase

The enzyme GlcNAc-1-phosphotransferase exists as a hexameric 540kDa glycoprotein complex comprised of two disulfide-linked 166kDa α-subunits, two disulfide-linked 51-kDa β-subunits, and two non-covalently associated 56-kDa γ-subunits (Fig 1.3) [61]. A single gene, *GNPTAB*, encodes the α and β subunits and a separate gene on a different chromosome, *GNPTG*, encodes the γ subunit [62-64]. Both genes are highly conserved across several species including humans, mice, rats, cows, and zebrafish [65].

The α/β gene product undergoes proteolysis at the lysine 928 – aspartic acid 929 peptide bond yielding two distinct subunits. It has been shown that this bond is cleaved by site-1 protease (S1P) within the TGN and S1P-deficient cells fail to cleave the α/β precursor, exhibiting an I-cell like phenotype in vitro [66].

Proteolytic cleavage is prerequisite for phosphotransferase activity and several studies have determined the α/β subunits contain the catalytic activity of the enzyme as well as the ability to recognize lysosomal proteins [67-70]. S1P cleavage generates the transmembrane α- and β-subunits.

The mature α-subunit is a type II transmembrane protein with a 19 amino acid N-terminal cytoplasmic tail, 22 amino acid transmembrane region, and an 886 amino acid luminal domain containing 17 potential N-glycosylation sites. The luminal portion contains six domains with homology to bacterial capsule biosynthesis domains, two Notch receptor-like repeats, and a binding domain for the transcriptional co-repressor DMAP1 [62, 67]. A coiled-coil domain is present within the α-subunit from residues 80-120, and similar domains have been implicated in protein-protein interactions [71]. The mature β-subunit is a type 1 transmembrane protein, with similarly sized cytoplasmic and transmembrane regions as the α-subunit, and a smaller, conserved 284 residue luminal domain containing three potential N-glycosylation sites [67].

The specific functions of the γ subunit have been elusive. It was initially believed the mannose receptor homology (MRH) domain of the γ-subunits mediated lysosomal protein recognition and it has been shown the γ-subunit can enhance phosphorylation of some, but not all lysosomal proteins, and is dispensable for others [69]. Additional data suggests that γ subunit can function to stabilize α/β and limited proteolysis of γ may represent a mechanism of regulation of M6P biosynthesis in macrophages [72, 73].

Recognition of Lysosomal Proteins

Specific recognition of N-glycans on lysosomal enzymes is a critical parameter to achieve selective trafficking to the lysosomal compartment. The observation that GlcNAc-1-phosphotransferase has a 100-fold higher specificity for lysosomal enzymes compared to other proteins suggests that lysosomal proteins contain a specific recognition determinant [21, 74]. Primary sequence studies of lysosomal enzymes known to bear M6P show very little sequence homology and denatured lysosomal enzymes are not recognized by GlcNAc-1-phosphotransferase suggesting elements of secondary or tertiary structure are important for recognition. A number of studies suggested a role for specific lysine residues in recognition [75-77].

Mutation of lysines within proximity to N-linked oligosaccharides of DNase I, a lysosomal enzyme known to bear M6P, significantly reduced the level of mannose phosphorylation [75, 78]. In a complementary approach, addition of lysines to the primary sequence of pepsinogen, a non-lysosomal secretory protein with high homology and tertiary structure to cathepsin D, was sufficient to confer recognition by GlcNAc-1-phosphotransferase and phosphorylation of the N-glycan [79-82]. Substitution of the carboxy-terminal region of pepsinogen with that of cathepsin D further enhanced recognition and mannose phosphorylation. These studies revealed that two lysines in correct orientation to each other and an N-glycan are key recognition elements between lysosomal proteins and GlcNAc-1-phosphotransferase. However, it was noted that additional residues

could further enhance recognition likely through interactions with the DMAP domain.

In vitro studies of have further elucidated the function of α/β- and γ-subunits in protein recognition. In many cases, the γ-subunit may be dispensable for protein recognition but interacts with the high mannose oligosaccharide and facilitates transfer of a second M6P residue to the α3 arm. Further, γ also appears to stabilize α/β in a conformation enhancing substrate recognition and binding on a specific subset of acid hydrolases [69].

Uncovering of the M6P Trafficking Marker

As previously mentioned, after the GlcNAc-phosphate is transferred onto select mannose residues it must be "uncovered" to reveal the M6P recognition marker for recognition by specific receptors. The second enzyme involved in biosynthesis of the recognition marker, "Uncovering Enzyme or UCE" is a 272-kDa tetramer of four 68-kDa subunits arranged as two homodimers linked by disulfide bonds. UCE is synthesized as an inactive precursor and is processed within the TGN by furin convertase [58]. Unlike many other Golgi enzymes, UCE is a type-1 transmembrane glycoprotein found within the TGN and at the plasma membrane. Amino-terminal cytoplasmic residues mediate Golgi retention, exit, and assembly into clathrin-coated vesicles for retrograde transport back to the TGN [83]. Uncovering the M6P recognition marker appears to take place as a late event within the Golgi network [59, 84]. Though there are no known human

mutations in UCE, it has been shown that mutagenic disruption of UCE activity leads to hypersecretion of lysosomal enzymes [85].

The Structure and Function of Mannose-6-Phosphate Receptors

After the terminal M6P marker is exposed by the activity of UCE, lysosomal proteins are trafficked out of the TGN by high-affinity receptors and released within the low pH environment of endosomes or lysosomes. Two receptors have been identified for their ability to bind M6P. Both M6PRs are type 1 transmembrane glycoproteins with large extracytoplasmic domains and a short c-terminal cytoplasmic tail, but are significantly different from each other. The first receptor identified was a large 300kDa receptor found to bind M6P in the absence of cations. Study of cells deficient in this receptor revealed normal trafficking of some lysosomal enzymes and led to the discovery of a second, smaller 45kDa M6PR [86, 87]. These receptors, termed the cation-independent M6P receptor (CI-MPR) and the cation-dependent M6P receptor (CD-MPR), bind glycans bearing M6P in a 1:1 stoichiometry and are depicted in Figure 1.4. On the basis of their unique M6P binding properties these receptors have been classified as P-type lectins.

Mannose-6-Phosphate Ligand Binding Properties of the M6PRs

Both receptors bind glycans bearing two M6P residues with highest affinity, one M6P with intermediate affinity, and the CI-MPR binds weakly to

“covered” M6P glycan structures. Optimal ligand binding occurs at pH ~6.5 within the TGN, and no binding is detectable below pH 5, consistent with their function [88]. The CD-MPR has a single extracellular domain and has been shown to function as a dimer, with each monomer interacting with one M6P-glycan [89]. The CI-MPR has an extended extracellular domain of 15 repeats that resemble the structure and sequence of the CD-MPR [90]. This shared homology suggests that the two receptors evolved from a common ancestor. Structural studies of the soluble extracellular region of the CI-MPR revealed a unique, compact structure not unlike that of avidin. Despite having 15 repeats sharing high degrees of homology, only domains 3, 5 and 9 have been shown to bind M6P. Domain 9 preferentially binds phosphomonoesters and domain 5 preferentially binds phosphodiesters [91, 92]. Based off the crystal structure, it is not likely a diphosphorylated glycan is capable of binding in both domains 3 and 9 of a single CI-MPR monomer. However, it is possible that a diphosphorylated glycan can span the binding sites on different CI-MPR dimers. Alternatively, the receptor is flexible and may be capable of binding two different phosphorylated N-glycans on a single lysosomal protein [93]. There is evidence that the CI-MPR is capable of binding other modified mannose glycans via domains 1 and 3, including mannose-6-sulfate and methylated M6P. It is postulated that chondroitin sulfate may interact with the receptor in place of mannose-6-sulfate, but the significance of these uncommon interactions is currently not known [94, 95].

In addition to their structural differences, the MPRs also appear to bind with different affinities to lysosomal proteins. Comparison of several cell lines

including those lacking either a single or both M6PRs indicated that loss of a single M6PR leads to partial impairment of sorting, while loss of both receptors causes significant missorting and accumulation of I-cell like undigested material [89, 96]. Analysis of lysosomal enzymes secreted into the media of these cell types indicates that the receptors interact preferentially with different lysosomal enzymes, despite the fact that both receptors bind the M6P epitope. This suggests both receptors are required for efficient sorting of lysosomal enzymes and lysosomal targeting may vary in different cell types or tissues.

Trafficking and Localization of the M6PRs

Within the cell, the M6PRs are primarily localized within the TGN and late endosomes and cycle between these compartments, but never reach the lysosome where they may be degraded. Sorting signals within the cytoplasmic tails of both receptors interact with a number of factors including adapter protein 1 (AP1) and Golgi-localized, gamma-ear containing, ADP-ribosylation factor binding proteins (GGAs) and recruit clathrin for the assembly of clathrin-coated vesicles [97-100]. Upon reaching the endosomal network, as the pH decreases, lysosomal proteins are released from the M6PRs. Late endosomes engage in dynamic fission and fusion with lysosomes, selectively delivering contents to the lysosomal compartment. The CI-MPR, but not the CD-MPR, may then move from the endosomes to the plasma membrane [89].

It is interesting to note that even under normal conditions, some newly synthesized lysosomal enzymes are not targeted to the lysosome and are

secreted into the extracellular space despite bearing M6P [101, 102]. Secreted lysosomal proteins that bear M6P may be recaptured, either the same cell or adjacent cells, by the CI-MPR at the plasma membrane.

At the membrane, the CI-MPR is capable of binding many different ligands and is internalized via clathrin-coated pits and, mediated by AP2, return to the endosomal network [88]. Several pathways exist for the M6PRs to return to the TGN from the endosomal-lysosomal network, though many of the specific details of these different pathways are presently not known.

The CI-MPR and Other Substrates

At the plasma membrane CI-MPR has been reported to bind several other ligands independent of M6P. These ligands include insulin-like growth factor II (IGF-II), retinoic acid, plasminogen, and urokinase-type plasminogen activator receptor (uPAR), heparanase, and serglycin [94, 103-106]. Of these ligands, the interaction between the CI-MPR and IGF-II has been most studied. Domain 11 is reported to bind IGF-II and attenuates signaling at the cell surface, negatively regulating cell growth [105]. Interaction with retinoic acid suppresses proliferation and may induce both apoptosis and generation of autophagosomes through mechanisms that are not fully elucidated [106, 107]. The binding of uPAR has proven somewhat ambiguous. Studies have shown that uPAR binds to domain 1 of the full-length CI-MPR, but uPAR can bind to the 260kDa serum form of the receptor in a M6P-dependant fashion. Regulation of uPAR and subsequent activation of plasminogen, functions as an early step in tissue remodeling and

wound healing. Elevated uPAR mediated activation of plasminogen has been reported in malignant tumors [108-110]. Further, loss of heterozygosity of the CI-MPR has been reported in human cancers and the receptor may play a key role in regulation of cancer cell growth and adhesion through these and other mechanisms [111].

M6P-Independent Routes to the Lysosome

Although the M6P pathway to the lysosome exists as the primary mechanism by which many proteins reach the lysosome, it has become appreciated that alternative membrane-bound receptors are also involved in lysosomal sorting of proteins. Characterization of ML-II patients determined that extent of mannose phosphorylation on lysosomal proteins is cell and tissue specific and some enzymes may traffic to the lysosome using alternative pathways [112]. Tissue and cellular analysis of enzyme content from hepatocytes and leukocytes, kidney, liver, spleen, and brain isolated from ML-II patients revealed relatively normal levels of some lysosomal enzymes despite an inability to generate M6P-containing glycans [112]. Other studies focused on the expression and localization of the M6PRs revealed that receptor-deficient cells traffic some enzymes normally [113, 114]. These findings jointly supported the idea that some lysosomal enzymes may reach the enzymes through alternate mechanisms.

Indeed, certain lysosomal hydrolases are now known to traffic to the lysosome independent of mannose phosphorylation. Thus far, two receptors have been identified capable of M6P-independent lysosomal trafficking:

lysosomal integral membrane protein-2 (limp-2), and sortilin. Limp-2 has been shown to deliver the enzyme glucocerebrosidase, the enzyme defective in patients with Gaucher disease, to the lysosome. Recently, mutations in the gene encoding limp-2 have been shown to cause a severe disease characterized by progressive epilepsy and renal dysfunction [115, 116]. The second receptor was identified due to a high degree of homology to the yeast protein Vps10p known to sort carboxypeptidase gamma to the lysosome-like vacuole [117]. Sortilin appears to bind multiple ligands including prosaposin, acid sphingomyelinase, and cathepsins H and D and direct them to the lysosome. Sortilin is one of five members of the Vps10p domain receptor family, primarily localized to the TGN and endosomes and are capable of cycling between compartments [118]. It is interesting to note that the cytoplasmic tail of sortilin closely resembles that of the M6PRs. Many of the same motifs within the M6PRs are also present within sortilin, limp-2, and other lysosomal membrane proteins targeted to the endosomal network [119]. Sortilin also shares the same GGA-mediated retrograde transport of the M6PRs.

Additionally, there are examples of proteins such as cathepsin D and H that are capable of reaching the lysosome via both the M6PRs and sortilin. The basis for multiple routes to the lysosome is presently not well understood. It is possible that multiple mechanisms exists either for purposes of redundancy or for targeting enzymes to distinct lysosomes which serve different functions, such as secretory lysosomes or autophagosomes.

Evolutionary Origins of the Mannose-6-Phosphate Sorting Machinery

The elements of the M6P sorting pathway appear to be highly conserved amongst vertebrates. The M6P dependent mechanism for sorting lysosomal proteins was first discovered in human cells and is present in several animals including mammals, birds, amphibians, and fish. However, the evolutionary origin of the pathway and what elements are present in lower organisms remains unclear. Lysosomal enzymes appear to be targeted without the use of any identified M6PRs in yeast, trypanosomes, and protozoans [120].

The soil amoeba *Acanthamoeba castellanii* and the slime mold *Dictyostelium discoideum* synthesize a M6P structure on some proteins that are capable of recognition by mammalian CI-MPR, but not the CD-MPR. Studies of *Acanthamoeba* have shown that its GlcNAc-1-phosphotransferase enzyme recognizes the lysosomal proteins cathepsin D and uteroferrin with greater specificity than non-lysosomal proteins *in vitro*, though not as precise as rat enzyme [57, 121]. Although *Dictyostelium* also contains a gene encoding for a GlcNAc-1-phosphotransferase that recognizes α1,2 linked mannose residues, the enzyme is not specific for lysosomal proteins. The enzyme has a 27% amino acid identity to the human GlcNAc-1-phosphotransferase and two key differences: the absence of both a gamma subunit and a DMAP binding domain, suggested to mediate protein-protein interactions and potentially an important recognition element [74, 122]. No other elements of the M6P sorting pathway have been identified in either organism to date.

Amongst lower eukaryotes, *Drosophila melanogaster* GlcNAc-1-phosphotransferase shares a 45.5% amino acid identity with humans, but is less than half the size and not believed to function. In a related fruit fly, *Ceratitis capitata*, enzymatic activity has been reported at low, but detectable, levels [123]. However, while mannose receptor homology (MRH) domain-containing receptors have been identified in insects, none appear to be able to bind M6P-glycans. The closest homologue to a M6PR, drosophila lysosomal enzyme receptor protein (Lerp), is a type I transmembrane protein containing 5 repeats similar to the CI-MPR each with P-type lectin conserved cysteine residues but lacking key arginine residues shown to be required for binding M6P. Lerp has been shown to contain the same C-terminal trafficking motifs as the M6PRs, and can compensate for lack of M6PRs in mammalian cells in a M6P-independent fashion [124].

Though elements of the M6P sorting pathway are present in many organisms, the complete machinery appears to be present only in vertebrates. The point at which the full sorting pathway arose has yet to be determined.

Defects in the Turnover of Glycans Leads to Disease

Lysosomes contain 50-60 highly specific glycosidases required for normal turnover of a variety of macromolecules including the metabolism of glycolipids, glycoproteins, and mucopolysaccharides. More than 45 diseases are known which impair the degradation of these molecules, leading to accumulation of undigested material [125-127]. These lysosomal storage disorders (LSDs) are

progressive in nature and share overlapping symptoms as well as distinct features. These progressive disorders are characterized by multisystem defects including craniofacial, skeletal and cardiac abnormalities, variable neurological deficits and ocular problems, detailed in Table 1.1 [128, 129]. It is not clear if storage of undegraded material in the lysosome leads to pathological symptoms characteristic of each disorder. Pathology is likely cell and tissue specific and influenced by the balance of biosynthesis and degradation of the defective enzyme's substrate [130, 131].

As discussed above, Mucolipidosis II (GlcNAc-1-phosphotransferase deficiency) is a debilitating pediatric LSD caused by defects in the biosynthesis of mannose 6-phosphate residues, the recognition signal for targeting of soluble acid hydrolases to the lysosome [22, 64, 102, 132]. Unlike most LSDs that are characterized by loss of specific lysosomal hydrolase, ML-II is unique since the hydrolases are still made but many are secreted into the extracellular space due to impaired lysosomal targeting [133]. The pathological mechanisms of many LSDs including ML-II remain poorly understood, representing a barrier to therapeutic development.

Molecular Basis of Mucolipidosis II

To date nearly 100 different mutations have been identified within the *GNPTAB* gene. Sequencing of the *GNPTAB* gene in ML-II patients has confirmed that homozygous and compound heterozygous mutations causing either premature truncation or frameshift of the gene produces no enzyme or an

enzyme with nearly no functional activity. Almost all patients with the severe ML-II α/β are associated with nonsense or frameshift mutations [62, 65, 134].

Missense and splice site mutations have also been identified within *GNPTAB* and result in up to 10% residual activity. To date, 18 patient mutations have been identified in *GNPTG* including include missense, frameshift and splice mutations. Patients with these mutations often present a more mildly progressive form of the disease termed ML-III α/β or ML-III γ respectively [135, 136]. The clinical and molecular diagnosis of ML-II/III can be further confirmed by biochemical analysis of lysosomal enzymes.

Cellular and Biochemical Pathology of Mucolipidosis II

Patients affected by ML-II/III exhibit defective lysosomal targeting of enzymes due to defects in the biosynthesis of M6P. The lack of normal lysosomal targeting results in secretion and intracellular deficiency of acid hydrolases. As a result, material accumulates within the lysosome and result in dense inclusions that have been observed in patient fibroblasts and mesenchymal cells. High levels of acid hydrolases have been detected within the serum of patients, where they may have deleterious effects [133].

Several cell types and tissues isolated from ML-II patients appear to contain normal acid hydrolase levels despite complete loss of GlcNAc-1-phosphotransferase activity [133, 137]. This is not well understood but may be the result of independent lysosomal targeting pathways or alternate routes to the lysosome, such as secretion and recapture at the plasma membrane. These cells

still contain the characteristic dense inclusions and large cytoplasmic vacuoles and have been identified as lysosomal compartments. Studies of these compartments have demonstrated the presence of lysosomal membrane proteins, acid hydrolases, and the storage of glycoconjugates that have accumulated in significant quantities [133, 137]. Much of the ML-II pathology appears cell and tissue specific, as evidenced by extensive vacuolization and generation of autolysosomes in exocrine gland cells, but not in brain, liver and muscle [138, 139].

Despite extensive investigation into the molecular pathology of ML-II, it is still not clear which characteristics of the disease are primary mechanisms of disease and which are secondary pathological phenotypes.

Clinical Characteristics of Mucolipidosis II

Mutations within the GNPTAB gene, which result in a complete loss of enzymatic activity, give rise to ML-II, while partial loss of activity is responsible for the milder ML-III. Although multiple systems are affected in patients with ML-II, the pathology primarily affects bone and joints and is visibly notable in the coarse facial features and skeletal abnormalities present at birth. Clinical features present at birth include a characteristic set of skeletal phenotypes (termed dysotosis multiplex), short hands and fingers, dislocated hip, thoracic deformity, thickened, waxy skin, gingival hypertrophy, and coarse craniofacial features such as a flattened face and nasal bridge, shallow orbits, and a prominent mouth,

shown in Figure 1.5. Birth weight is reported to be low to normal, and post-natal growth often ceases in the second year of life [133, 137].

All children are reported to have thickening of the mitral valve leading to cardiac complications, and thickening of airway mucosa and thoracic cage leading to respiratory insufficiency. Patients affected by ML-II rarely live past the first decade often as a result of frequent respiratory tract infections or congestive heart failure [140]. Autopsies have reported cytoplasmic lysosomal inclusions in myocardium, brain, and liver. Symptoms are similar in ML-III patients with a slower clinical course. The progressive nature of this disorder typically delays clinical diagnosis until later in life, and although the severity is variable life expectancy extends into adulthood [141]. The most notable sites of pathology in both ML-II/III appear in bone and cartilage and will be discussed below.

Bone and Cartilage are the Main Sites of Pathology in ML-II

Cartilage and bone abnormalities are commonly found in LSDs, including ML-II/III. These skeletal and cartilage defects are hallmarks of LSDs and it is possible that some pathology is shared between them. The craniofacial cartilage defects observed in ML-II are apparent at birth, while others, such as restriction of the hip, shoulder, and knee joints, are progressive in nature, particularly in ML-III [137, 141, 142]. Patients affected by the milder and slowly progressive ML-III experience gradual restriction of movement in all joints and prominent hip deterioration by adolescence. Alterations in cell-shape and hypertrophic chondrocytes have been documented in ML-II, and serve as indicators of

increased cartilage catabolism. Cell morphology is recognized as a phenotypic parameter of the differentiation state and health of chondrocytes within cartilage [138, 139, 143-145].

Post-mortem studies of patients revealed inhibition of growth plate calcification, signs of high bone turnover, and membrane bound vacuoles within chondrocytes, osteoblasts, osteocytes, and stromal fibroblasts. Isolation and microscopic analysis of patient precursor chondrocytes revealed membrane tethered granular vesicles, comprised of predominantly proteoglycans [138, 139, 143, 146]. Given the serious consequences of imbalanced extracellular matrix (ECM) homeostasis and matrix degradation, the role of chondrocytes and surrounding synovial fibroblasts may be significant in the cartilage and joint pathologies of ML-II.

Mammalian Models of ML-II

Efforts to determine the underlying pathological mechanisms behind ML-II have been hindered by the lack of animal models that are genetically accessible and amenable to investigation during early development. Investigation into the molecular pathology of ML-II has taken place primarily with feline and murine models, though both differ slightly in their phenotypic presentation. The feline model displays characteristics similar to the human condition including facial dysmorphia, skeletal defects, impaired lysosomal targeting, and retinal clouding [147-149]. However, the feline genome is incomplete and not well annotated.

The GNPTAB knockout mouse exhibits retinal degeneration, smaller stature, pathological lesions in exocrine glands, accumulation of autolysosomes, and hypertrophic chondrocytes but no overt cartilage or bone defects as seen in humans [70, 150, 151]. Fibroblasts and mesenchymal cells isolated from the mouse did not develop cytoplasmic inclusions characteristic of ML-II and ML-III patients [152]. Osteoclasts isolated from these mice have altered secretory lysosome formation, which corresponds with elevated levels in cathepsin K and tartrate resistant alkaline phosphatase (TRAP) [153]. Recently, a GNPTAB knock-in mouse was generated by insertion of a single cytosine corresponding to mutations found in patients with ML-II. This mouse presents a similar disease course to humans including severe skeletal abnormalities, inclusions within fibroblasts and tissue, and premature death [154].

Though murine and feline animal models recapitulate many aspects of the human disease, study of early developmental processes is difficult as they occur *in utero*.

Zebrafish as a Developmental Model of ML-II

The freshwater teleost *Danio rerio*, also known as zebrafish, is a well-established model organism for studying vertebrate development and organogenesis. External development and optical clarity throughout embryogenesis make this system well suited to developmental, genetic, and biochemical analysis. Large scale genetic screens of zebrafish have leveraged these traits with noteworthy success and have identified hundreds of mutant

phenotypes in various aspects of development and those which resemble various known human diseases, including CDGs and LSDs [155-159].

In order to gain insight into the early developmental parameters of the disease a zebrafish model of ML-II was developed in our lab using morpholino-based knockdown technology. Early characterization of morphant embryos revealed multiple phenotypes in systems consistent with the human disease including craniofacial defects, abnormal cartilage development, altered chondrocyte morphology, motility defects, and profound cardiac abnormalities. Striking changes were noted in both the timing and steady state level of type II collagen deposition and Sox9 expression in craniofacial cartilage, indicating altered ECM production or homeostasis [158]. Investigation of this animal model of ML-II suggests that development of structures dependent upon coordinated ECM biosynthesis and turnover, such as cartilage and bone, may be uniquely sensitive to defects in lysosomal targeting.

This process is particularly important in early development, as differentiation of chondro- progenitor cells depends upon the surrounding components of the ECM, as discussed below.

Development of Craniofacial Cartilage

Cartilage and bone development begins with the mesenchymal condensation of chondrocyte precursors derived from either the cells of the cranial neural crest (CNC) in the case of craniofacial cartilage, or the lateral plate mesoderm in the case of the vertebrate limb. These multi-potential cells

differentiate into a variety of cell types including chondrocytes and osteoblasts. After mesenchymal cell migration, highly ordered epithelium-derived cell-cell and cell-matrix signals drive proliferation and differentiation during chondrogenesis terminating in endochondral ossification [160, 161]. Prior to condensation, precursor chondrocytes express high levels of hyaluronan, and type I collagen [162]. Condensation is initiated by TGF-β, which increases synthesis of fibronectin. Upon being embedded in matrix-rich lacunae, chondrocyte precursors no longer secrete collagen type I, and instead secrete a matrix predominantly comprised of aggrecan and collagen type II, which serves as an early marker for committed chondrocytes [160-163]. Coordination between fibroblast growth factors (FGFs), hedgehog, bone morphogenic proteins (BMPs), and Wnt pathways establish the temporal-spatial differentiation of chondrocytes along the pathway from cartilage to bone [164, 165]. Differentiation of precursor chondrocytes is required for the continued progression of skeletogenesis. Sox9, a member of the HMG box transcription factor family, is one of the earliest markers for cells undergoing condensation and is required for expression of type II collagen [166, 167].

Molecular Composition of Cartilage

Articular cartilage consists of a hydrated, proteoglycan and glycosaminoglycan (GAG) rich matrix. Within the matrix, type II collagen triple helical fibers forms a highly ordered network, each collagen molecule associates with other lateral collagen molecules in a staggered array. Trimeric collagen is

joined with adjacent molecules via an almidine-derived crosslink, joining the telopeptide of one collagen to the triple helix of another. This arrangement yields a stiff matrix capable of resisting tensile forces the cartilage is exposed to *in vivo*. Type II collagen and aggrecan are the principal molecules of the ECM, making up 95% of its dry weight [161, 168, 169]. Aggrecan exists in association with the GAG hyaluronic acid (HA) and link proteins in a large proteoglycan aggregate filling the interstitial spaces between the collagen matrix. Monomeric aggrecan is approximately 2.5MDa, consisting of a 250kDa core protein to which numerous chondroitin sulfate (CS) and keratan sulfate (KS) GAG chains are attached. The long polysaccharide chains of aggrecan within the ECM are highly hydrated, providing the cartilage with the osmotic properties necessary to resist compressive loads. Depletion of proteoglycans is considered to be reversible (33% of all HA is turned over daily in human adults), disruption and degradation of the collagen network is considered permanent because of the extremely limited ability of cartilage to regenerate [170-172].

Cathepsin Proteases are Involved in Many Normal Physiological Processes

Cathepsin proteases are members of the papain family and are synthesized as inactive zymogens requiring processing to become mature and active enzymes. Lysosomal cathepsins require the addition of M6P residues to their N-glycans for proper trafficking to the lysosomal compartment via the M6PRs [173-177]. Activation of cathepsins requires removal of the N-terminal propeptide either via furin processing, proteolytic processing, and autocatalytic

processing within a low pH environment [178-181]. Emerging data supports the role of GAG chains in promoting or enhancing the activation of these proteases, but is not well understood in a biological context [182-185].

Cathepsin proteases were first identified for their ability to degrade a wide variety of proteins, and later recognized as important constituents of the lysosome [186-188]. Cathepsin gene knockouts have revealed that loss of individual cathepsins does not impair lysosomal protein turnover, although lysosomal cathepsins have diverse functions critical for the development and normal function of many organisms [189-194]. Pycnodysostosis, a human disease characterized by severe skeletal abnormalities results from loss of cathepsin K activity. Cathepsin K null mice recapitulate the human disease, suggesting cathepsin K is required for normal bone development and remodeling [190, 195, 196]. A role has also been illustrated for cathepsin K, and possibly other cathepsins, in the endosomal processing and subsequent signaling of Toll-like receptors, which recognize pathogens and illicit elements of the innate immune system [197]. Immune function requires major histocompatibility complex (MHC) class II invariant chain processing and antigen presentation, mediated via Cathepsin S in humans and cathepsin L in mice [191, 198]. Cathepsin L has been found to prevent cardiac hypertrophy in murine models through blocking AKT/GSK3β signaling, is required for terminal keratinocyte differentiation, and the balance between cystatin M/E and cathepsin L is required for tissue integrity of epidermis, hair follicles, and the corneal epithelium [199-201]. Initially implicated in generation of amyloid plaques, Cathepsin B has

recently been shown to degrade β-amyloid precursor proteins into harmless fragments, and is believed to have a neuroprotective effect [202]. Cathepsin D is known to play a role in apoptosis and autophagy and within the developing heart, cathepsin D expression outlines areas of programmed cell death. The cysteine cathepsins B, C, and L also play roles in apoptosis, possibly in redundant and cell-type specific mechanisms [191, 192, 203-207].

Matrix Metalloproteinase are Effectors of Development and Physiology

Divided into broad groups based on substrate specificity, MMPs are key mediators in physiological turnover of the ECM. Collagenases, stromelysins, and gelatinases have all been shown to play distinct roles in the normal turnover of collagens, aggrecan, fibronectin, laminin and other matrix proteins [208-211]. Degradation of collagen requires sequential activity of MMPs; collagenases first cleave the triple-helical collagen followed by subsequent cleavage into smaller fragments by the gelatinases. Collagen fragments are then internalized via endocytosis and degraded into amino acids within the lysosome by cathepsins [212, 213]. ECM remodeling mediated by MMPs is required for tissue morphogenesis and cell migration, as evidenced by endothelial cell migration during sprouting angiogenesis in tissue and bone [214, 215]. MMPs also regulate the bioavailability of growth factors sequestered within the ECM, including TGF-β and FGF. MMPs 1 and 3 have been shown to degrade perlecan, releasing bound FGF [215]. MMPs 2, 9, 13, and 14 have been shown to activate latent TGF-β, which is capable of increasing MMP and type II collagen expression [216-218].

Studies of wound healing have established the role of MT-MMP1 in keratinocyte migration at the wound site and dermis contraction [219, 220]. Regulated primarily at the level of transcript, dysregulation of MMPs activity leads to pathological ECM degradation [221-223].

Pathological ECM Degradation is Mediated by Proteases

The cartilage matrix is turned over throughout life, particularly during growth and development as cells must migrate and reorganize. It is believed that degradation products within the environment of the matrix can be catalysts leading to increased catabolism [161]. A number of enzymes and signaling pathways have been well studied using human and animal models of osteoarthritis (OA) and rheumatoid arthritis (RA). The expression and synthesis of several classes of MMPs and cathepsins are increased in arthritic conditions [224-226]. Three collagenases, MMP-1, 8, and 13 and two gelatinases, MMP-2 and 9 are found at increased levels in synovial fluid, chondrocytes, and cartilage explants from patients with RA and OA. MMP-9 does not appear to be expressed in normal cartilage, suggesting that its selective upregulation may contribute to the progressive degradation in OA [168, 227]. Expression of MMPs is strongly associated with increased levels of inflammatory cytokines IL-1B, IL-18, and TNF-α in arthritic conditions [227-230].

Several cathepsins have been shown to exhibit proteolytic activity on ECM substrates and have been implicated in generation of inflammatory responses [225, 231-234]. Cathepsin K has been identified as the critical protease in

osteoclast mediated bone resorption and cartilage degradation. Recent studies have shown cathepsin K to function efficiently as both an aggrecanase and a collagenase when bound to CS or dermatan sulfate (DS). Upon binding to CS, cathepsin K is substantially more stable at neutral pH and functions as a potent collagenase [225, 233, 235]. Cathepsins B, L, G, and S have all been shown to degrade matrix proteoglycans such as fibronectin and aggrecan and accumulate in the synovial fluid of arthritic patients [234, 236]. Evidence in the literature supports the idea that there may be some relationship between cathepsins and MMPs in degradation of matrix substrates. Cathepsin B can degrade tissue-inhibitors of metalloproteinases (TIMPs), the endogenous inhibitors of MMPs, while cathepsin G is known to activate MMP-9 and stimulate MMP expression through the generation of fibronectin fragments [237-239].

Increased cathepsin and MMP activities are also associated with mucopolysaccharidoses (MPS), a class of LSD resulting from impaired GAG turnover. MPS patients suffer from numerous joint and skeletal abnormalities similar to those in ML-II. Studies show an increase in cathepsin S and MMP-12 activity in the aortas of MPS I mice, as well as increased levels of pro-inflammatory cytokines [240, 241]. Crossing the MPS I mouse into a cathepsin S null mouse relieved aortic abnormalities similar to those seen in ML-II patients (data not published, personal communication from Ponder KP). Further studies using MPS VI and VII animal models have shown substantial increases in MMP activity, as well as significantly elevated levels of pro-inflammatory cytokines, suggesting that impaired GAG metabolism seen in MPS disorders leads to

increased ECM destruction [242, 243]. These studies have shown that TLR signaling is elevated, and use of TNF-α antagonists reduces cartilage catabolism and improves bone and joint health [244, 245]. Increased activity of these proteases within the ECM leads to numerous deleterious effects.

Dissertation Overview

Significant progress has been made since the discovery of “I-cell” disease over forty years ago. We now have a better understanding of the genetics of the disease, the enzymes and proteins involved, and how defects in the mannose-6-phosphate biosynthetic pathway leads to a severe disease. Presently, many of the cellular and molecular pathologies that have been observed in both patients and animal models do not have a well-defined pathogenic mechanism. For example, it is still not understood if the accumulation of material within lysosomes is disease-causing or if it is an observable symptom of the disease progression. Nor is it understood why these inclusions appear to be cell and tissue specific or why acid hydrolase levels appear normal in certain tissues. These and other factors remain an obstacle to the treatment of ML-II. Based on the evidence that loss of Man-6-P biosynthesis impairs the normal chondrocyte differentiation in ML-II zebrafish, we hypothesized that loss of M6P on the lysosomal cathepsin proteases disrupts the biosynthesis or maintenance of the ECM and contributes to the bone and cartilage pathology of ML-II. This dissertation explores this hypothesis by characterizing the expression and activity of cathepsin and MMPs during early development in a zebrafish model for ML-II. The findings presented show that several proteases are increased, cathepsin K activity is required in

wild-type embryos, cathepsin K is subject to tight regulation, and is inappropriately activated in ML-II. Suppression of cathepsin K, by either pharmacological or genetic means, rescues many of the craniofacial abnormalities observed in the zebrafish ML-II model. Further, the data presented highlights the extent of mannose phosphorylation of cathepsin proteases in zebrafish, loss of M6P leads to loss of intracellular cathepsin activity, and loss of mannose phosphorylation of cathepsin K is sufficient to generate craniofacial cartilage abnormalities. The mechanisms that underlie the role of lysosomal and matrix proteases in the cartilage pathology of ML-II are discussed.

References

1. Schachter, H., et al., *Intracellular localization of liver sugar nucleotide glycoprotein glycosyltransferases in a Golgi-rich fraction.* J Biol Chem, 1970. **245**(5): p. 1090-100.

2. Schachter, H., *The subcellular sites of glycosylation.* Biochem Soc Symp, 1974(40): p. 57-71.

3. Varki, A., J.D. Esko, and K.J. Colley, *Cellular Organization of Glycosylation*, in *Essentials of Glycobiology*, A. Varki, et al., Editors. 2009: Cold Spring Harbor (NY).

4. Capasso, J.M. and C.B. Hirschberg, *Mechanisms of glycosylation and sulfation in the Golgi apparatus: evidence for nucleotide sugar/nucleoside monophosphate and nucleotide sulfate/nucleoside monophosphate antiports in the Golgi apparatus membrane.* Proc Natl Acad Sci U S A, 1984. **81**(22): p. 7051-5.

5. Capasso, J.M. and C.B. Hirschberg, *Effect of nucleotides on translocation of sugar nucleotides and adenosine 3'-phosphate 5'-phosphosulfate into Golgi apparatus vesicles.* Biochim Biophys Acta, 1984. **777**(1): p. 133-9.

6. Guillen, E., C. Abeijon, and C.B. Hirschberg, *Mammalian Golgi apparatus UDP-N-acetylglucosamine transporter: molecular cloning by phenotypic correction of a yeast mutant.* Proc Natl Acad Sci U S A, 1998. **95**(14): p. 7888-92.

7. Fleischer, B., *Mechanism of glycosylation in the Golgi apparatus.* J Histochem Cytochem, 1983. **31**(8): p. 1033-40.

8. Lucas, J.J. and C.J. Waechter, *Polyisoprenoid glycolipids involved in glycoprotein biosynthesis.* Mol Cell Biochem, 1976. **11**(2): p. 67-78.

9. Kornfeld, R. and S. Kornfeld, *Assembly of asparagine-linked oligosaccharides.* Annu Rev Biochem, 1985. **54**: p. 631-64.

10. Rini, J., J. Esko, and A. Varki, *Glycosyltransferases and Glycan-processing Enzymes*, in *Essentials of Glycobiology*, A. Varki, et al., Editors. 2009: Cold Spring Harbor (NY).

11. Hammond, C. and A. Helenius, *Folding of VSV G protein: sequential interaction with BiP and calnexin.* Science, 1994. **266**(5184): p. 456-8.

12. Hammond, C., I. Braakman, and A. Helenius, *Role of N-linked oligosaccharide recognition, glucose trimming, and calnexin in glycoprotein folding and quality control.* Proc Natl Acad Sci U S A, 1994. **91**(3): p. 913-7.

13. Zhang, Q., M. Tector, and R.D. Salter, *Calnexin recognizes carbohydrate and protein determinants of class I major histocompatibility complex molecules.* J Biol Chem, 1995. **270**(8): p. 3944-8.

14. Hebert, D.N., B. Foellmer, and A. Helenius, *Glucose trimming and reglucosylation determine glycoprotein association with calnexin in the endoplasmic reticulum.* Cell, 1995. **81**(3): p. 425-33.

15. Dewald, B. and O. Touster, *A new alpha-D-mannosidase occurring in Golgi membranes.* J Biol Chem, 1973. **248**(20): p. 7223-33.

16. Tulsiani, D.R., et al., *alpha-D-Mannosidases of rat liver Golgi membranes. Mannosidase II is the GlcNAcMAN5-cleaving enzyme in glycoprotein biosynthesis and mannosidases Ia and IB are the enzymes converting Man9 precursors to Man5 intermediates.* J Biol Chem, 1982. **257**(7): p. 3660-8.

17. Tabas, I. and S. Kornfeld, *N-asparagine-linked oligosaccharides: processing.* Methods Enzymol, 1982. **83**: p. 416-29.

18. Tulsiani, D.R., T.M. Harris, and O. Touster, *Swainsonine inhibits the biosynthesis of complex glycoproteins by inhibition of Golgi mannosidase II.* J Biol Chem, 1982. **257**(14): p. 7936-9.

19. Natowicz, M., J.U. Baenziger, and W.S. Sly, *Structural studies of the phosphorylated high mannose-type oligosaccharides on human beta-glucuronidase.* J Biol Chem, 1982. **257**(8): p. 4412-20.

20. Hickman, S., L.J. Shapiro, and E.F. Neufeld, *A recognition marker required for uptake of a lysosomal enzyme by cultured fibroblasts.* Biochem Biophys Res Commun, 1974. **57**(1): p. 55-61.

21. Reitman, M.L. and S. Kornfeld, *Lysosomal enzyme targeting. N-Acetylglucosaminylphosphotransferase selectively phosphorylates native lysosomal enzymes.* J Biol Chem, 1981. **256**(23): p. 11977-80.

22. Reitman, M.L. and S. Kornfeld, *UDP-N-acetylglucosamine:glycoprotein N-acetylglucosamine-1-phosphotransferase. Proposed enzyme for the phosphorylation of the high mannose oligosaccharide units of lysosomal enzymes.* J Biol Chem, 1981. **256**(9): p. 4275-81.

23. Harpaz, N. and H. Schachter, *Control of glycoprotein synthesis. Bovine colostrum UDP-N-acetylglucosamine:alpha-D-mannoside beta 2-N-acetylglucosaminyltransferase I. Separation from UDP-N-acetylglucosamine:alpha-D-mannoside beta 2-N-acetylglucosaminyltransferase II, partial purification, and substrate specificity.* J Biol Chem, 1980. **255**(10): p. 4885-93.

24. Harpaz, N. and H. Schachter, *Control of glycoprotein synthesis. Processing of asparagine-linked oligosaccharides by one or more rat liver Golgi alpha-D-mannosidases dependent on the prior action of UDP-N-acetylglucosamine: alpha-D-mannoside beta 2-N-acetylglucosaminyltransferase I.* J Biol Chem, 1980. **255**(10): p. 4894-902.

25. Stanley, P., H. Schachter, and N. Taniguchi, *N-Glycans*, in *Essentials of Glycobiology*, A. Varki, et al., Editors. 2009: Cold Spring Harbor (NY).

26. Mulloy, B., G.W. Hart, and P. Stanley, *Structural Analysis of Glycans*, in *Essentials of Glycobiology*, A. Varki, et al., Editors. 2009: Cold Spring Harbor (NY).

27. Duksin, D. and P. Bornstein, *Changes in surface properties of normal and transformed cells caused by tunicamycin, an inhibitor of protein glycosylation.* Proc Natl Acad Sci U S A, 1977. **74**(8): p. 3433-7.

28. Leavitt, R., S. Schlesinger, and S. Kornfeld, *Tunicamycin inhibits glycosylation and multiplication of Sindbis and vesicular stomatitis viruses.* J Virol, 1977. **21**(1): p. 375-85.

29. Campbell, R.M., et al., *Complex asparagine-linked oligosaccharides in Mgat1-null embryos.* Glycobiology, 1995. **5**(5): p. 535-43.

30. Ioffe, E., Y. Liu, and P. Stanley, *Essential role for complex N-glycans in forming an organized layer of bronchial epithelium.* Proc Natl Acad Sci U S A, 1996. **93**(20): p. 11041-6.

31. Lin, X., et al., *Disruption of gastrulation and heparan sulfate biosynthesis in EXT1-deficient mice.* Dev Biol, 2000. **224**(2): p. 299-311.

32. Shi, S. and P. Stanley, *Protein O-fucosyltransferase 1 is an essential component of Notch signaling pathways.* Proc Natl Acad Sci U S A, 2003. **100**(9): p. 5234-9.

33. Freeze, H.H., *Genetic defects in the human glycome.* Nat Rev Genet, 2006. **7**(7): p. 537-51.

34. Ungar, D., et al., *Retrograde transport on the COG railway.* Trends Cell Biol, 2006. **16**(2): p. 113-20.

35. Freeze, H.H. and H. Schachter, *Genetic Disorders of Glycosylation*, in *Essentials of Glycobiology*, A. Varki, et al., Editors. 2009: Cold Spring Harbor (NY).

36. Arvan, P. and J. Lee, *Regulated and constitutive protein targeting can be distinguished by secretory polarity in thyroid epithelial cells.* J Cell Biol, 1991. **112**(3): p. 365-76.

37. de Virgilio, M., et al., *Degradation of a short-lived glycoprotein from the lumen of the endoplasmic reticulum: the role of N-linked glycans and the unfolded protein response.* Mol Biol Cell, 1999. **10**(12): p. 4059-73.

38. Wang, X.Z., et al., *Signals from the stressed endoplasmic reticulum induce C/EBP-homologous protein (CHOP/GADD153).* Mol Cell Biol, 1996. **16**(8): p. 4273-80.

39. Lukacs, G.L., et al., *Conformational maturation of CFTR but not its mutant counterpart (delta F508) occurs in the endoplasmic reticulum and requires ATP.* EMBO J, 1994. **13**(24): p. 6076-86.

40. Glozman, R., et al., *N-glycans are direct determinants of CFTR folding and stability in secretory and endocytic membrane traffic.* J Cell Biol, 2009. **184**(6): p. 847-62.

41. Lau, K.S., et al., *Complex N-glycan number and degree of branching cooperate to regulate cell proliferation and differentiation.* Cell, 2007. **129**(1): p. 123-34.

42. Cholon, D.M., et al., *Modulation of endocytic trafficking and apical stability of CFTR in primary human airway epithelial cultures.* Am J Physiol Lung Cell Mol Physiol, 2010. **298**(3): p. L304-14.

43. Esko, J.D. and N. Sharon, *Microbial Lectins: Hemagglutinins, Adhesins, and Toxins*, in *Essentials of Glycobiology*, A. Varki, et al., Editors. 2009: Cold Spring Harbor (NY).

44. Sharon, N. and H. Lis, *History of lectins: from hemagglutinins to biological recognition molecules.* Glycobiology, 2004. **14**(11): p. 53R-62R.

45. Cummings, R.D. and F.T. Liu, *Galectins*, in *Essentials of Glycobiology*, A. Varki, et al., Editors. 2009: Cold Spring Harbor (NY).

46. Cummings, R.D. and R.P. McEver, *C-type Lectins*, in *Essentials of Glycobiology*, A. Varki, et al., Editors. 2009: Cold Spring Harbor (NY).

47. Epperson, T.K., et al., *Noncovalent association of P-selectin glycoprotein ligand-1 and minimal determinants for binding to P-selectin.* J Biol Chem, 2000. **275**(11): p. 7839-53.

48. Guyer, D.A., et al., *P-selectin glycoprotein ligand-1 (PSGL-1) is a ligand for L-selectin in neutrophil aggregation.* Blood, 1996. **88**(7): p. 2415-21.

49. Waheed, A., A. Hasilik, and K. von Figura, *Processing of the phosphorylated recognition marker in lysosomal enzymes. Characterization and partial purification of a microsomal alpha-N-acetylglucosaminyl phosphodiesterase.* J Biol Chem, 1981. **256**(11): p. 5717-21.

50. Fratantoni, J.C., C.W. Hall, and E.F. Neufeld, *The defect in Hurler's and Hunter's syndromes: faulty degradation of mucopolysaccharide.* Proc Natl Acad Sci U S A, 1968. **60**(2): p. 699-706.

51. Hickman, S. and E.F. Neufeld, *A hypothesis for I-cell disease: defective hydrolases that do not enter lysosomes.* Biochem Biophys Res Commun, 1972. **49**(4): p. 992-9.

52. Fratantoni, J.C., C.W. Hall, and E.F. Neufeld, *Hurler and Hunter syndromes: mutual correction of the defect in cultured fibroblasts.* Science, 1968. **162**(3853): p. 570-2.

53. Leroy, J.G. and R.I. Demars, *Mutant Enzymatic and Cytological Phenotypes in Cultured Human Fibroblasts.* Science, 1967. **157**(3790): p. 804-806.

54. Kornfeld, S., et al., *Steps in the phosphorylation of the high mannose oligosaccharides of lysosomal enzymes.* Ciba Found Symp, 1982(92): p. 138-56.

55. Kelly, T.E., et al., *Mucolipidosis III: clinical and laboratory findings.* Birth Defects Orig Artic Ser, 1975. **11**(6): p. 295-9.

56. Sly, W.S., *The missing link in lysosomal enzyme targeting.* J Clin Invest, 2000. **105**(5): p. 563-4.

57. Couso, R., et al., *Phosphorylation of the oligosaccharide of uteroferrin by UDP-GlcNAc:glycoprotein N-acetylglucosamine-1-phosphotransferases from rat liver, Acanthamoeba castellani, and Dictyostelium discoideum requires alpha 1,2-linked mannose residues.* J Biol Chem, 1986. **261**(14): p. 6326-31.

58. Do, H., et al., *Human mannose 6-phosphate-uncovering enzyme is synthesized as a proenzyme that is activated by the endoprotease furin.* J Biol Chem, 2002. **277**(33): p. 29737-44.

59. Rohrer, J. and R. Kornfeld, *Lysosomal hydrolase mannose 6-phosphate uncovering enzyme resides in the trans-Golgi network.* Mol Biol Cell, 2001. **12**(6): p. 1623-31.

60. Varki, A. and S. Kornfeld, *Identification of a rat liver alpha-N-acetylglucosaminyl phosphodiesterase capable of removing "blocking" alpha-N-acetylglucosamine residues from phosphorylated high mannose oligosaccharides of lysosomal enzymes.* J Biol Chem, 1980. **255**(18): p. 8398-401.

61. Bao, M., et al., *Bovine UDP-N-acetylglucosamine:lysosomal-enzyme N-acetylglucosamine-1-phosphotransferase. I. Purification and subunit structure.* J Biol Chem, 1996. **271**(49): p. 31437-45.

62. Tiede, S., et al., *Mucolipidosis II is caused by mutations in GNPTA encoding the alpha/beta GlcNAc-1-phosphotransferase.* Nat Med, 2005. **11**(10): p. 1109-12.

63. Paik, K.H., et al., *Identification of mutations in the GNPTA (MGC4170) gene coding for GlcNAc-phosphotransferase alpha/beta subunits in Korean patients with mucolipidosis type II or type IIIA.* Hum Mutat, 2005. **26**(4): p. 308-14.

64. Raas-Rothschild, A., et al., *Molecular basis of variant pseudo-hurler polydystrophy (mucolipidosis IIIC).* J Clin Invest, 2000. **105**(5): p. 673-81.

65. Kollmann, K., et al., *Mannose phosphorylation in health and disease.* Eur J Cell Biol, 2010. **89**(1): p. 117-23.

66. Marschner, K., et al., *A key enzyme in the biogenesis of lysosomes is a protease that regulates cholesterol metabolism.* Science, 2011. **333**(6038): p. 87-90.

67. Kudo, M., et al., *The alpha- and beta-subunits of the human UDP-N-acetylglucosamine:lysosomal enzyme N-acetylglucosamine-1-phosphotransferase [corrected] are encoded by a single cDNA.* J Biol Chem, 2005. **280**(43): p. 36141-9.

68. Kudo, M., M.S. Brem, and W.M. Canfield, *Mucolipidosis II (I-cell disease) and mucolipidosis IIIA (classical pseudo-hurler polydystrophy) are caused by mutations in the GlcNAc-phosphotransferase alpha / beta -subunits precursor gene.* Am J Hum Genet, 2006. **78**(3): p. 451-63.

69. Qian, Y., et al., *Functions of the alpha, beta, and gamma subunits of UDP-GlcNAc:lysosomal enzyme N-acetylglucosamine-1-phosphotransferase.* J Biol Chem, 2010. **285**(5): p. 3360-70.

70. Lee, W.S., et al., *Murine UDP-GlcNAc:lysosomal enzyme N-acetylglucosamine-1-phosphotransferase lacking the gamma-subunit retains substantial activity toward acid hydrolases.* J Biol Chem, 2007. **282**(37): p. 27198-203.

71. Lupas, A., M. Van Dyke, and J. Stock, *Predicting coiled coils from protein sequences.* Science, 1991. **252**(5010): p. 1162-4.

72. Encarnacao, M., et al., *Post-translational modifications of the gamma-subunit affect intracellular trafficking and complex assembly of GlcNAc-1-phosphotransferase.* J Biol Chem, 2011. **286**(7): p. 5311-8.

73. Pohl, S., et al., *Proteolytic processing of the gamma-subunit is associated with the failure to form GlcNAc-1-phosphotransferase complexes and mannose 6-phosphate residues on lysosomal enzymes in human macrophages.* J Biol Chem, 2010. **285**(31): p. 23936-44.

74. Lang, L., et al., *Lysosomal enzyme phosphorylation. Recognition of a protein-dependent determinant allows specific phosphorylation of oligosaccharides present on lysosomal enzymes.* J Biol Chem, 1984. **259**(23): p. 14663-71.

75. Nishikawa, A., et al., *The phosphorylation of bovine DNase I Asn-linked oligosaccharides is dependent on specific lysine and arginine residues.* J Biol Chem, 1997. **272**(31): p. 19408-12.

76. Cuozzo, J.W. and G.G. Sahagian, *Lysine is a common determinant for mannose phosphorylation of lysosomal proteins.* J Biol Chem, 1994. **269**(20): p. 14490-6.

77. Cuozzo, J.W., et al., *Lysine-based structure responsible for selective mannose phosphorylation of cathepsin D and cathepsin L defines a common structural motif for lysosomal enzyme targeting.* J Biol Chem, 1998. **273**(33): p. 21067-76.

78. Nishikawa, A., et al., *Identification of amino acids that modulate mannose phosphorylation of mouse DNase I, a secretory glycoprotein.* J Biol Chem, 1999. **274**(27): p. 19309-15.

79. Baranski, T.J., A.B. Cantor, and S. Kornfeld, *Lysosomal enzyme phosphorylation. I. Protein recognition determinants in both lobes of procathepsin D mediate its interaction with UDP-GlcNAc:lysosomal enzyme N-acetylglucosamine-1-phosphotransferase.* J Biol Chem, 1992. **267**(32): p. 23342-8.

80. Cantor, A.B., T.J. Baranski, and S. Kornfeld, *Lysosomal enzyme phosphorylation. II. Protein recognition determinants in either lobe of procathepsin D are sufficient for phosphorylation of both the amino and carboxyl lobe oligosaccharides.* J Biol Chem, 1992. **267**(32): p. 23349-56.

81. Cantor, A.B. and S. Kornfeld, *Phosphorylation of Asn-linked oligosaccharides located at novel sites on the lysosomal enzyme cathepsin D.* J Biol Chem, 1992. **267**(32): p. 23357-63.

82. Steet, R., W.S. Lee, and S. Kornfeld, *Identification of the minimal lysosomal enzyme recognition domain in cathepsin D.* J Biol Chem, 2005. **280**(39): p. 33318-23.

83. Lee, W.S., et al., *Multiple signals regulate trafficking of the mannose 6-phosphate-uncovering enzyme.* J Biol Chem, 2002. **277**(5): p. 3544-51.

84. Mullis, K.G. and R.H. Kornfeld, *Characterization and immunolocalization of bovine N-acetylglucosamine-1-phosphodiester alpha-N-acetylglucosaminidase.* J Biol Chem, 1994. **269**(3): p. 1727-33.

85. Boonen, M., et al., *Mice lacking mannose 6-phosphate uncovering enzyme activity have a milder phenotype than mice deficient for N-acetylglucosamine-1-phosphotransferase activity.* Mol Biol Cell, 2009. **20**(20): p. 4381-9.

86. Hoflack, B. and S. Kornfeld, *Purification and characterization of a cation-dependent mannose 6-phosphate receptor from murine P388D1 macrophages and bovine liver.* J Biol Chem, 1985. **260**(22): p. 12008-14.

87. Sahagian, G.G., J. Distler, and G.W. Jourdian, *Characterization of a membrane-associated receptor from bovine liver that binds phosphomannosyl residues of bovine testicular beta-galactosidase.* Proc Natl Acad Sci U S A, 1981. **78**(7): p. 4289-93.

88. Dahms, N.M., L.J. Olson, and J.J. Kim, *Strategies for carbohydrate recognition by the mannose 6-phosphate receptors.* Glycobiology, 2008. **18**(9): p. 664-78.

89. Ghosh, P., N.M. Dahms, and S. Kornfeld, *Mannose 6-phosphate receptors: new twists in the tale.* Nat Rev Mol Cell Biol, 2003. **4**(3): p. 202-12.

90. Olson, L.J., N.M. Dahms, and J.J. Kim, *The N-terminal carbohydrate recognition site of the cation-independent mannose 6-phosphate receptor.* J Biol Chem, 2004. **279**(32): p. 34000-9.

91. Kim, J.J., L.J. Olson, and N.M. Dahms, *Carbohydrate recognition by the mannose-6-phosphate receptors.* Curr Opin Struct Biol, 2009. **19**(5): p. 534-42.

92. Song, X., et al., *Glycan microarray analysis of P-type lectins reveals distinct phosphomannose glycan recognition.* J Biol Chem, 2009. **284**(50): p. 35201-14.

93. Bohnsack, R.N., et al., *Cation-independent mannose 6-phosphate receptor: a composite of distinct phosphomannosyl binding sites.* J Biol Chem, 2009. **284**(50): p. 35215-26.

94. Lemansky, P., et al., *The cation-independent mannose 6-phosphate receptor is involved in lysosomal delivery of serglycin.* J Leukoc Biol, 2007. **81**(4): p. 1149-58.

95. Lemansky, P., et al., *Targeting myeloperoxidase to azurophilic granules in HL-60 cells.* J Leukoc Biol, 2003. **74**(4): p. 542-50.

96. Qian, M., et al., *Proteomics analysis of serum from mutant mice reveals lysosomal proteins selectively transported by each of the two mannose 6-phosphate receptors.* Mol Cell Proteomics, 2008. **7**(1): p. 58-70.

97. Ghosh, P., et al., *Mammalian GGAs act together to sort mannose 6-phosphate receptors.* J Cell Biol, 2003. **163**(4): p. 755-66.

98. Ghosh, P. and S. Kornfeld, *Phosphorylation-induced conformational changes regulate GGAs 1 and 3 function at the trans-Golgi network.* J Biol Chem, 2003. **278**(16): p. 14543-9.

99. Rohrer, J., et al., *A determinant in the cytoplasmic tail of the cation-dependent mannose 6-phosphate receptor prevents trafficking to lysosomes.* J Cell Biol, 1995. **130**(6): p. 1297-306.

100. Ghosh, P. and S. Kornfeld, *The GGA proteins: key players in protein sorting at the trans-Golgi network.* Eur J Cell Biol, 2004. **83**(6): p. 257-62.

101. Kornfeld, S., *Trafficking of lysosomal enzymes in normal and disease states.* J Clin Invest, 1986. **77**(1): p. 1-6.

102. Kornfeld, S., *Trafficking of lysosomal enzymes.* Faseb J, 1987. **1**(6): p. 462-8.

103. Godar, S., et al., *M6P/IGFII-receptor complexes urokinase receptor and plasminogen for activation of transforming growth factor-beta1.* Eur J Immunol, 1999. **29**(3): p. 1004-13.

104. Vignon, F. and H. Rochefort, *Interactions of pro-cathepsin D and IGF-II on the mannose-6-phosphate/IGF-II receptor.* Breast Cancer Res Treat, 1992. **22**(1): p. 47-57.

105. Dahms, N.M., D.A. Wick, and M.A. Brzycki-Wessell, *The bovine mannose 6-phosphate/insulin-like growth factor II receptor. Localization of the insulin-like growth factor II binding site to domains 5-11.* J Biol Chem, 1994. **269**(5): p. 3802-9.

106. Kang, J.X., Y. Li, and A. Leaf, *Mannose-6-phosphate/insulin-like growth factor-II receptor is a receptor for retinoic acid.* Proc Natl Acad Sci U S A, 1997. **94**(25): p. 13671-6.

107. MacDonald, R.G., et al., *Growth inhibition and differentiation of the human colon carcinoma cell line, Caco-2, by constitutive expression of insulin-like*

growth factor binding protein-3. J Gastroenterol Hepatol, 1999. **14**(1): p. 72-8.

108. Odekon, L.E., F. Blasi, and D.B. Rifkin, *Requirement for receptor-bound urokinase in plasmin-dependent cellular conversion of latent TGF-beta to TGF-beta.* J Cell Physiol, 1994. **158**(3): p. 398-407.

109. Olson, L.J., et al., *Structure of uPAR, plasminogen, and sugar-binding sites of the 300 kDa mannose 6-phosphate receptor.* EMBO J, 2004. **23**(10): p. 2019-28.

110. Kreiling, J.L., et al., *Binding of urokinase-type plasminogen activator receptor (uPAR) to the mannose 6-phosphate/insulin-like growth factor II receptor: contrasting interactions of full-length and soluble forms of uPAR.* J Biol Chem, 2003. **278**(23): p. 20628-37.

111. Antoniades, H.N., et al., *Expression of insulin-like growth factors I and II and their receptor mRNAs in primary human astrocytomas and meningiomas; in vivo studies using in situ hybridization and immunocytochemistry.* Int J Cancer, 1992. **50**(2): p. 215-22.

112. Waheed, A., et al., *Deficiency of UDP-N-acetylglucosamine:lysosomal enzyme N-acetylglucosamine-1-phosphotransferase in organs of I-cell patients.* Biochem Biophys Res Commun, 1982. **105**(3): p. 1052-8.

113. Ullrich, K., et al., *Recognition of human urine alpha-N-acetylglucosaminidase by rat hepatocytes. Involvement of receptors specific for galactose, mannose 6-phosphate and mannose.* Biochem J, 1979. **180**(2): p. 413-9.

114. Ullrich, K. and K. von Figura, *Endocytosis of beta-N-acetylglucosaminidase from sections of mucolipidosis-II and-III fibroblasts by non-parenchymal rat liver cells.* Biochem J, 1979. **182**(1): p. 245-7.

115. Barriocanal, J.G., et al., *Biosynthesis, glycosylation, movement through the Golgi system, and transport to lysosomes by an N-linked carbohydrate-independent mechanism of three lysosomal integral membrane proteins.* J Biol Chem, 1986. **261**(35): p. 16755-63.

116. Reczek, D., et al., *LIMP-2 is a receptor for lysosomal mannose-6-phosphate-independent targeting of beta-glucocerebrosidase.* Cell, 2007. **131**(4): p. 770-83.

117. Cooper, A.A. and T.H. Stevens, *Vps10p cycles between the late-Golgi and prevacuolar compartments in its function as the sorting receptor for multiple yeast vacuolar hydrolases.* J Cell Biol, 1996. **133**(3): p. 529-41.

118. Canuel, M., et al., *Sortilin mediates the lysosomal targeting of cathepsins D and H.* Biochem Biophys Res Commun, 2008. **373**(2): p. 292-7.

119. Coutinho, M.F., M.J. Prata, and S. Alves, *A shortcut to the lysosome: The mannose-6-phosphate-independent pathway.* Mol Genet Metab, 2012.

120. Allen, C.L., et al., *Dileucine signal-dependent and AP-1-independent targeting of a lysosomal glycoprotein in Trypanosoma brucei.* Mol Biochem Parasitol, 2007. **156**(2): p. 175-90.

121. Lang, L., R. Couso, and S. Kornfeld, *Glycoprotein phosphorylation in simple eucaryotic organisms. Identification of UDP-GlcNAc:glycoprotein N-acetylglucosamine-1-phosphotransferase activity and analysis of substrate specificity.* J Biol Chem, 1986. **261**(14): p. 6320-5.

122. Lang, L., et al., *Lysosomal enzyme phosphorylation in human fibroblasts. Kinetic parameters offer a biochemical rationale for two distinct defects in the uridine diphospho-N-acetylglucosamine:lysosomal enzyme precursor N-acetylglucosamine-1-phosphotransferase.* J Clin Invest, 1985. **76**(6): p. 2191-5.

123. Guillen, E.Q.-A., A. Couso, R., *UDP-N-Acetylglucosamine: Glycoprotein N-Acetylglucosamine-I-Phosphotransferase Activity in Pupae of the Mediterranean Fruit Fly Ceratitis capitata.* Insect Biochem. Molec. Biol., 1994. **24**(2): p. 6.

124. Dennes, A., et al., *The novel Drosophila lysosomal enzyme receptor protein mediates lysosomal sorting in mammalian cells and binds mammalian and Drosophila GGA adaptors.* J Biol Chem, 2005. **280**(13): p. 12849-57.

125. Freeze, H.H., *Genetic Disorders of Glycan Degradation*, in *Essentials of Glycobiology*, A. Varki, et al., Editors. 2009: Cold Spring Harbor (NY).

126. Neufeld, E.F., T.W. Lim, and L.J. Shapiro, *Inherited disorders of lysosomal metabolism.* Annu Rev Biochem, 1975. **44**: p. 357-76.

127. Winchester, B.G., *Lysosomal metabolism of glycoconjugates.* Subcell Biochem, 1996. **27**: p. 191-238.

128. Meikle, P.J. and J.J. Hopwood, *Lysosomal storage disorders: emerging therapeutic options require early diagnosis.* Eur J Pediatr, 2003. **162 Suppl 1**: p. S34-7.

129. Beutler, E., *Lysosomal storage diseases: natural history and ethical and economic aspects.* Mol Genet Metab, 2006. **88**(3): p. 208-15.

130. Beutler, E., et al., *Enzyme replacement therapy for Gaucher disease.* Blood, 1991. **78**(5): p. 1183-9.

131. Beutler, E., *Gaucher disease: multiple lessons from a single gene disorder.* Acta Paediatr Suppl, 2006. **95**(451): p. 103-9.

132. Cathey, S.S., et al., *Molecular order in mucolipidosis II and III nomenclature.* Am J Med Genet A, 2008. **146A**(4): p. 512-3.

133. Kornfeld, S. and W.S. Sly, *I-Cell Disease and Pseudo-Hurler Polydystrophy: Disorders of Lysosomal Enzyme Phosphorylation and Localization*, in *The Metabolic and Molecular Bases of Inherited Disease*2001, McGraw Hill. p. 3469-3482.

134. Cathey, S.S., et al., *Phenotype and genotype in mucolipidoses II and III alpha/beta: a study of 61 probands.* J Med Genet, 2010. **47**(1): p. 38-48.

135. Encarnacao, M., et al., *Molecular analysis of the GNPTAB and GNPTG genes in 13 patients with mucolipidosis type II or type III - identification of eight novel mutations.* Clin Genet, 2009. **76**(1): p. 76-84.

136. Persichetti, E., et al., *Identification and molecular characterization of six novel mutations in the UDP-N-acetylglucosamine-1-phosphotransferase gamma subunit (GNPTG) gene in patients with mucolipidosis III gamma.* Hum Mutat, 2009. **30**(6): p. 978-84.

137. Leroy, J.G., S. Cathey, and M.J. Friez, *Mucolipidosis II*, in *GeneReviews*, R.A. Pagon, et al., Editors. 1993: Seattle (WA).

138. Kerr, D.A., et al., *Mucolipidosis type III alpha/beta: the first characterization of this rare disease by autopsy.* Arch Pathol Lab Med, 2011. **135**(4): p. 503-10.

139. Kobayashi, H., et al., *Pathology of the first autopsy case diagnosed as mucolipidosis type III alpha/beta suggesting autophagic dysfunction.* Mol Genet Metab, 2011. **102**(2): p. 170-5.

140. Patriquin, H.B., et al., *Neonatal mucolipidosis II (I-cell disease): clinical and radiologic features in three cases.* AJR Am J Roentgenol, 1977. **129**(1): p. 37-43.

141. Leroy, J.G., S.S. Cathey, and M.J. Friez, *Mucolipidosis III Alpha/Beta*, in *GeneReviews*, R.A. Pagon, et al., Editors. 1993: Seattle (WA).

142. Saul, R.A., et al., *Prenatal mucolipidosis type II (I-cell disease) can present as Pacman dysplasia.* Am J Med Genet A, 2005. **135**(3): p. 328-32.

143. Terashima, Y., et al., *I-cell disease. Report of three cases.* Am J Dis Child, 1975. **129**(9): p. 1083-90.

144. Pazzaglia, U.E., et al., *Bone changes of mucolipidosis II at different ages. Postmortem study of three cases.* Clin Orthop Relat Res, 1992(276): p. 283-90.

145. Pazzaglia, U.E., et al., *Neonatal mucolipidosis 2. The spontaneous evolution of early bone lesions and the effect of vitamin D treatment. Report of two cases.* Pediatr Radiol, 1989. **20**(1-2): p. 80-4.

146. Kawashima, I., et al., *Cytochemical analysis of storage materials in cultured skin fibroblasts from patients with I-cell disease.* Clin Chim Acta, 2007. **378**(1-2): p. 142-6.

147. Mazrier, H., et al., *Inheritance, biochemical abnormalities, and clinical features of feline mucolipidosis II: the first animal model of human I-cell disease.* J Hered, 2003. **94**(5): p. 363-73.

148. Hubler, M., et al., *Mucolipidosis type II in a domestic shorthair cat.* J Small Anim Pract, 1996. **37**(9): p. 435-41.

149. Bosshard, N.U., et al., *Spontaneous mucolipidosis in a cat: an animal model of human I-cell disease.* Vet Pathol, 1996. **33**(1): p. 1-13.

150. Gelfman, C.M., et al., *Mice lacking alpha/beta subunits of GlcNAc-1-phosphotransferase exhibit growth retardation, retinal degeneration, and secretory cell lesions.* Invest Ophthalmol Vis Sci, 2007. **48**(11): p. 5221-8.

151. Boonen, M., et al., *Vacuolization of mucolipidosis type II mouse exocrine gland cells represents accumulation of autolysosomes.* Mol Biol Cell, 2011. **22**(8): p. 1135-47.

152. Vogel, P., et al., *Comparative pathology of murine mucolipidosis types II and IIIC.* Vet Pathol, 2009. **46**(2): p. 313-24.

153. van Meel, E., et al., *Disruption of the Man-6-P targeting pathway in mice impairs osteoclast secretory lysosome biogenesis.* Traffic, 2011. **12**(7): p. 912-24.

154. Kollmann, K., et al., *Lysosomal dysfunction causes neurodegeneration in mucolipidosis II 'knock-in' mice.* Brain, 2012. **135**(Pt 9): p. 2661-75.

155. Haffter, P., et al., *The identification of genes with unique and essential functions in the development of the zebrafish, Danio rerio.* Development, 1996. **123**: p. 1-36.

156. Driever, W., et al., *A genetic screen for mutations affecting embryogenesis in zebrafish.* Development, 1996. **123**: p. 37-46.

157. Cline, A., et al., *A Zebrafish Model Of PMM2-CDG Reveals Altered Neurogenesis And A Substrate-Accumulation Mechanism For N-Linked Glycosylation Deficiency.* Mol Biol Cell, 2012.

158. Flanagan-Steet, H., C. Sias, and R. Steet, *Altered chondrocyte differentiation and extracellular matrix homeostasis in a zebrafish model for mucolipidosis II.* Am J Pathol, 2009. **175**(5): p. 2063-75.

159. Louwette, S., et al., *NPC1 defect results in abnormal platelet formation and function: studies in Niemann-Pick disease type C1 patients and zebrafish.* Hum Mol Genet, 2012.

160. Goldring, M.B., K. Tsuchimochi, and K. Ijiri, *The control of chondrogenesis.* J Cell Biochem, 2006. **97**(1): p. 33-44.

161. Onyekwelu, I., M.B. Goldring, and C. Hidaka, *Chondrogenesis, joint formation, and articular cartilage regeneration.* J Cell Biochem, 2009. **107**(3): p. 383-92.

162. DeLise, A.M., L. Fischer, and R.S. Tuan, *Cellular interactions and signaling in cartilage development.* Osteoarthritis Cartilage, 2000. **8**(5): p. 309-34.

163. Voss, B., J. Rauterberg, and K.M. Muller, *The perivascular connective matrix.* Pathol Res Pract, 1994. **190**(9-10): p. 969-83.

164. Day, T.F., et al., *Wnt/beta-catenin signaling in mesenchymal progenitors controls osteoblast and chondrocyte differentiation during vertebrate skeletogenesis.* Dev Cell, 2005. **8**(5): p. 739-50.

165. Niswander, L., *Pattern formation: old models out on a limb.* Nat Rev Genet, 2003. **4**(2): p. 133-43.

166. Gerber, H.P., et al., *VEGF couples hypertrophic cartilage remodeling, ossification and angiogenesis during endochondral bone formation.* Nat Med, 1999. **5**(6): p. 623-8.

167. Bridgewater, L.C., et al., *Adjacent DNA sequences modulate Sox9 transcriptional activation at paired Sox sites in three chondrocyte-specific enhancer elements.* Nucleic Acids Res, 2003. **31**(5): p. 1541-53.

168. Martel-Pelletier, J., et al., *Cartilage in normal and osteoarthritis conditions.* Best Pract Res Clin Rheumatol, 2008. **22**(2): p. 351-84.

169. Buckwalter, J.A. and H.J. Mankin, *Articular cartilage: tissue design and chondrocyte-matrix interactions.* Instr Course Lect, 1998. **47**: p. 477-86.

170. Brittberg, M., et al., *A critical analysis of cartilage repair.* Acta Orthop Scand, 1997. **68**(2): p. 186-91.

171. Stern, R., *Hyaluronan catabolism: a new metabolic pathway.* Eur J Cell Biol, 2004. **83**(7): p. 317-25.

172. Miller, D.R., et al., *Identification of fibronectin in preparations of osteoarthritic human cartilage.* Connect Tissue Res, 1984. **12**(3-4): p. 267-75.

173. Galjart, N.J., et al., *Human lysosomal protective protein has cathepsin A-like activity distinct from its protective function.* J Biol Chem, 1991. **266**(22): p. 14754-62.

174. Glickman, J.N. and S. Kornfeld, *Mannose 6-phosphate-independent targeting of lysosomal enzymes in I-cell disease B lymphoblasts.* J Cell Biol, 1993. **123**(1): p. 99-108.

175. Nishimura, Y., K. Furuno, and K. Kato, *Biosynthesis and processing of lysosomal cathepsin L in primary cultures of rat hepatocytes.* Arch Biochem Biophys, 1988. **263**(1): p. 107-16.

176. Tanaka, Y., R. Tanaka, and M. Himeno, *Lysosomal cysteine protease, cathepsin H, is targeted to lysosomes by the mannose 6-phosphate-independent system in rat hepatocytes.* Biol Pharm Bull, 2000. **23**(7): p. 805-9.

177. Tanaka, Y., et al., *Lysosomal cysteine protease, cathepsin B, is targeted to lysosomes by the mannose 6-phosphate-independent pathway in rat hepatocytes: site-specific phosphorylation in oligosaccharides of the proregion.* J Biochem, 2000. **128**(1): p. 39-48.

178. McQueney, M.S., et al., *Autocatalytic activation of human cathepsin K.* J Biol Chem, 1997. **272**(21): p. 13955-60.

179. Menard, R., et al., *Autocatalytic processing of recombinant human procathepsin L. Contribution of both intermolecular and unimolecular*

events in the processing of procathepsin L in vitro. J Biol Chem, 1998. **273**(8): p. 4478-84.

180. Pungercar, J.R., et al., *Autocatalytic processing of procathepsin B is triggered by proenzyme activity.* FEBS J, 2009. **276**(3): p. 660-8.

181. Rojnik, M., et al., *The influence of differential processing of procathepsin H on its aminopeptidase activity, secretion and subcellular localization in human cell lines.* Eur J Cell Biol, 2012. **91**(10): p. 757-64.

182. Beckman, M., et al., *Activation of cathepsin D by glycosaminoglycans.* FEBS J, 2009. **276**(24): p. 7343-52.

183. Caglic, D., et al., *Glycosaminoglycans facilitate procathepsin B activation through disruption of propeptide-mature enzyme interactions.* J Biol Chem, 2007. **282**(45): p. 33076-85.

184. Vasiljeva, O., et al., *Recombinant human procathepsin S is capable of autocatalytic processing at neutral pH in the presence of glycosaminoglycans.* FEBS Lett, 2005. **579**(5): p. 1285-90.

185. Novinec, M., et al., *Conformational flexibility and allosteric regulation of cathepsin K.* Biochem J, 2010. **429**(2): p. 379-89.

186. Bergmann, M. and J.S. Fruton, *Regarding the General Nature of Catheptic Enzymes.* Science, 1936. **84**(2169): p. 89-90.

187. Hsu, L. and A.L. Tappel, *Lysosomal Enzymes of Rat Intestinal Mucosa.* J Cell Biol, 1964. **23**: p. 233-40.

188. Coffey, J.W. and C. De Duve, *Digestive activity of lysosomes. I. The digestion of proteins by extracts of rat liver lysosomes.* J Biol Chem, 1968. **243**(12): p. 3255-63.

189. Deussing, J., et al., *Cathepsins B and D are dispensable for major histocompatibility complex class II-mediated antigen presentation.* Proc Natl Acad Sci U S A, 1998. **95**(8): p. 4516-21.

190. Saftig, P., et al., *Impaired osteoclastic bone resorption leads to osteopetrosis in cathepsin-K-deficient mice.* Proc Natl Acad Sci U S A, 1998. **95**(23): p. 13453-8.

191. Chapman, H.A., R.J. Riese, and G.P. Shi, *Emerging roles for cysteine proteases in human biology.* Annu Rev Physiol, 1997. **59**: p. 63-88.

192. Ivanova, S., et al., *Lysosomes in apoptosis.* Methods Enzymol, 2008. **442**: p. 183-99.

193. Repnik, U., et al., *Lysosomes and lysosomal cathepsins in cell death.* Biochim Biophys Acta, 2012. **1824**(1): p. 22-33.

194. Turk, V., et al., *Cysteine cathepsins: from structure, function and regulation to new frontiers.* Biochim Biophys Acta, 2012. **1824**(1): p. 68-88.

195. Khan, B., Z. Ahmed, and W. Ahmad, *A novel missense mutation in cathepsin K (CTSK) gene in a consanguineous Pakistani family with pycnodysostosis.* J Investig Med, 2010. **58**(5): p. 720-4.

196. Naeem, M., S. Sheikh, and W. Ahmad, *A mutation in CTSK gene in an autosomal recessive pycnodysostosis family of Pakistani origin.* BMC Med Genet, 2009. **10**: p. 76.

197. Asagiri, M., et al., *Cathepsin K-dependent toll-like receptor 9 signaling revealed in experimental arthritis.* Science, 2008. **319**(5863): p. 624-7.

198. Nakagawa, T.Y., et al., *Impaired invariant chain degradation and antigen presentation and diminished collagen-induced arthritis in cathepsin S null mice.* Immunity, 1999. **10**(2): p. 207-17.

199. Benavides, F., et al., *Protective role of cathepsin L in mouse skin carcinogenesis.* Mol Carcinog, 2011.

200. Tang, Q., et al., *Lysosomal cysteine peptidase cathepsin L protects against cardiac hypertrophy through blocking AKT/GSK3beta signaling.* J Mol Med, 2009. **87**(3): p. 249-60.

201. Zeeuwen, P.L., et al., *The cystatin M/E-cathepsin L balance is essential for tissue homeostasis in epidermis, hair follicles, and cornea.* FASEB J, 2010. **24**(10): p. 3744-55.

202. Mueller-Steiner, S., et al., *Antiamyloidogenic and neuroprotective functions of cathepsin B: implications for Alzheimer's disease.* Neuron, 2006. **51**(6): p. 703-14.

203. Cirman, T., et al., *Selective disruption of lysosomes in HeLa cells triggers apoptosis mediated by cleavage of Bid by multiple papain-like lysosomal cathepsins.* J Biol Chem, 2004. **279**(5): p. 3578-87.

204. Jaattela, M., C. Cande, and G. Kroemer, *Lysosomes and mitochondria in the commitment to apoptosis: a potential role for cathepsin D and AIF.* Cell Death Differ, 2004. **11**(2): p. 135-6.

205. Wu, G.S., et al., *Potential role for cathepsin D in p53-dependent tumor suppression and chemosensitivity.* Oncogene, 1998. **16**(17): p. 2177-83.

206. Zuzarte-Luis, V., et al., *Lysosomal cathepsins in embryonic programmed cell death.* Dev Biol, 2007. **301**(1): p. 205-17.

207. Zuzarte-Luis, V., et al., *Cathepsin D gene expression outlines the areas of physiological cell death during embryonic development.* Dev Dyn, 2007. **236**(3): p. 880-5.

208. Hsu, C.C. and S.C. Lai, *Matrix metalloproteinase-2, -9 and -13 are involved in fibronectin degradation of rat lung granulomatous fibrosis caused by Angiostrongylus cantonensis.* Int J Exp Pathol, 2007. **88**(6): p. 437-43.

209. Imai, K., et al., *Degradation of decorin by matrix metalloproteinases: identification of the cleavage sites, kinetic analyses and transforming growth factor-beta1 release.* Biochem J, 1997. **322 (Pt 3)**: p. 809-14.

210. Komori, T., *Regulation of bone development and extracellular matrix protein genes by RUNX2.* Cell Tissue Res, 2010. **339**(1): p. 189-95.

211. Overall, C.M., *Molecular determinants of metalloproteinase substrate specificity: matrix metalloproteinase substrate binding domains, modules, and exosites.* Mol Biotechnol, 2002. **22**(1): p. 51-86.

212. Scott, P.G. and C.H. Pearson, *Cathepsin D: cleavage of soluble collagen and crosslinked peptides.* FEBS Lett, 1978. **88**(1): p. 41-5.

213. Burleigh, M.C., A.J. Barrett, and G.S. Lazarus, *Cathepsin B1. A lysosomal enzyme that degrades native collagen.* Biochem J, 1974. **137**(2): p. 387-98.

214. van Hinsbergh, V.W. and P. Koolwijk, *Endothelial sprouting and angiogenesis: matrix metalloproteinases in the lead.* Cardiovasc Res, 2008. **78**(2): p. 203-12.

215. Whitelock, J.M., et al., *The degradation of human endothelial cell-derived perlecan and release of bound basic fibroblast growth factor by stromelysin, collagenase, plasmin, and heparanases.* J Biol Chem, 1996. **271**(17): p. 10079-86.

216. Cambier, S., et al., *Integrin alpha(v)beta8-mediated activation of transforming growth factor-beta by perivascular astrocytes: an angiogenic control switch.* Am J Pathol, 2005. **166**(6): p. 1883-94.

217. Hyytiainen, M., C. Penttinen, and J. Keski-Oja, *Latent TGF-beta binding proteins: extracellular matrix association and roles in TGF-beta activation.* Crit Rev Clin Lab Sci, 2004. **41**(3): p. 233-64.

218. Yu, Q. and I. Stamenkovic, *Cell surface-localized matrix metalloproteinase-9 proteolytically activates TGF-beta and promotes tumor invasion and angiogenesis.* Genes Dev, 2000. **14**(2): p. 163-76.

219. Romer, J., et al., *Plasminogen and wound healing.* Nat Med, 1996. **2**(7): p. 725.

220. Romer, J., et al., *Impaired wound healing in mice with a disrupted plasminogen gene.* Nat Med, 1996. **2**(3): p. 287-92.

221. Windsor, L.J., et al., *Cell type-specific regulation of SL-1 and SL-2 genes. Induction of the SL-2 gene but not the SL-1 gene by human keratinocytes in response to cytokines and phorbolesters.* J Biol Chem, 1993. **268**(23): p. 17341-7.

222. Kurschat, P., et al., *Identification of activated matrix metalloproteinase-2 (MMP-2) as the main gelatinolytic enzyme in malignant melanoma by in situ zymography.* J Pathol, 2002. **197**(2): p. 179-87.

223. Mauch, S., et al., *Matrix metalloproteinase-19 is expressed in myeloid cells in an adhesion-dependent manner and associates with the cell surface.* J Immunol, 2002. **168**(3): p. 1244-51.

224. Hornebeck, W., et al., *[Proteolysis directed by the extracellular matrix].* J Soc Biol, 2003. **197**(1): p. 25-30.

225. Li, Z., et al., *Regulation of collagenase activities of human cathepsins by glycosaminoglycans.* J Biol Chem, 2004. **279**(7): p. 5470-9.

226. Yasuda, T., *Cartilage destruction by matrix degradation products.* Mod Rheumatol, 2006. **16**(4): p. 197-205.

227. Fernandes, J.C., J. Martel-Pelletier, and J.P. Pelletier, *The role of cytokines in osteoarthritis pathophysiology.* Biorheology, 2002. **39**(1-2): p. 237-46.

228. Burrage, P.S., K.S. Mix, and C.E. Brinckerhoff, *Matrix metalloproteinases: role in arthritis.* Front Biosci, 2006. **11**: p. 529-43.

229. Pujol, J.P., et al., *Interleukin-1 and transforming growth factor-beta 1 as crucial factors in osteoarthritic cartilage metabolism.* Connect Tissue Res, 2008. **49**(3): p. 293-7.

230. Rucavado, A., et al., *Increments in cytokines and matrix metalloproteinases in skeletal muscle after injection of tissue-damaging toxins from the venom of the snake Bothrops asper.* Mediators Inflamm, 2002. **11**(2): p. 121-8.

231. Hou, W.S., et al., *Comparison of cathepsins K and S expression within the rheumatoid and osteoarthritic synovium.* Arthritis Rheum, 2002. **46**(3): p. 663-74.

232. Ishidoh, K. and E. Kominami, *Procathepsin L degrades extracellular matrix proteins in the presence of glycosaminoglycans in vitro.* Biochem Biophys Res Commun, 1995. **217**(2): p. 624-31.

233. Li, Z., et al., *Collagenase activity of cathepsin K depends on complex formation with chondroitin sulfate.* J Biol Chem, 2002. **277**(32): p. 28669-76.

234. Martel-Pelletier, J., J.M. Cloutier, and J.P. Pelletier, *Cathepsin B and cysteine protease inhibitors in human osteoarthritis.* J Orthop Res, 1990. **8**(3): p. 336-44.

235. Selent, J., et al., *Selective inhibition of the collagenase activity of cathepsin K.* J Biol Chem, 2007. **282**(22): p. 16492-501.

236. Konttinen, Y.T., et al., *Acidic cysteine endoproteinase cathepsin K in the degeneration of the superficial articular hyaline cartilage in osteoarthritis.* Arthritis Rheum, 2002. **46**(4): p. 953-60.

237. Son, E.D., et al., *Cathepsin G increases MMP expression in normal human fibroblasts through fibronectin fragmentation, and induces the conversion of proMMP-1 to active MMP-1.* J Dermatol Sci, 2008.

238. Wilson, T.J., K.C. Nannuru, and R.K. Singh, *Cathepsin G-mediated activation of pro-matrix metalloproteinase 9 at the tumor-bone interface promotes transforming growth factor-beta signaling and bone destruction.* Mol Cancer Res, 2009. **7**(8): p. 1224-33.

239. Baici, A., et al., *Cathepsin B in osteoarthritis: uncontrolled proteolysis in the wrong place.* Semin Arthritis Rheum, 2005. **34**(6 Suppl 2): p. 24-8.

240. Ma, X., et al., *Upregulation of elastase proteins results in aortic dilatation in mucopolysaccharidosis I mice.* Mol Genet Metab, 2008. **94**(3): p. 298-304.

241. Metcalf, J.A., et al., *Upregulation of elastase activity in aorta in mucopolysaccharidosis I and VII dogs may be due to increased cytokine expression.* Mol Genet Metab, 2009.

242. Simonaro, C.M., et al., *Joint and bone disease in mucopolysaccharidoses VI and VII: identification of new therapeutic targets and biomarkers using animal models.* Pediatr Res, 2005. **57**(5 Pt 1): p. 701-7.

243. Simonaro, C.M., et al., *Mechanism of glycosaminoglycan-mediated bone and joint disease: implications for the mucopolysaccharidoses and other connective tissue diseases.* Am J Pathol, 2008. **172**(1): p. 112-22.

244. Eliyahu, E., et al., *Anti-TNF-alpha therapy enhances the effects of enzyme replacement therapy in rats with mucopolysaccharidosis type VI.* PLoS One, 2011. **6**(8): p. e22447.

245. Simonaro, C.M., et al., *Involvement of the Toll-like receptor 4 pathway and use of TNF-alpha antagonists for treatment of the mucopolysaccharidoses.* Proc Natl Acad Sci U S A, 2010. **107**(1): p. 222-7.

Figures

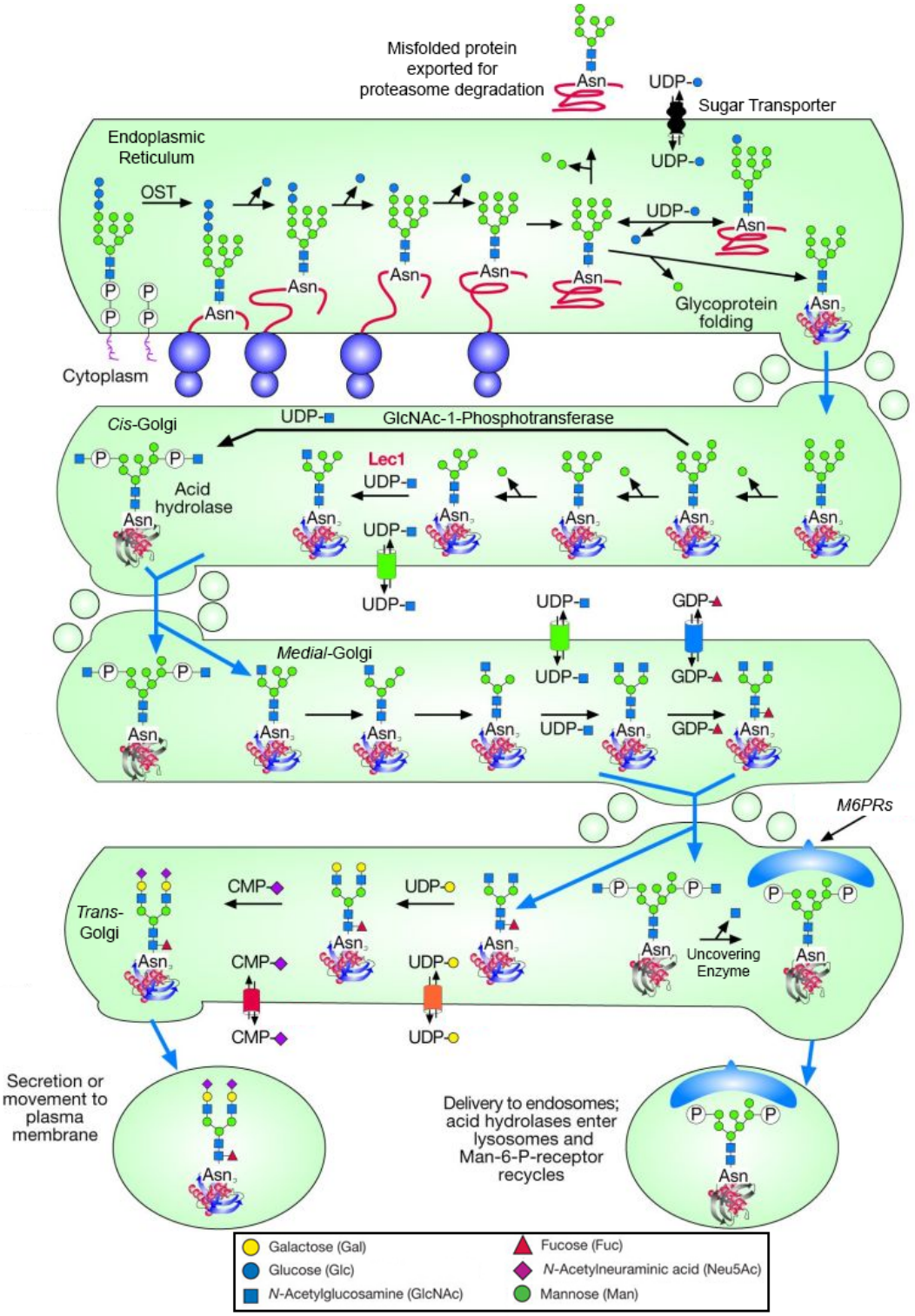
Misfolded protein exported for proteasome degradation
Asn
UDP-
Sugar Transporter
Endoplasmic Reticulum
OST
Glycoprotein folding
Cytoplasm
Cis-Golgi
GlcNAc-1-Phosphotransferase
Lec1
Acid hydrolase
Medial-Golgi
GDP-
M6PRs
Trans-Golgi
CMP-
Uncovering Enzyme
Secretion or movement to plasma membrane
Delivery to endosomes; acid hydrolases enter lysosomes and Man-6-P-receptor recycles
Galactose (Gal)
Glucose (Glc)
N-Acetylglucosamine (GlcNAc)
Fucose (Fuc)
N-Acetylneuraminic acid (Neu5Ac)
Mannose (Man)

FIGURE 1.1. Biosynthesis and Processing of N-Glycans. The biosynthesis of the mature 14 sugar lipid linked oligosaccharide (LLO) begins with the addition of a chitobiose core on a dolichol phosphate intermediate followed by the addition of nine mannose and three glucose residues. The mature LLO is transferred *en bloc* onto nascent polypeptide chains by the membrane-bound enzyme complex oligosaccharyl transferase, or OST. The glycoprotein then undergoes removal of two glucose residues as the protein folds. The remaining glucose plays an important role in folding through binding to ER chaperone lectins. Glycoprotein folding is time-dependent, and if a protein is not able to reach a productive fold it is targeted for ER associated degradation (ERAD). Following proper folding, the third glucose and a single mannose are removed and the glycoproteins are packaged and transported to the *cis*-Golgi. Within the Golgi, glycoproteins may be further processed and enter into the constitutive secretory pathway, or designated for lysosomal targeting by the addition of M6P. GlcNAc-1-Phosphotransferase modifies select oligosaccharides on lysosomal proteins within the *cis*-Golgi with a GlcNAc-1-phosphate and these lysosomal proteins evade further processing by Golgi-mannosidases. Within the *trans*-Golgi, “Uncovering enzyme” removes the N-acetyl glucosamine generating the M6P trafficking signal required for lysosomal sorting. Adapted with permission from publisher. *Essentials of Glycobiology* [3].

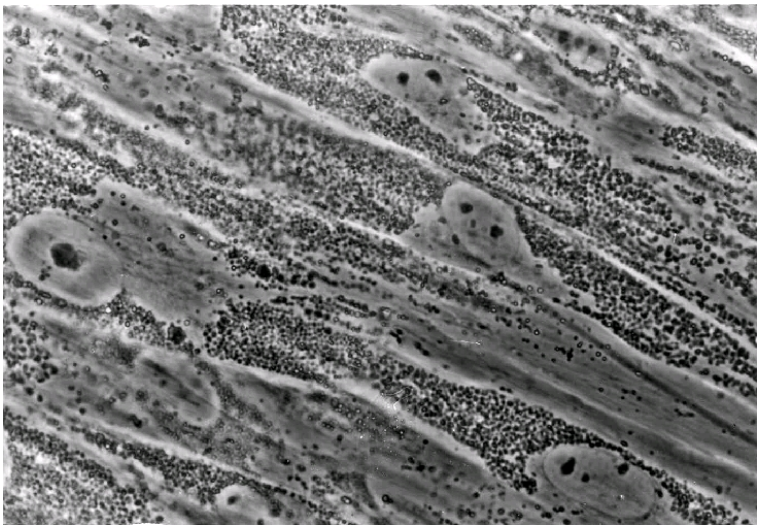

FIGURE 1.2. Cultured skin fibroblasts from a ML-III alpha/beta patient. Light contrast microscopy highlights the namesake “I-cell” phenotype observed in ML-II and ML-III cells. Dense lysosomal inclusions appear to fill the cytoplasm, sparing only a zone near the nucleus containing the ER and Golgi. Reproduced with permission from Publisher. Leroy, J. et al. [35].

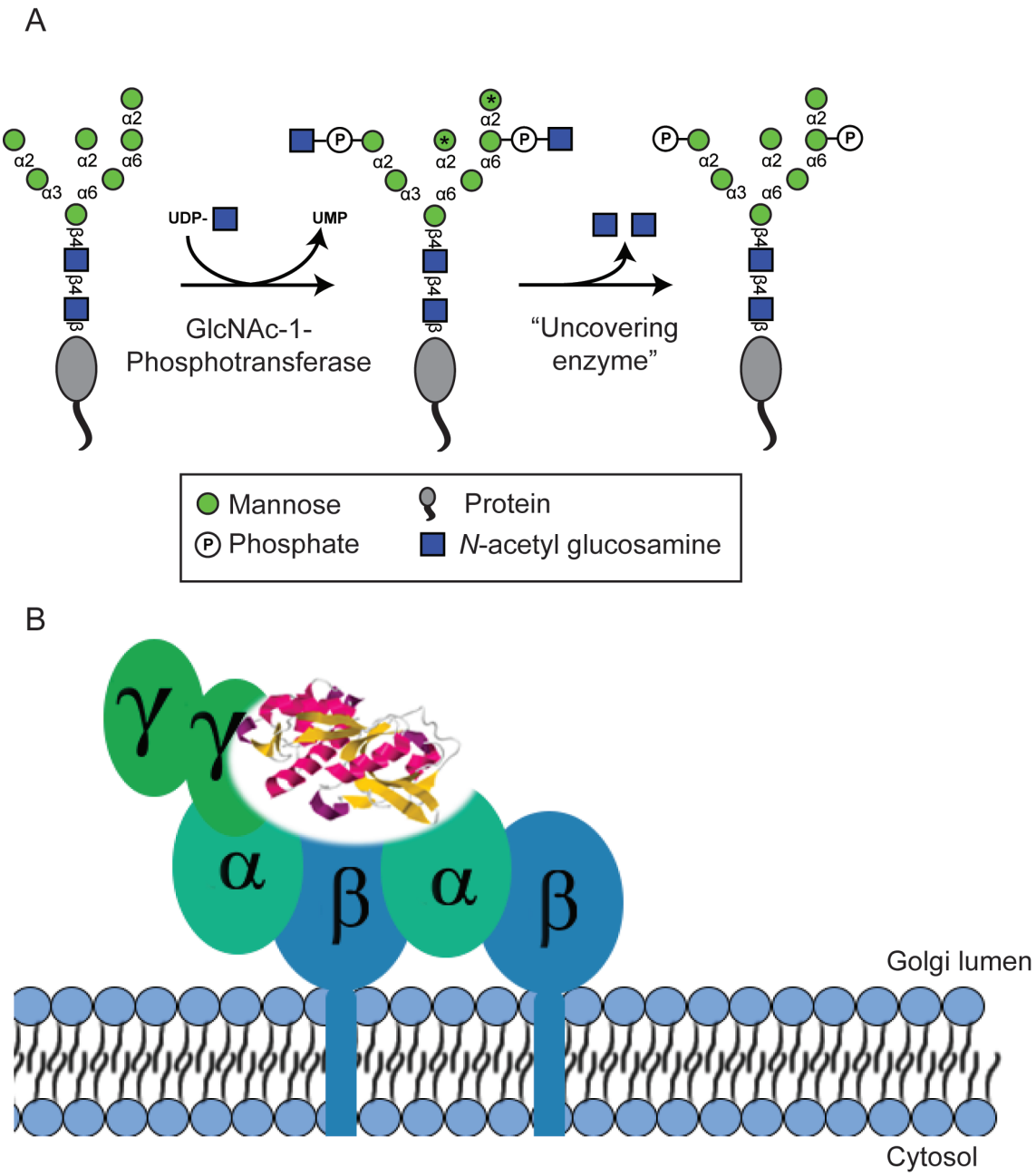

FIGURE 1.3. GlcNAc-1-Phosphotransferase catalyzes the biosynthesis of mannose-6-phosphate. An illustration of M6P biosynthesis. (A) Schematic representation of the two-step enzymatic process generating the M6P trafficking marker. Asterisks represent alternative M6P sites reported on a N-glycan. (B) A representation of GlcNAc-1-phosphotransferase and cathepsin K.

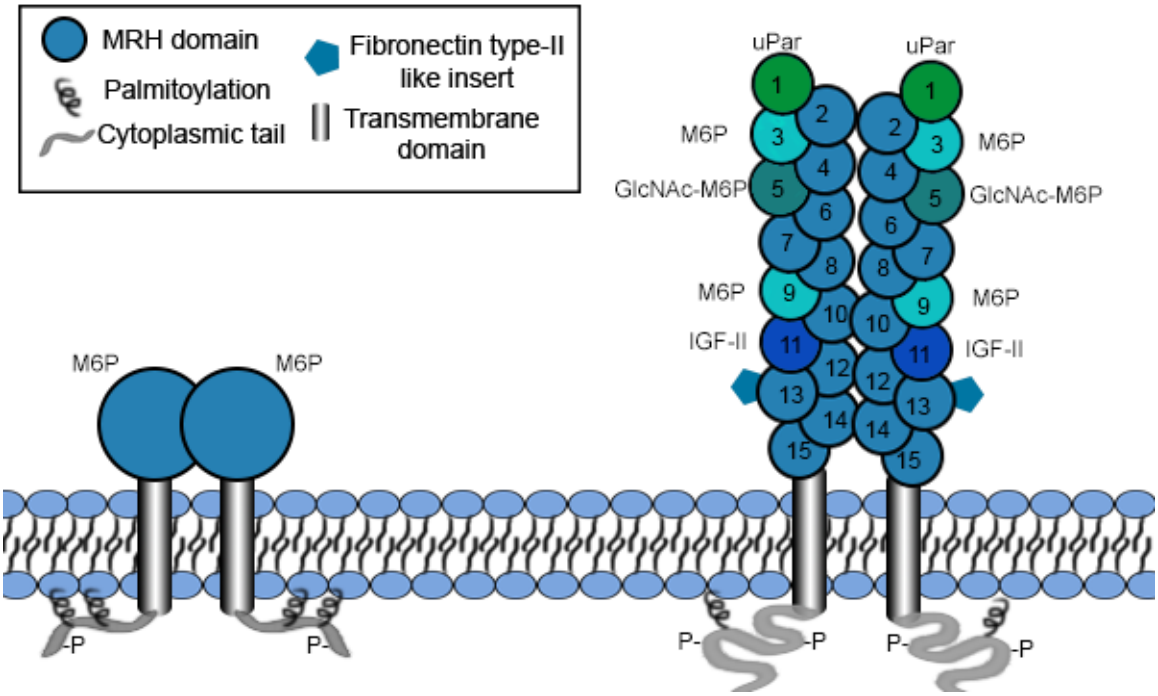

FIGURE 1.4. Domain structure of the two Mannose-6-phosphate receptors. The M6PRs are transmembrane glycoprotein P-type lectins that target M6P-modified lysosomal proteins to the endosomal network. Both M6PRs are type-1 transmembrane glycoproteins with large extracytoplasmic domains and a short c-terminal cytoplasmic tail which is palmitoylated and phosphorylated. The CI-MPR binds M6P in domains 3, 5, and 9, but domain 5 (teal) binds covered phosphodiesters. Domain 1 (green) binds uPar and plasminogen, and IGF-II is capable of binding at domain 11 (dark blue). Domain 13 contains a fibronectin type-II like insertion that may bind collagen.

Table 1.1 Lysosomal Storage Disorders

Disorder	Defective enzyme/protein	Storage Material	Clinical Symptoms
Defects in Glycoprotein Degradation			
α-Mannosidosis (types I and II)	α-mannosidase	glycoproteins	*type I:* infantile onset, progressive mental retardation, hepatomegaly, death between 3 and 12 years *type II:* juvenile/adult onset, milder, slowly progressive
β-Mannosidosis	β-mannosidase	glycoproteins	severe quadriplegia, death by 15 months in most severe cases; mild cases have mental retardation, angiokeratoma, facial dysmorphism
Aspartylglucosaminuria	aspartyl-glucosaminidase		progressive, coarse facies, mental retardation
Sialidosis (mucolipidosis I)	sialidase	glycoproteins & glycolipids	progressive, severe mucopolysaccharidosis-like features, mental retardation
Schindler (types I and II)	α-*N*-acetyl-galactosaminidase	glycoproteins	*type I:* infantile onset, neuroaxonal dystrophy. severe psychomotor and mental retardation, cortical blindness, neurodegeneration *type II:* mild intellectual impairment, angiokeratoma, corpus diffusum
Galactosialidosis	protective protein/cathepsin A	glycoproteins & glycolipids	coarse facies, skeletal dysplasia, early death
Fucosidosis	α-fucosidase	glycoproteins & glycolipids	spectrum of severities includes psychomotor retardation, coarse facies, growth retardation
GM1 gangliosidosis	β-galactosidase	glycoproteins & glycolipids	progressive neurological disease and skeletal dysplasia in severe infantile form
GM2 gangliosidosis	β-hexosaminidase	glycoproteins & glycolipids	severe form: neurodegeneration with death by 4 years less severe form: slower onset of symptoms and variable symptoms, all relating to various parts of the central nervous system
Defects in Glycosaminoglycan Degradation			
Hurler Syndrome (MPS I H)	α-L-iduronidase	DS, HS	*Hurler:* corneal clouding, organomegaly, heart disease, mental retardation, death in childhood *Hurler/Scheie and Scheie:* less severe, individuals survive longer
Hunter Syndrome (MPS II)	iduronate-2-sulfatase	DS, HS	*severe:* organomegaly, no corneal clouding, mental retardation, death before 15 years *less severe:* normal intelligence, short stature, survival age 20–60
Sanfilippo A (MPS III A)	heparan N-sulfatase	HS	profound mental deterioration, hyperactivity, relatively mild somatic manifestations
Sanfilippo B (MPS III B)	α-*N*-acetylglucos aminidase	HS	similar to III A
Sanfilippo C (MPS III C)	acetyl CoA: α-glucosaminide acetyltransferase	HS	similar to III A
Sanfilippo D (MPS III D)	*N*-acetylglucosamine 6-sulfatase	HS	similar to III A
Morquio A (MPS IV A)	galactose-6-sulfatase	KS, CS	distinctive skeletal abnormalities, corneal clouding, odontoid hypoplasia, milder forms known to exist
Morquio B (MPS IV B)	β-galactosidase	KS	same as IV A
Maroteaux-Lamy (MPS VI)	*N*-acetylgalactosamine 4-sulfatase	DS	corneal clouding, normal intelligence, survival to teens in severe form; milder forms known to exist
Sly Syndrome (MPS VII)	β-glucuronidase	DS, HS, CS	wide spectrum of severity, including hydrops fetalis and neonatal form
Multiple Sulfatase Deficiency	sulfatase modifying factor converts cysteine→formyl glycine	all sulfated glycans	hypotonia, retarded psychomotor development, quadriplegia
Defects in Glycolipid Degradation			
Tay–Sachs	β-hexosaminidase A	GM2 ganglioside & glycolipids	*severe:* neurodegeneration, death by 4 years *less severe:* slower onset of symptoms, variable symptoms all relating to parts of the nervous system
Sandhoff	β-hexosaminidase A and B	GM2 ganglioside & glycolipids	same as Tay–Sachs
GM1 gangliosidosis	β-glalactosidase	GM1 ganglioside	progressive neurological disease and skeletal dysplasia in severe infantile form
Sialidosis	Sialidase		progressive, severe mucopolysaccharidosis-like features, mental retardation
Fabry	α-galactosidase	Globotriasylceramide	severe pain, angiokeratoma, corneal opacities, death from renal or cerebrovascular disease
Gaucher's	β-glucoceramidase	Glucosylceramide	*severe:* childhood or infancy onset, hepatosplenomegaly, neurodegeneration *mild:* child/adult onset, no neurodegenerative course
Krabbe	β-galactoceramidase	Galactoceramide	early onset with progression to severe mental and motor deterioration infantile, juvenile, and adult forms can include mental regression, peripheral neuropathy, seizures, dementia
Saposin deficiency	saposin precursor	GM2 ganglioside & glycolipids	similar to Tay–Sachs and Sandhoff

Figure 1.5. Clinical features of children with ML-II and ML-III. (A-C) A 6 year old patient with ML-II with severe bone dysplasia, developmental delay, stiffening of the joints, coarse facial features and gingival hypertrophy. (B) Shallow orbits, thick skin, and a depressed nasal bridge are prominent in profile. (C) Short, broad hands and contractures of knee and ankle joints are common features. (D-G) Clinical manifestations observed in a female ML-II patient at 17 years. The ML-III patient does not have dwarfed stature like that seen in ML-II, however linear growth is affected by severe lumbar and spine abnormalities, as shown in (D), similar to bone dysplasias associated with ML-II. Contractures of hips and knees cause the squatting appearance seen in standing posture. (G) Limited range of motion is observed in the shoulders. Adapted with permission from from publisher. Cathey, SS. et al. [134].

CHAPTER 2: EXCESSIVE ACTIVITY OF CATHEPSIN K IS ASSOCIATED WITH THE CARTILAGE DEFECTS IN A ZEBRAFISH MODEL FOR MUCOLIPIDOSIS II[1]

[1] Petrey, A.C., et al. Disease Models and Mechanisms, 2012. **5**(2): p. 177-90.
Reprinted here with permission of publisher.

Abstract

The severe pediatric disorder, mucolipidosis II (ML-II; I-cell disease), is caused by defects in mannose 6-phosphate (Man-6-P) biosynthesis. Patients with ML-II exhibit multiple developmental defects including skeletal, craniofacial and joint abnormalities. To date, the molecular mechanisms that underlie these clinical manifestations are poorly understood. Taking advantage of a zebrafish model for ML-II, we previously showed that the cartilage morphogenesis defects in this model are associated with altered chondrocyte differentiation and excessive deposition of type II collagen, indicating that aspects of development that rely on proper extracellular matrix homeostasis are sensitive to decreases in Man-6-P biosynthesis. To further investigate the molecular bases for the cartilage phenotypes, we analyzed the transcript abundance of several genes in chondrocyte-enriched cell populations isolated from wild-type WT and ML-II zebrafish embryos. Increased levels of cathepsin and matrix metalloproteinase (MMP) transcripts were noted in ML-II cell populations. This increase in transcript abundance corresponded with elevated and sustained activity of several cathepsins (K, L and S) and MMP-13 during early development. Unlike MMP-13, in which higher levels of enzyme was also detected, sustained activity of cathepsin K appeared to result from abnormal processing and activation of this enzyme at later stages. Inhibition of cathepsin K activity by pharmacological or genetic means not

only reduced the activity of this enzyme but led to a broad reduction in additional protease activity, significant correction of the cartilage morphogenesis phenotype and reduced type II collagen staining in ML-II embryos. Our findings suggest a central role for excessive cathepsin K activity in the developmental aspects of ML-II cartilage pathogenesis and highlight the utility of the zebrafish system to address the biochemical underpinnings of metabolic disease.

Introduction

The autosomal recessive lysosomal disease mucolipidosis II (ML-II; I-cell disease) is caused by defects in the biosynthesis of mannose 6-phosphate (Man-6-P) residues [1]. These residues serve as the key recognition marker for the sorting of lysosomal hydrolases to lysosomes by Man-6-P receptors [2]. ML-II arises from mutations in the single gene encoding the alpha/beta subunits of the GlcNAc-1-phosphotransferase enzyme (*GNPTAB*) [3-7]. The clinical manifestations of this disorder are diverse, encompassing skeletal and craniofacial defects, impaired speech and cognitive function and recurrent lung infections [8]. Indeed, many of the abnormalities associated with ML-II are noted at birth, highlighting the rapidly progressive nature of the disease and its impact on prenatal development [9, 10]. Although a clearer delineation of the genetic bases for this disorder has emerged in recent years, the molecular and cellular mechanisms that drive pathology in ML-II patients and the specific Man-6-P

modified proteins implicated in individual affected tissues remain incompletely understood.

In an effort to address the developmental pathogenesis of this disorder, we previously generated and characterized a novel morpholino-based model for ML-II using the vertebrate organism zebrafish (*Danio rerio*) [11]. *GNPTAB*-depleted embryos exhibited decreased mannose phosphorylation of lysosomal hydrolases, craniofacial and cardiac defects, impaired motility and altered development of pectoral fins and otic vesicles. Focusing on the cellular and molecular basis for the craniofacial cartilage defects in this model, we demonstrated striking changes in the timing and expression of two chondrogenic factors (e.g. the extracellular matrix (ECM) protein, type II collagen, and the transcription factor, Sox9) in craniofacial elements, which were associated with abnormal morphogenetic movements of the chondrocytes in cartilage elements. These findings suggested that loss of Man-6-P biosynthesis impaired the normal chondrocyte differentiation program in the ML-II zebrafish. Since the development of craniofacial cartilage relies heavily on the timed deposition and remodeling of ECM proteins, we hypothesized that disruption in the biosynthesis and/or proper maintenance of the ECM contributes to the disease process in ML-II.

In light of the fact ECM deposition and turnover occurs at stages within developing cartilage that were most strongly affected in ML-II embryos, proteins and enzymes responsible for the biosynthesis, remodeling and clearance of proteins such as collagen are likely to play a key role in the altered craniofacial

development noted in this model. The consequences of impaired expression and activity of several classes of proteolytic enzymes, including ADAMTS proteases, matrix metalloproteinases (MMPs) and cathepsins, on the development and homeostasis of bone and cartilage is evidenced by animal models and human patients with defects in these proteases [12-14]. Moreover, recent work in animal models of mucopolysaccharidoses (MPS) has suggested a role for both cathepsins and MMPs in the pathogenesis of lysosomal disorders [15-17]. Subsequent studies have also identified increases in both the transcript abundance and activity of these proteases, implicating disruption of specific signaling pathways [18, 19]. Since most lysosomal cathepsins are modified by Man-6-P residues and may be hypersecreted when mannose phosphorylation is lost, these proteases are ideal candidates for the initiation and progression of the phenotypes associated with ML-II.

Taking advantage of methodologies that are highly amenable in the zebrafish system, we conducted a targeted investigation of molecules involved in ECM deposition, remodeling and turnover in WT and ML-II embryos. Our results showed that the transcript abundance of several ECM proteins, cathepsins and MMP enzymes were altered in chondrocyte-enriched cell populations isolated from ML-II embryos. Focusing our subsequent analyses on the proteases, we further demonstrated that the activities of cathepsins K, L and S as well as MMP-13 were elevated and sustained during developmental stages and in tissues most affected in ML-II embryos. Suppression of one of these activities, cathepsin K, to near WT levels was not only sufficient to reduce the activity of several other

proteases in the ML-II zebrafish but also partially corrected the craniofacial phenotypes in these embryos. Together, these data suggest a central role for excessive cathepsin K activity in the cartilage pathogenesis of ML-II and further highlight the utility of the zebrafish system to address both the developmental and biochemical underpinnings of metabolic disease.

Results

Cells isolated from Tg(fli1a:EGFP) zebrafish embryos express high levels of transcripts encoding ECM proteins and ECM remodeling enzymes.

Transcript abundance profiling in isolated populations of zebrafish cells has emerged as an effective way to identify changes in gene expression that are associated with the development of specific cell types and tissues. This methodology has proven useful in both normal embryos as well as disease models [20, 21]. In an effort to further explore the molecular basis of the cartilage phenotypes in the ML-II model, GFP-positive and -negative cells were isolated by FACS from dissociated WT and ML-II *Tg*(*fli1a*:EGFP) embryos, and quantitative real time PCR (qRT-PCR) analysis was performed on a targeted set of transcripts. *Tg*(*fli1a*:EGFP) embryos express EGFP in endothelial cells, certain hematopoetic cells, and pharyngeal arch neural crest-derived cells, which yield the chondrocytes of craniofacial cartilage [20]. Due to the expansion of craniofacial structures in embryos 2 and 3 days post fertilization (dpf), isolated GFP-positive cells from dissociated embryos are highly enriched for

chondrocytes and their precursors. The genes targeted for qRT-PCR analyses included several collagens and other ECM proteins, enzymes involved in collagen biosynthesis and multiple classes of proteases capable of modifying and/or degrading the ECM (Table I). The choice of targets was primarily guided by our earlier assessment of the craniofacial phenotypes in the ML-II embryos, which indicated that stages of cartilage development that rely heavily on the deposition and/or remodeling of ECM proteins (such as collagens) were particularly sensitive to reduced Man-6-P biosynthesis [11]. GFP-positive and –negative cells were effectively separated from dissociated embryos, with GFP-positive cells representing ~8% and ~20% of the total cells isolated from 2 and 3 dpf embryos, respectively (Figure 2.1A). Diagnostic FACS analysis of the sorted GFP+ and GFP- cell populations revealed they were 99.2% and 99.9% pure, respectively. Consistent with the enrichment of chondrocytes within the GFP-positive cell population and the requirement for active synthesis and turnover of the ECM during chondrocyte development, the relative level of several transcripts, including collagens I, II and X and the matrix metalloproteinases, in WT embryos were found to be higher in the GFP-positive cells when compared to GFP-negative cells (Figure 2.1B).

Transcript abundance of several proteases and ECM proteins was increased in chondrocyte enriched cell populations isolated from ML-II zebrafish.

Comparison of WT and ML-II GFP positive cells at 2 and 3 dpf revealed differences in the transcript abundance of several target genes (Figure 2.2). Overall transcript levels of several genes were shown to increase in WT embryos between 2 and 3 dpf, suggesting that dynamic changes in gene expression occur during this developmental period (suppl. Figure 1). Significant increases were detected in the transcripts of several cathepsins and MMPs (but not ADAMTS proteases) in ML-II embryos at these stages, with cathepsin L being the most striking elevation measured. Notable changes in the ECM targets analyzed included a profound decrease in aggrecan expression in ML-II GFP-positive cells, likely reflecting the abnormal differentiation of chondrocytes in the ML-II embryos [22]. Consistent with our previous analyses, which demonstrated the sustained expression of type II collagen in ML-II craniofacial cartilages, higher levels of *col2a1* transcripts were also observed in ML-II embryos at 3 and 5 dpf (Figure 2.2, suppl. Figure 1). Importantly, no significant changes were seen in the apparent expression of genes related to ER stress (*bip and hsp70*, data not shown) and inflammation (*tlr4;* Figure 2.2), and the transcript abundance of several growth factors (*tgfß*; data not shown) was comparable in WT and ML-II sorted cell populations. Most of the transcripts analyzed were elevated in ML-II embryos (GFP-positive and negative) at 5 dpf. This increase may relate to the compromised health and impaired yolk utilization of the ML-II embryos by this

later stage. It is unlikely, however, that global effects on health would account for the increased transcript abundance in ML-II embryos at 2 and 3 dpf, since the embryos are viable, and with the exception of specific phenotypes, do not display the same signs of deteriorating health noted in 5 dpf embryos.

Although differences in the transcript abundance of several genes were evident in multiple individual samples, a collective analysis of four independent biological replicates indicated that only a subset of these transcript changes were statistically significant. The disparity in transcript abundance between data sets likely reflects biological variability, since technical replicate analysis from the same biological sample was highly reproducible. Thus, the high degree of variability between the biological replicates may mask additional important differences for some of the transcripts analyzed, but those transcripts indicated with *p*-values in Figure 2.2 were consistently and significantly altered in abundance in the biological replicates.

Cathepsin activity was greatly increased and sustained during early development of ML-II zebrafish embryos.

To determine whether the increased abundance of cathepsin transcripts was associated with a corresponding increase in enzymatic activity, *in vitro* enzyme assays were performed on WT and ML-II zebrafish lysates. For all enzymes tested, the normalized activity values shown represent only the activity that could be specifically blocked with the respective inhibitors. As shown in Figure 2.3A, statistically significant differences in the activity of several cathepsins were

detected between WT and ML-II embryos across a developmental timeline spanning 1 to 4 dpf. With the exception of the aspartyl protease cathepsin D, the activity of all cathepsins tested was relatively low in WT embryos at 1 dpf. By 2 dpf, an increase in the activity of cathepsin K, but not S and L, was detected in WT embryos. The disappearance of cathepsin K activity by 3 dpf suggested that this protease is subject to tight regulation in normally developing embryos. Unlike WT, the activities of cathepsins K, L, and S all increased substantially at 2 dpf in ML-II embryos. Although these activities also decreased at 3 and 4 dpf, the levels in ML-II embryos remained significantly higher than that detected in WT embryos. The activity of cathepsin D was also moderately elevated in ML-II embryos at all four stages but did not exhibit the same sustained activity profile as the other cathepsins tested. To gauge the specificity of these effects, we also tested cathepsin activity in ML-II embryos that had been rescued by over-expression of WT GlcNAc-1-phosphotransferase mRNA (Figure 2.3B). Rescued embryos exhibited cathepsin activity levels that were similar to WT embryos, indicating that the increased activity of these enzymes was specifically due to loss of GlcNAc-1-phosphotransferase activity. Moreover, over-expression of GlcNAc-1-phosphotransferase mRNA in WT embryos did not result in any significant change in cathepsin activity.

As an additional gauge of the specificity of increased cathepsin activity, several glycosidase enzyme activities were measured in 3 dpf WT and ML-II whole embryos. These analyses were important to assess whether the increased cathepsin activity was indicative of a general stimulation in lysosomal

enzymes. We did not, however, detect any substantial changes in the activity of these glycosidases in the ML-II embryos (suppl. Figure 2). These data suggest that the increases in cathepsin protease activity likely occur independent of a global increase in the expression and/or activity of other lysosomal proteins.

Cathepsin K is temporally and spatially expressed in developing cartilage during zebrafish embryogenesis.

In an effort to determine whether any of the assayed cathepsins were candidate contributors toward the cartilage defects in ML-II embryos, we assessed whether their individual activities were globally or regionally increased. WT and ML-II embryos were separated into head and tail sections (diagrammed in Figure 2.4A) and each of these pools assayed for protease activity. The results of this analysis, shown in Figure 2.4B and C, clearly demonstrated that the vast majority of elevated cathepsin activity was present in the heads of ML-II embryos, suggesting that these enzymes may be upregulated in cell types that are enriched within this region (i.e. precursors of cartilage and bone). Interestingly, MMP activity was increased in both the head and tail extracts of ML-II embryos, indicating that elevated MMP activity may contribute to disease onset or progression in other affected tissues.

In light of its known role in the maintenance of bone and cartilage homeostasis and its sustained activity during stages of cartilage development, further investigation of cathepsin K's role in the ML-II cartilage morphogenesis defects was warranted. To specifically localize the expression of cathepsin K

within the head, *in situ* hybridization and immunohistochemical experiments were performed (Figure 2.4). Consistent with a role for the enzyme in the development and maturation of cartilage, cathepsin K transcript was detected primarily in the head at 2 and 3 dpf with strong staining present in regions of craniofacial development (Figure 2.4 D-G). At 2 dpf, cathepsin K transcript was particularly prominent in the ventral portion of tissues posterior to the eye. By 3 dpf, cathepsin K transcript was visible throughout regions that generally correspond to Meckel's (M) cartilage and the ceratobranchials (CB). Although the overall staining pattern was similar between WT and ML-II embryos at both 2 and 3 dpf, cathepsin K staining was notably absent from the pectoral fins (Figure 2.4D and E, black arrows) of ML-II embryos. This is likely due to the fact that, although the fin itself can form, it lacks *fli1*:EGFP-positive chondrocytes in morphant embryos. Interestingly, *in situ* analyses also demonstrated a consistent increase in cathepsin K transcript within the developing heart of ML-II embryos at 3 dpf (Figure 2.4F and G, black arrows). Immunohistochemical analyses performed on sections of WT *fli1*:EGFP embryos at 3 and 4 dpf confirmed that cathepsin K protein is expressed in the developing chondrocytes and, to a lesser extent, the perichondrial fibroblasts that surround them. This was true for multiple structures, including the Meckel's and trabecular cartilages (Figure 2.4 H-J). Within chondrocytes, cathepsin K expression was most evident in discrete cellular puncta, possibly corresponding to lysosomes. Its expression was also detected in the cellular sheath surrounding elements of the notochord (data not shown). Collectively these data suggest a role for cathepsin K during

cartilage development and support the idea that increases in its activity may underlie the craniofacial defects noted in ML-II.

Increased processing of cathepsin K underlies its sustained activity in ML-II embryos.

The increased activity of the cathepsins could arise from several different mechanisms, including increased expression of the protein, decreased expression of endogenous protein inhibitors or enhanced conversion of inactive proenzymes into their mature active forms. To further explore the biochemical basis for the sustained increase in cathepsin K activity in ML-II embryos, cathepsin K protein was analyzed by Western blot in embryos 3 dpf (Figure 2.5A). Although the 42-kDa procathepsin K band was present in both lysates at this stage, there were clear differences in the extent of proteolytic processing to lower molecular weight intermediates and the 32-kDa mature form of the enzyme. In particular, the mature form of cathepsin K was highly enriched in ML-II compared to WT samples. The increased abundance of the mature form corresponds with the detection of excessive cathepsin K activity in ML-II embryos. In order to further establish this relationship between proteolytic conversion of procathepsin K and enzymatic activity, additional experiments were performed in which both recombinant human procathepsin K (suppl. Figure 3), and 3 dpf WT and ML-II zebrafish lysates were acid treated prior to activity and Western blot analysis. These results demonstrated that acid treatment completely shifts recombinant procathepsin K to the mature form, which

corresponds with an increase in cathepsin K activity (suppl. Figure 3). While acid treatment of WT embryos also resulted in a 10-fold increase in cathepsin K activity, this level was still much lower than the robust activity noted in the ML-II embryos. Moreover, acid treatment only slightly increased cathepsin K activity in ML-II lysates. Although treatment of WT lysates with acid did convert the 42-kDa procathepsin K band to lower molecular weight intermediates, it did not generate the mature 32-kDa form. Since the mature form was below the limit of detection, it is possible that the measured activity in acid-treated WT lysates resulted from weak catalytic activity of the intermediate forms. Highly similar results were obtained when heads from 3 dpf WT and ML-II embryos were subjected to the same analysis (Figure 2.5B). From these data, we concluded that while acid treatment leads to procathepsin K activation, it appears that other mechanisms may be involved in the processing of intermediate forms of the enzyme to the 32-kDa mature band.

Having defined the molecular forms of cathepsin K, the electrophoretic mobility of this protease was then analyzed in WT and ML-II embryo lysates 2, 3 and 4 dpf (Figure 2.5C). As shown, the extent of processing of cathepsin K was generally increased in ML-II embryos at these stages, with the 32-kDa active form uniquely present in ML-II lysates at both 3 and 4 dpf. Although activity was highest in all samples at 2 dpf, low levels of protein were detected, possibly due to the instability of the mature form of the protein relative to the intermediate and pro- forms. Collectively, these observations are highly consistent with the increased activity of this protease during development (Figure 2.3) and indicate

that abnormal processing of cathepsin K underlies its sustained activity in ML-II embryos.

Inhibition of cathepsin K effectively reduces the activity of other cathepsins.

The above experiments establish that cathepsin activity was increased in ML-II embryos and that this increase correlated temporally and spatially with the craniofacial defects noted in these embryos. In order to begin defining the role of cathepsin K in the onset and progression of these phenotypes, its activity and expression were independently suppressed in ML-II embryos using either a cathepsin K-specific enzyme inhibitor or one of two cathepsin K-targeting morpholinos. The morpholinos used included a splice blocker (SB), which inhibited processing of the cathepsin K mRNA, and a translation blocker (TB) that spanned the start codon. Both approaches were first titrated to determine an effective dose of the inhibitor or morpholino that would reduce cathepsin K activity to levels comparable to WT (see Material and Methods and suppl. Figure 4 for details of this titration). It was important to avoid doses that would eliminate the activity or expression of cathepsin K, as this could result in additional phenotypes not relevant to ML-II.

The effects of the inhibitor treatment were dose-dependent and varied with the timing of inhibitor administration. For example, addition of 5μM cathepsin K inhibitor to WT and ML-II embryos at 1 dpf resulted in developmental abnormalities. While cathepsin K activity may be required at these early time

points for normal development, control experiments demonstrated that the observed toxicity was primarily due to the presence of DMSO (data not shown). In contrast, this same concentration of inhibitor applied at 2 dpf effectively reduced the cathepsin K activity in ML-II embryos to WT levels without an observed increase in developmental defects. Surprisingly, addition of inhibitor was not only found to effectively reduce cathepsin K activity, but also the activities of the other cathepsins and general MMP activity (Figure 2.6A). *In vitro* analyses of the cathepsin K inhibitor demonstrated that at the low doses used it specifically affects cathepsin K activity, with no significant effect on the other proteases (suppl. Figure 4). This suggests that the corresponding reductions noted in the activity of the additional proteases following *in vivo* administration of the inhibitor may stem from loss of cathespin K activity itself. As with pharmacological manipulation, inhibition of cathepsin K by morpholino knockdown in the ML-II embryos also resulted in a reduction in cathepsin K activity albeit not to WT levels (see suppl. Figure 4). This was true for both of the cathepsin K-specific MOs tested. Similarly, when the other protease activities were measured in the cathepsin K/ML-II double morphants at 3 dpf, reductions comparable to those noted in the inhibitor-treated embryos were seen (Figure 2.6B).

Cathepsin K inhibition rescues multiple aspects of the craniofacial phenotypes in ML-II zebrafish.

We next tested whether the reduction in cathepsin K activity and the corresponding decrease in the activities of the other proteases would improve the craniofacial phenotypes in ML-II morphant embryos. For these experiments, ML-II embryos were either treated at 2 dpf with the cathepsin K inhibitor for a period of 2 d or sequentially injected at the one cell stage with morpholinos to inhibit both GlcNAc-1-phosphotransferase and cathepsin K expression. To ensure specificity with morpholino-based inhibition of cathepsin K, similar analyses were independently performed using both the splice blocking and translation blocking cathepsin K morpholinos (phenotypic data for SB MO is shown). All of the treated embryos were initially analyzed at 4 dpf by Alcian blue staining (Figure 2.7A and B, respectively). Importantly, several aspects of the craniofacial phenotypes that typify ML-II embryos were significantly corrected following reduction of cathepsin K activity or expression. The degree of phenotypic correction was quantified by multiple parameters, which are diagramed schematically in Figure 2.7C and the results detailed in Figure 2.7D and E. Parameters scored included: 1) whether Meckel's (M) cartilage reached the palate (P), 2) the shape of the anterior jaw, as represented by the ratio of the long and short axes (see figure legend), 3) the angle between the two ceratohyal (CH) cartilages, and 4) whether the pectoral fins contained Alcian blue positive cartilage. Suppression of cathepsin K activity following addition of either 2.5μM or 5μM inhibitor resulted in significant amelioration of all of these phenotypes in

13.9% and 22.2% of the animals treated, respectively. Interestingly, following pharmacological inhibition, the craniofacial structures of ML-II animals were either completely rescued (indistinguishable from WT) or appeared unaffected by the treatment, perhaps suggesting variable penetration of the inhibitor. In contrast, MO-inhibition of cathepsin K expression yielded a broader range of corrected phenotypes. In the case of the SB MO, we found that 15.9% of the embryos tested exhibited full rescue of craniofacial phenotypes, while 69.2% exhibited partial rescue, most often due to incomplete recovery of either the angle between the CH cartilages or the presence of pectoral fin cartilage. Together, these results suggested that cathepsin K plays a central role in the onset of the craniofacial phenotypes in the ML-II embryos.

Inhibition of cathepsin K leads to recovery of ML-II cellular morphology and reductions in type II collagen expression.

Previous work on the zebrafish ML-II model revealed significant disruptions in the distribution of cells within multiple structures, including the trabecular and Meckel's cartilages. In particular, ML-II cells were drastically underintercalated compared to the WT cells [11]. In addition, ML-II chondrocytes expressed significantly higher levels of type II collagen. This was most evident at later time points (4-6 dpf). To further assess whether cathepsin K inhibition also improved these aspects of the ML-II craniofacial phenotypes, ML-II morphants and ML-II/cathepsin K double morphants were generated in the *fli1*:EGFP transgenic background. A subset of the WT and ML-II *fli1*:EGFP embryos was

also treated with the cathepsin K pharmacological inhibitor. Embryos were collected 4 dpf and stained immunohistochemically for the presence of type II collagen (Figure 2.8). In most cases, striking decreases in the expression of type II collagen were noted in cathepsin K-inhibited ML-II embryos. Less reduction in collagen staining was, however, noted in the inhibitor-treated embryos. This may reflect either the overall permeability of the inhibitor or the need for additional dosing to obtain a maximal effect. Although MO treatment was slightly more effective, inhibition of cathepsin K expression by either method (MO or inhibitor) also resulted in significant recovery of the morphology and distribution of chondrocytes within the ML-II cartilages. For example, while 85±5% of the WT trabecular chondrocytes were fully intercalated, only 6±4%% of the cells comprising the morphant cartilages had completed this process. MO-inhibition of cathepsin K in ML-II embryos significantly improved this phenotype with 60±9% intercalation noted. The improved cellular distribution was also associated with changes in cell shape. Unlike morphant cells, which often lacked the elongated shape of mature chondrocytes, ML-II/cathespin K double morphant chondrocytes reverted to a flat, narrow cell (Figure 2.8A and B). Similar improvements were noted when *fli1*:EGFP WT and ML-II embryos were treated with 5μM cathepsin K inhibitor. Here again the degree of recovery somewhat less than with MO inhibition, but the chondrocytes of drug-treated morphants showed increased intercalation compared to DMSO-treated morphant embryos (0% and 48±10%, respectively; Figure 2.8C and D). These data suggest an intimate link between increased cathepsin K activity and the persistent expression of type II collagen.

Discussion

The mechanisms that underlie the molecular and cellular pathogenesis of lysosomal storage disorders are beginning to emerge, in part due to the investigation of animal models for these diseases [17, 19, 23-28]. The use of zebrafish as a model system to study these disorders is particularly attractive since the initial pathogenic mechanisms that arise during development can be studied, taking advantage of the genetic and experimental accessibility of this system. The previous generation and characterization of a zebrafish model for ML-II revealed multiple phenotypes within tissues, such as craniofacial cartilage, that are also affected in human ML-II patients [11]. To further explore the molecular basis for these phenotypes, a targeted set of gene expression changes were analyzed in chondrocyte-enriched cell populations isolated from WT and ML-II embryos. These analyses revealed increases in the transcript abundance and activity of several proteases involved in ECM turnover and remodeling, including the cathepsins and MMPs. The subsequent analyses of these enzymes uncovered a key role for excessive cathepsin K activity in the cartilage lesions noted in ML-II embryos. Surprisingly, inhibition of cathepsin K activity not only resulted in phenotypic correction of the cartilage defects but also lead to a general suppression of multiple protease activities in ML-II embryos.

The ability to isolate and biochemically analyze specific cell populations using transgenically-labeled zebrafish embryos, such as the *fli1a*:EGFP line, is a promising means to address the mechanisms that account for tissue-specific

pathology in disease models with this organism. In light of the increasing number of transgenic lines that have been generated in recent years, the investigation of most major organ systems and tissues within these models is possible. The expression of *fli1* in zebrafish is detected in endothelial cells and angioblasts as well as a subset of neural crest cells, including precursors of craniofacial chondrocytes [20]. Because not all labeled cells are chondrocytes, we believe that some of the changes in transcript abundance detected in GFP+ cells may be relevant to pathogenesis outside craniofacial cartilage. It is worth noting the significant transcript abundance increases in the GFP- cell populations, in particular with regard to cathepsin L and the MMPs in 2 dpf and 3 dpf embryos, respectively. Since these enzymes are known to play roles in ECM remodeling in many tissues including the brain and heart [29-31], it will be of interest to determine whether their inappropriate expression and activity mediates additional aspects of ML-II pathogenesis. Parallel experiments on ML-II embryos generated in transgenic lines that label different cell populations are ongoing and should further address such tissue-specific mechanisms.

The basis for the increased transcript abundance of the cathepsins and MMPs in the cell populations isolated from ML-II *fli1a*:EGFP embryos is unclear. These data might reflect inappropriate stimulation of gene-specific transcription. Transcriptional stimulation could arise in response to accumulation of lysosomal storage and the need for increased lysosomal biogenesis, a response that has recently been shown to be coordinated by the transcription factor TFEB [32, 33]. The increase observed in the cathepsins would be consistent with a TFEB-

dependent mechanism. However, no stimulation in other lysosomal components was noted including the activity of several glycosidases (suppl. Figure 2). Furthermore, no obvious signs of either intralysosomal storage or lysosomal proliferation in the ML-II zebrafish embryos were detected [11]. Due to the fact that transcriptional upregulation of specific cathepsins has been observed in the context of cancer cells as well as tissues of animal models of MPS disorders [15, 29], it is plausible that the changes in cathepsin expression are independent of a global increase in lysosomal biogenesis. However, this was not the case with cathepsin K - where post-translational modes of regulation (i.e. proteolytic activation) likely represent the primary mechanism leading to increased activity within the ML-II embryo.

The results demonstrated that substantial cathepsin K activity was required in WT embryos at 2 dpf and this enzyme was subject to tight regulation via its proteolytic activation. Since cathepsin K is a very potent collagenase with the ability to cleave triple-helical collagens at multiple sites [34-36], it is likely that this activity is needed during discrete developmental time points to assist in the degradation and turnover of collagens, which are continually replaced and remodeled during embryonic development [37]. Our results indicate that multiple cell types including craniofacial chondrocytes express and/or secrete cathepsin K in early zebrafish embryos. *In situ* analysis of cathepsin K expression (Figure 2.4) at 2 and 3 dpf revealed an abundance of transcripts throughout the craniofacial region, and the immunostaining experiments confirm its expression in chondrocytes. The complete range of cathepsin K-expressing cells in the

developing embryo is not currently known, but osteoclasts, the major cathepsin K-expressing cells in postnatal mammals, are not a plausible source since these cells do not appear to arise at these early stages [38].

The data suggests that the increased activity of cathepsin K in the ML-II embryos at later stages (3 and 4 dpf) arises due to sustained processing of cathepsin K, a mechanism that is supported by the unique presence of mature cathepsin K on Western blots of whole embryo lysates (Figure 2.5). The mechanism underlying this apparent sustained activation in the morphants is not known, but since this enzyme typically undergoes autocatalytic activation at low pH, this phenomenon may indicate abnormal acidification of cathepsin K-containing vesicles [39-41]. Importantly, however, we found that acid treatment was most effective in reducing the procathepsin K to its intermediate forms but not to the mature 32-kDa form. We believe the increased activity of cathepsin K in the ML-II background more likely reflects additional processing to its highly active mature form. This additional processing may result from decreased mannose phosphorylation of cathepsin K, its subsequent hypersecretion and contact with cell surface proteases within the extracellular space. Unlike cathepsin D, cathepsin K was recently shown to be hypersecreted from osteoclasts isolated from *GNPTAB(-/-)* mice, indicating enzyme-specific sorting of acid hydrolases in mice [42]. Exploring whether cathepsin-specific missorting is evident in zebrafish, how enzyme hypersecretion and activation are related and what mechanisms control this process are all necessary areas for future investigation.

An intriguing finding in this work is the observation that reduction of cathepsin K activity results in decreased activity of other proteases such as cathepsin L, a phenomenon that we confirmed is not the result of non-specific drug inhibition (suppl. Figure 4). Since cathepsins are known to activate other cathepsins as well as MMPs [43], it is possible that the reduction observed was due to a block in the proteolytic activation of proteases by cathepsin K. Due to the extended timeframe of the rescue experiments, however, it is also plausible that inhibition of cathepsin K activity reversed a broader pathogenic cascade. Nonetheless, cathepsin K inhibition, by two separate methods, resulted in significant phenotypic correction of the craniofacial phenotypes as assessed by both Alcian blue staining and type II collagen expression. These results are encouraging from a clinical standpoint since they support cathepsin K as a potential therapeutic target for alleviation of the developmental defects associated with ML-II. We are actively investigating whether cathepsin K inhibition also leads to correction of other phenotypes and whether inhibition of the other elevated cathepsins will impact ML-II pathogenesis.

Taken together, our results demonstrate that cathepsin K plays a critical role in the development of the cartilage phenotypes in ML-II zebrafish and provide the basis for investigating the role of cathepsins in non-craniofacial defects. They also highlight the importance of this class of enzymes during normal craniofacial development, as evidenced by the tight control of cathepsin K activation within the developing embryo. To our knowledge this work provides the first demonstration of a role for cathepsin K during development of embryonic

cartilages. Further studies are needed to better define the physiological function of cathepsin activity at these stages and how these activities are intertwined in the maturation program of chondrocytes and other cell types.

Materials and Methods

Fish strains

Wild-type zebrafish were obtained from Fish 2U (Gibsonton, FL) and maintained using standard protocols. Embryos were staged according to the criteria established by Kimmel [44]. In some cases, 0.003% 1-phenyl-2-thiourea was added to the growth medium to block pigmentation. All MO-generated phenotypes were tested in several genetic backgrounds, including a wild-type strain from a commercial source (Fish 2U). Analyses of craniofacial phenotypes were performed in both the F2U wild-type strain and Tg (*fli1a*:EGFP)^{y1} transgenic line [45]. Handling and euthanasia of fish for all experiments were carried out in compliance with University of Georgia's policies. This protocol has been approved by the University of Georgia Institutional Animal Care and Use Committee (permit number: A2009 8-144).

Anti-sense morpholino injection and mRNA rescue

Expression of N-acetylglucosamine-1-phosphotransferase (alpha/beta subunit, *GNPTAB*) was inhibited by injection of morpholino oligonucleotides (MO) as previously described [11]. Experiments involving mRNA rescue in the morphant background were performed following injection of full-length phosphotransferase

mRNA as previously described [11]. The expression of cathepsin K (*ctsk*) was inhibited using either 0.2 nL of a 500uM (0.1 μM) solution of a splice blocking MO (TGTAACAATACTTACCATGTCACCA) directed against the exon 1 – intron 1 junction or 0.2 nL of a 500uM (0.1μM) solution of a translation blocking MO (GAGGGAATCCGCCAAATCTACCCAT) directed at the *ctsk* ATG. The specificity of the *ctsk* MOs and the concentrations necessary to reduced Ctsk activity (in ML-II embryos) to WT levels was determined by introducing a range of MO (0.01-0.5 μM) concentrations into both the WT and ML-II morphant backgrounds. For experiments involving inhibition of *ctsk* in the ML-II background, the MOs were injected sequentially at the one cell stage. The degree of *ctsk* inhibition for various MO concentrations was then determined by RT-PCR analysis of the *ctsk* mRNA (in the case of the splice blocker) and/or activity assays (used in both cases as described below) (see supplemental Figure 4). In light of the fact that neither the splice blocking nor the translation blocking MOs resulted in embryonic phenotypes when injected alone into WT embryos, we did not assess off target effects by mRNA recovery. It is important to note that for both cases, the goal was reduction not elimination of *ctsk* expression.

Embryo dissociation and cell sorting

Wild-type and morphant *fli1*:EGFP embryos were collected at the indicated stages in Ca^{2+}-free Ringers solution. Embryonic yolks were removed by gentle passage through a flame polished Pasteur pipette. Embryos were subsequently

rinsed for 15 minutes in Ca^{2+}-free Ringer's solution. Dissociated-cellular suspensions were generated by soaking the embryos in 0.25% trypsin, followed by repeated passage through 23- and 25-gauge syringes. Cellular dissociation was monitored microscopically. When cellular aggregates were no longer visible, the suspensions were filtered through sterile 40-μm Falcon filters to remove debris. Cells were collected following centrifugation and suspended in L-15 growth medium (minus phenol red) containing 1% FBS. GFP-positive and GFP-negative cells were subsequently isolated by Fluorescence Activated Cell Scanning (FACS) and collected in L-15 medium containing 10% FBS and 10% fish embryonic extract (generated as previously described). GFP-positive and – negative cells were harvested by centrifugation and re-suspended in RLT buffer, flash frozen, and stored at -80°C until RNA could be prepared (via RNeasy Plus kit, Qiagen).

Quantitative real-time PCR analysis of transcript abundance

Total RNA was isolated from sorted cell populations using the RNeasy Plus kit (Qiagen). Samples were quantitated with a NanoDrop spectophotometer (Thermo) and stored at -80°C. First strand cDNA synthesis was performed using the SuperScript VILO cDNA synthesis kit with 125 ng of total RNA. A 10-fold dilution of the cDNA synthesis reaction was used as the template source for qRT-PCR reactions. RNA samples were checked for genomic DNA (gDNA) contamination using a control cDNA synthesis reaction without reverse transcriptase.

Sequences for *D. rerio* genes used in this study were obtained from ZFIN and NCBI databases. Primer pairs used for quantitative real time PCR (qRT-PCR) were designed within a single exon sequence of an individual gene as described previously for mouse genes [46]. Primer pairs were validated for specificity (amplification of a single product) and efficiency using *D. rerio* gDNA as a template.

Quantitative RT-PCR reactions for individual genes were run in technical triplicate on four independent cell populations. Reactions consisted of 2.5 ul SYBR Green Supermix (Bio-Rad), 1.25 ml diluted cDNA synthesis reaction and 1.25 ul of gene specific-primer pair (125 nM final concentration). Amplification conditions and data analysis were performed as described previously (Nairn et al Methods in Enzymology). Several housekeeping genes were evaluated as normalization controls and ribosomal protein L4 (*rpl4*) was determined to be the most uniformly expressed gene.

The relative transcript abundance of each gene (normalized to *rpl4*) was determined for each of the four biological samples at each growth stage. These values were then evaluated for statistically significant changes in abundance when comparing wild type and morphant samples. A non-parametric Mann-Whitney test was used to determine statistically significant differences between samples with the InStat 3 software package (GraphPad Software, Inc.).

Whole-mount in situ hybridization

Whole-mount *in situ* hybridization was performed as previously described (Flanagan-Steet et al., 2009). An I.M.A.G.E. clone containing the full-length cathepsin K mRNA (Accession # BC092901) was purchased from Thermo-Fisher. A probe plasmid was generated following PCR amplification of a 1.2 kb fragment that included the entire coding region. This fragment was cloned into the EcoRI site of the pCSII vector and its orientation determined by PCR. The mRNA probe was generated from (HindIII) linearized plasmid DNA using T3 RNA polymerase.

Immunohistochemistry

Whole mount analysis of type II collagen expression was performed in the *fli1*:EGFP transgenic background as previously described (Flanagan-Steet et al., 2009). For immunohistochemical analysis of normal Ctsk expression, WT *fli1*:EGFP embryos were harvested and fixed in 4% paraformaldehyde (PFA) at 4°C overnight. The PFA was rinsed out with several changes of phosphate buffered saline (PBS), and embryos were taken through an ascending series of sucrose solutions (7, 15, 30%). The sucrose treated embryos were subsequently embedded and frozen in O.C.T. freezing media (TissueTek Corp). 40μm sections were cut on a Leica 1850 cryostat. The sections were incubated with blocking buffer (PBS+2% goat serum, 1% DMSO, 0.02% Triton X-100) for several hours at RT. This was followed by an overnight incubation at 4°C with rabbit anti-ctsk primary antibody diluted (1:75;cat#ab19027, Abcam) in blocking buffer. Sections

were rinsed with several changes of PBS+0.02% Triton-X-100; anti-rabbit Alexa 568 conjugated secondary antibody (diluted 1:400 in blocking buffer) was applied to the sections for 2 hrs at RT. Sections were again rinsed and coverslips mounted with Prolong Gold Mounting medium (Life Technologies Corporation) for microscopic analysis. In all cases immunohistochemical stains were visualized using an Olympus FV-100 laser scanning confocal microscope using ideal image parameters as defined by a 40xW (N.A.1.15) objective. Image acquisition and processing parameters were as previously described (Flanagan-Steet et al., 2009).

Protease activity assays

For the protease activity assays, WT and morphant embryos were dechorionated, deyolked (as described in embryo dissociation and cell sorting section above), and homogenized on ice by sonication in 10mM Tris pH 6.5, 1% Triton X-100. Embryo lysates were centrifuged at 15,000 rpm for 10 min at 4˚C and the protein concentration determined by Micro-BCA protein assay (Thermo Scientific). To gauge enzyme-specific substrate hydrolysis, equivalent samples were incubated with respective inhibitors or vehicle for 15 min at 4˚C before starting the assay. Enzymatic activities of cathepsins D (cat# 72097) and S (cat# 72099) were obtained using enzyme-specific kits from Anaspec (San Jose, Ca) and assays were performed according to manufacturer's specifications. The cysteine protease inhibitor E-64 (1 μM) was used to inhibit cathepsin S and pepstatin A (1 μM) was used to inhibit cathepsin D. For cathepsins K and L, 10

µg of lysate was assayed in a 100 µl reaction buffer (100mM sodium acetate, pH 5.5, 1mM DTT and 1mM EDTA) containing 10 µM of the respective substrates. The substrate for cathepsin K was $(Z\text{-Leu-Arg})_2$-Rhodamine 110 (cat# 219390) and the inhibitor Boc-Phe-Leu-NHNH-CO-NHNH-Leu-Z (1 µM, cat# 219373, Calbiochem, San Diego, Ca). For the determination of cathepsin L activity, the substrate $(Z\text{-Phe-Arg})_2$-R110 (cat# 350014) was obtained from Abbiotec (San Diego, Ca) and the cathepsin L inhibitor IV, 1-naphthalenesulfonyl-Ile-Trp-CHO (1 µM, cat# 219433) was also obtained from Calbiochem. The enzymatic activity of the MMPs was determined from the rate of hydrolysis of a general MMP substrate, QXL520 -γ-Abu-Pro-Cha-Abu-Smc-His-Ala-Dab (5-FAM)-Ala-Lys-NH_2, (cat# 60581-01) from Anaspec. According to the manufacturer, the substrate is cleaved by MMP-1, 2, 3, 7, 9, 12, and 13. MMPs were activated using *p*-aminophenylmercuric acetate (APMA). The metal ion chelator, EDTA, was used as an inhibitor. Fluorescence units were measured at various time intervals with a SpectraMax Genesis microplate fluorimeter from Molecular Devices (Sunnyvale, Ca) with excitation at 485nm and emission at 538nm. Reference standards were supplied with the assay reagents for cathepsin D and S, and MMPs. For cathepsins K and L, a rhodamine 110 standard was used.

Embryo extract preparation and immunoblot analysis of cathepsins

For analysis of cathepsin K and MMP-13 levels in wild-type and morphant embryos, lysates were prepared by overnight incubation of 50-75 embryos in 3% SDS, 10mM Tris pH 7.4, with a protease inhibitor cocktail (Sigma, St. Louis, MO,

USA). Lysates were then homogenized on ice by probe sonication, centrifuged at 15,000 rpm for 10 min at 4˚C and the protein concentration determined by Micro-BCA protein assay (Thermo Scientific). 100-125 µg of lysate was run on an SDS-PAGE gel and protein was transferred to a nitrocellulose membrane (Bio-Rad). Membranes were probed with a rabbit polyclonal anti-cathepsin K antibody (cat# ab19027, Abcam). Secondary goat anti-rabbit antibodies tagged with HRP were used to detect protein by chemiluminesence (GE Healthcare, Piscataway, NJ, USA).

In some cases, embryo lysates were treated with acid to reduce the pH to 4 for 1 h at 4˚C prior to subsequent analyses. The pH of the lysate was adjusted back to 5.5 prior to cathepsin K activity assays.

Small molecule in vivo inhibition of cathepsin K activity

At 24 hpf embryos were collected, dechorionated and 20-30 embryos placed per well into 6-well tissue culture plates. At 48 hpf embryos were treated with either 2.5 µM or 5.0 µM Cts K inhibitor, or control treated with 0.3% DMSO (which represents the highest amount present with the inhibitor). After two days of continuous drug treatment, embryos were subsequently collected (96 hpf) and processed for either Alcian blue staining or cathepsin enzyme assays.

Alcian blue staining and quantification of craniofacial phenotypes

Embryos were stained with Alcian blue as described previously [11]. Analysis of craniofacial structures was performed using the morphometric parameters

outlined in the results section. Stained embryos were photographed on an Olympus SZ-16 dissecting scope outfitted with Q-capture software and a Retiga 2000R color camera.

Acknowledgements

We wish to thank Julie Nelson (UGA Cell Sorting Facility) for her efforts in sorting dissociated zebrafish embryos and Sanjukta Sahu for technical assistance with immunohistochemistry.

References

1. Kollmann, K., et al., *Mannose phosphorylation in health and disease.* Eur J Cell Biol, 2010. **89**(1): p. 117-23.

2. Ghosh, P., N.M. Dahms, and S. Kornfeld, *Mannose 6-phosphate receptors: new twists in the tale.* Nat Rev Mol Cell Biol, 2003. **4**(3): p. 202-12.

3. Raas-Rothschild, A., et al., *Genomic organisation of the UDP-N-acetylglucosamine-1-phosphotransferase gamma subunit (GNPTAG) and its mutations in mucolipidosis III.* J Med Genet, 2004. **41**(4): p. e52.

4. Raas-Rothschild, A., et al., *Molecular basis of variant pseudo-hurler polydystrophy (mucolipidosis IIIC).* J Clin Invest, 2000. **105**(5): p. 673-81.

5. Reitman, M.L., A. Varki, and S. Kornfeld, *Fibroblasts from patients with I-cell disease and pseudo-Hurler polydystrophy are deficient in uridine 5'-diphosphate-N-acetylglucosamine: glycoprotein N-acetylglucosaminylphosphotransferase activity.* J Clin Invest, 1981. **67**(5): p. 1574-9.

6. Kornfeld, S., *Trafficking of lysosomal enzymes in normal and disease states.* J Clin Invest, 1986. **77**(1): p. 1-6.

7. Tiede, S., et al., *Mucolipidosis II is caused by mutations in GNPTA encoding the alpha/beta GlcNAc-1-phosphotransferase.* Nat Med, 2005. **11**(10): p. 1109-12.

8. Cathey, S.S., et al., *Phenotype and genotype in mucolipidoses II and III alpha/beta: a study of 61 probands.* J Med Genet, 2010. **47**(1): p. 38-48.

9. Herman, T.E. and W.H. McAlister, *Neonatal mucolipidosis II (I-cell disease) with dysharmonic epiphyseal ossification and butterfly vertebral body.* J Perinatol, 1996. **16**(5): p. 400-2.

10. Sprigz, R.A., et al., *Neonatal presentation of I-cell disease.* J Pediatr, 1978. **93**(6): p. 954-8.

11. Flanagan-Steet, H., C. Sias, and R. Steet, *Altered chondrocyte differentiation and extracellular matrix homeostasis in a zebrafish model for mucolipidosis II.* Am J Pathol, 2009. **175**(5): p. 2063-75.

12. Holmbeck, K. and L. Szabova, *Aspects of extracellular matrix remodeling in development and disease.* Birth Defects Res C Embryo Today, 2006. **78**(1): p. 11-23.

13. Lincoln, J., A.W. Lange, and K.E. Yutzey, *Hearts and bones: shared regulatory mechanisms in heart valve, cartilage, tendon, and bone development.* Dev Biol, 2006. **294**(2): p. 292-302.

14. Yasuda, Y., J. Kaleta, and D. Bromme, *The role of cathepsins in osteoporosis and arthritis: rationale for the design of new therapeutics.* Adv Drug Deliv Rev, 2005. **57**(7): p. 973-93.

15. Ma, X., et al., *Upregulation of elastase proteins results in aortic dilatation in mucopolysaccharidosis I mice.* Mol Genet Metab, 2008. **94**(3): p. 298-304.

16. Simonaro, C.M., et al., *Joint and bone disease in mucopolysaccharidoses VI and VII: identification of new therapeutic targets and biomarkers using animal models.* Pediatr Res, 2005. **57**(5 Pt 1): p. 701-7.

17. Simonaro, C.M., et al., *Mechanism of glycosaminoglycan-mediated bone and joint disease: implications for the mucopolysaccharidoses and other connective tissue diseases.* Am J Pathol, 2008. **172**(1): p. 112-22.

18. Metcalf, J.A., et al., *Upregulation of elastase activity in aorta in mucopolysaccharidosis I and VII dogs may be due to increased cytokine expression.* Mol Genet Metab, 2010. **99**(4): p. 396-407.

19. Metcalf, J.A., et al., *Mechanism of shortened bones in mucopolysaccharidosis VII.* Mol Genet Metab, 2009. **97**(3): p. 202-11.

20. Covassin, L., et al., *Global analysis of hematopoietic and vascular endothelial gene expression by tissue specific microarray profiling in zebrafish.* Dev Biol, 2006. **299**(2): p. 551-62.

21. Sumanas, S., T. Jorniak, and S. Lin, *Identification of novel vascular endothelial-specific genes by the microarray analysis of the zebrafish cloche mutants.* Blood, 2005. **106**(2): p. 534-41.

22. Knudson, C.B. and W. Knudson, *Cartilage proteoglycans.* Semin Cell Dev Biol, 2001. **12**(2): p. 69-78.

23. Haskins, M.E., *Animal models for mucopolysaccharidosis disorders and their clinical relevance.* Acta Paediatr Suppl, 2007. **96**(455): p. 56-62.

24. Boonen, M., et al., *Vacuolization of mucolipidosis type II mouse exocrine gland cells represents accumulation of autolysosomes.* Mol Biol Cell, 2011. **22**(8): p. 1135-47.

25. Gelfman, C.M., et al., *Mice lacking alpha/beta subunits of GlcNAc-1-phosphotransferase exhibit growth retardation, retinal degeneration, and secretory cell lesions.* Invest Ophthalmol Vis Sci, 2007. **48**(11): p. 5221-8.

26. Hubler, M., et al., *Mucolipidosis type II in a domestic shorthair cat.* J Small Anim Pract, 1996. **37**(9): p. 435-41.

27. Moro, E., et al., *A novel functional role of iduronate-2-sulfatase in zebrafish early development.* Matrix Biol, 2010. **29**(1): p. 43-50.

28. Vogel, P., et al., *Comparative pathology of murine mucolipidosis types II and IIIC.* Vet Pathol, 2009. **46**(2): p. 313-24.

29. Reiser, J., B. Adair, and T. Reinheckel, *Specialized roles for cysteine cathepsins in health and disease.* J Clin Invest, 2010. **120**(10): p. 3421-31.

30. Felbor, U., et al., *Neuronal loss and brain atrophy in mice lacking cathepsins B and L.* Proc Natl Acad Sci U S A, 2002. **99**(12): p. 7883-8.

31. Spira, D., et al., *Cell type-specific functions of the lysosomal protease cathepsin L in the heart.* J Biol Chem, 2007. **282**(51): p. 37045-52.

32. Sardiello, M. and A. Ballabio, *Lysosomal enhancement: a CLEAR answer to cellular degradative needs.* Cell Cycle, 2009. **8**(24): p. 4021-2.

33. Sardiello, M., et al., *A gene network regulating lysosomal biogenesis and function.* Science, 2009. **325**(5939): p. 473-7.

34. Selent, J., et al., *Selective inhibition of the collagenase activity of cathepsin K.* J Biol Chem, 2007. **282**(22): p. 16492-501.

35. Kafienah, W., et al., *Human cathepsin K cleaves native type I and II collagens at the N-terminal end of the triple helix.* Biochem J, 1998. **331 (Pt 3)**: p. 727-32.

36. Lecaille, F., et al., *Probing cathepsin K activity with a selective substrate spanning its active site.* Biochem J, 2003. **375**(Pt 2): p. 307-12.

37. Goldring, M.B., K. Tsuchimochi, and K. Ijiri, *The control of chondrogenesis.* J Cell Biochem, 2006. **97**(1): p. 33-44.

38. Witten, P.E., A. Hansen, and B.K. Hall, *Features of mono- and multinucleated bone resorbing cells of the zebrafish Danio rerio and their contribution to skeletal development, remodeling, and growth.* J Morphol, 2001. **250**(3): p. 197-207.

39. Dodds, R.A., et al., *Human osteoclast cathepsin K is processed intracellularly prior to attachment and bone resorption.* J Bone Miner Res, 2001. **16**(3): p. 478-86.

40. McQueney, M.S., et al., *Autocatalytic activation of human cathepsin K.* J Biol Chem, 1997. **272**(21): p. 13955-60.

41. Rieman, D.J., et al., *Biosynthesis and processing of cathepsin K in cultured human osteoclasts.* Bone, 2001. **28**(3): p. 282-9.

42. van Meel, E., et al., *Disruption of the Man-6-P Targeting Pathway in Mice Impairs Osteoclast Secretory Lysosome Biogenesis.* Traffic, 2011.

43. Okada, Y. and I. Nakanishi, *Activation of matrix metalloproteinase 3 (stromelysin) and matrix metalloproteinase 2 ('gelatinase') by human neutrophil elastase and cathepsin G.* FEBS Lett, 1989. **249**(2): p. 353-6.

44. Kimmel, C.B., et al., *Stages of embryonic development of the zebrafish.* Dev Dyn, 1995. **203**(3): p. 253-310.

45. Lawson, N.D. and B.M. Weinstein, *In vivo imaging of embryonic vascular development using transgenic zebrafish.* Dev Biol, 2002. **248**(2): p. 307-18.

46. Nairn, A.V., et al., *Regulation of glycan structures in animal tissues: transcript profiling of glycan-related genes.* J Biol Chem, 2008. **283**(25): p. 17298-313.

Figures

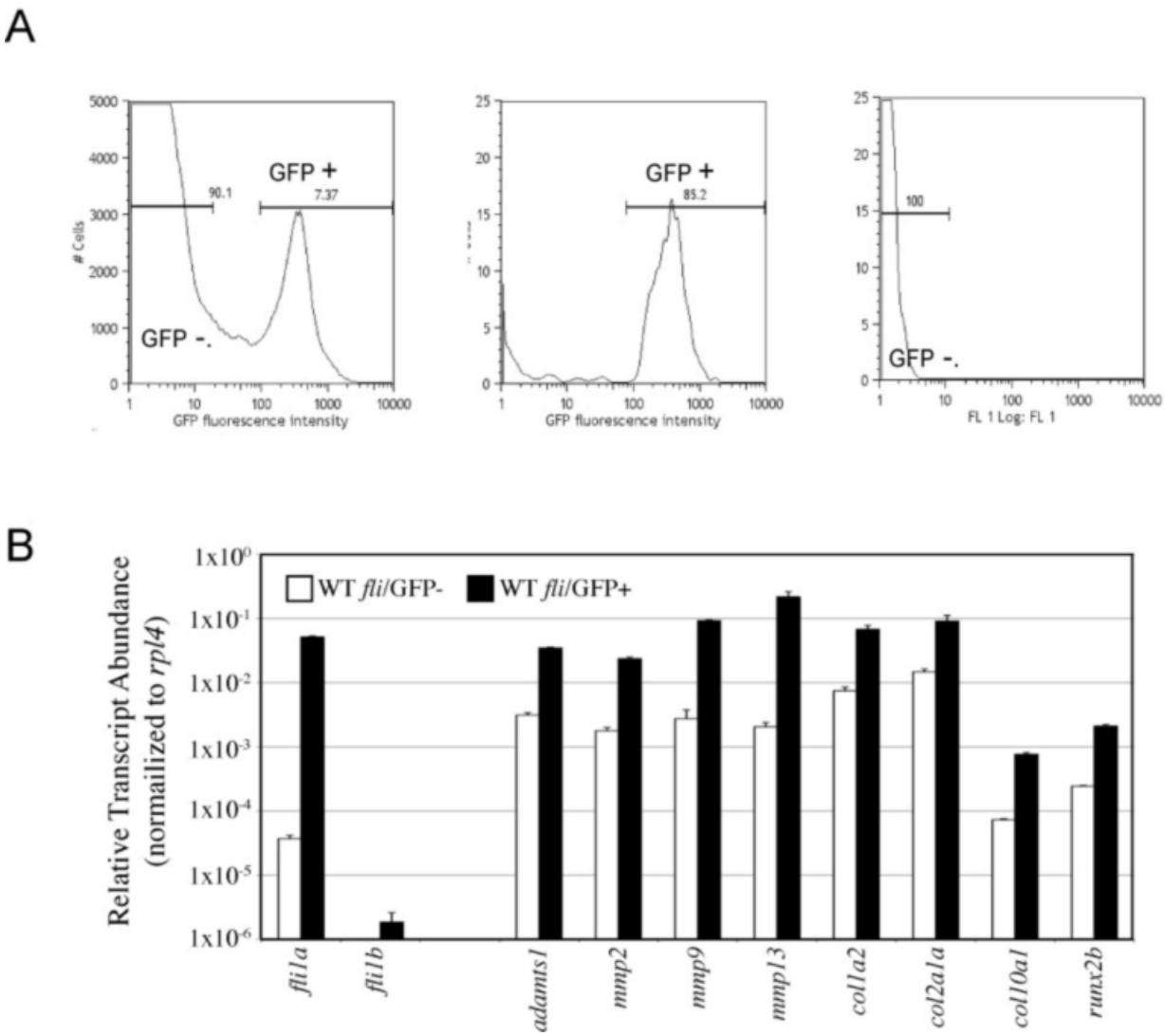

Figure 2.1. GFP-positive and –negative cells isolated from *Tg (fli1a:EGFP)* animals are highly pure and enriched for markers of craniofacial chondrocytes. (A) Representative profiles of diagnostic FACS performed on GFP+ and GFP- cells isolated from *Tg(fli1a:EGFP)* demonstrate that the individual pools are highly pure, containing only GFP positive or negative cells. (B) Comparison of relative transcript abundance of several genes in WT *fli1*:EGFP+ (open bars) and *fli1*:EGFP- (filled bars) sorted cell populations at 2 dpf. Data were normalized to a control gene (*rpl4*) and plotted on a $\log_{10}$ scale. Error bars represent the SEM from four independent biological samples. Individual gene names (italics) are listed along the bottom axis. Relative transcript abundance values less that $1x10^{-6}$ are below the threshold of detection.

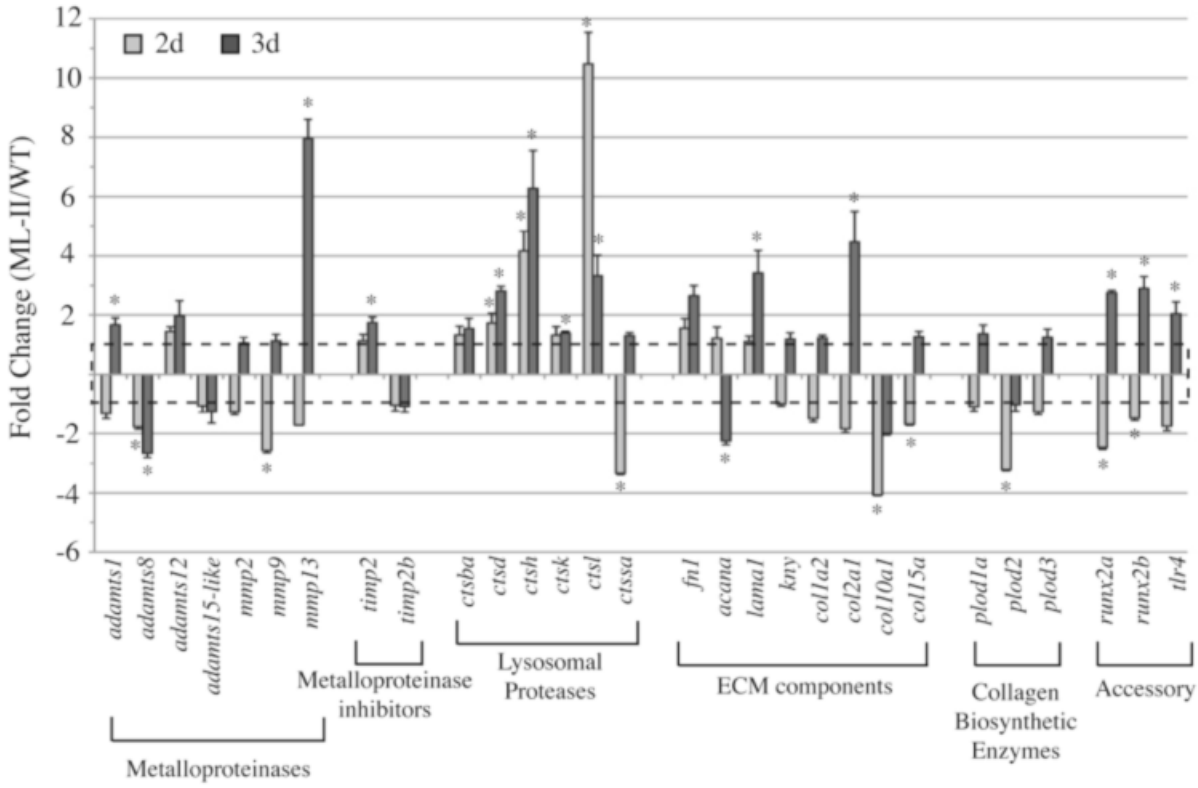

Figure 2.2. Transcript abundance of genes involved in ECM synthesis and modification is altered in 2 and 3 dpf ML-II morphants. The fold change in relative transcript abundance for ML-II fli/GFP+ cells relative to WT fli/GFP+ cells are shown for individual genes at 2 dpf (lighter bars) and 3 dpf (darker bars). A fold change of ±1 indicates that the expression is similar in both cell types (area indicated with dashed lines). Error bars represent the SEM from four independent biological samples. Asterisks indicate a statistically significant difference ($p<0.05$) between the transcript abundance for that gene between WT and ML-II sorted cells.

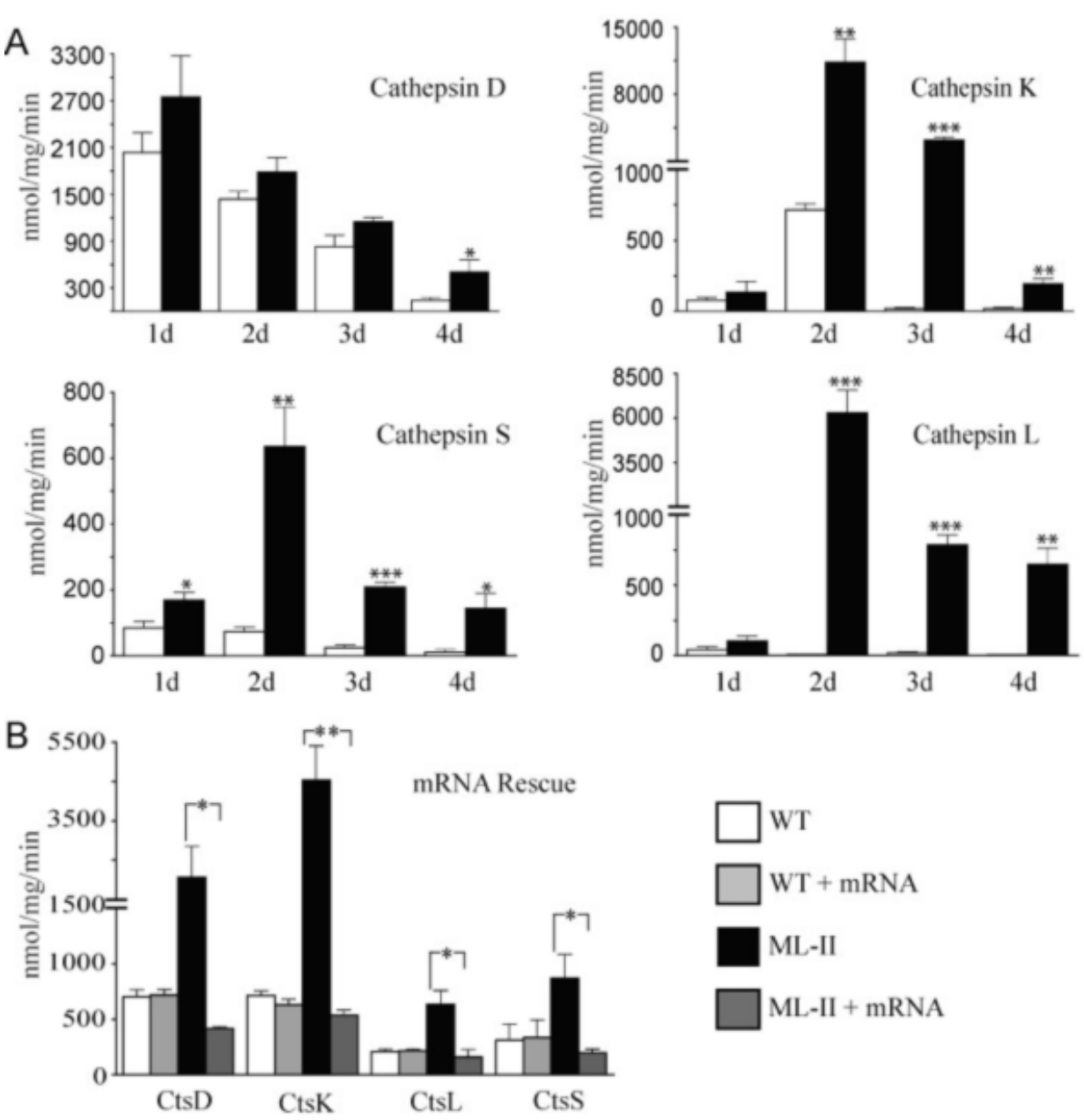

Figure 2.3. Cathepsin activity is elevated and sustained in ML-II zebrafish embryos. (A) Cathepsin activity was measured over a developmental time course (1-4 dpf) in WT and ML-II embryo lysates (~45 embryos/lysate) and normalized for total protein. Activity values (nmol/mg/min) are based on the rate of hydrolysis of cathepsin-specific fluorogenic peptide substrates; WT, n=4, ML-II n=6. (B) Introduction of GlcNAc-1-phosphotransferase mRNA normalizes cathepsin activity to WT levels at 3 dpf; WT and ML-II, n=3; (**P*<0.05, ***P*<0.01, ****P*<0.001, Student's *t*-test)

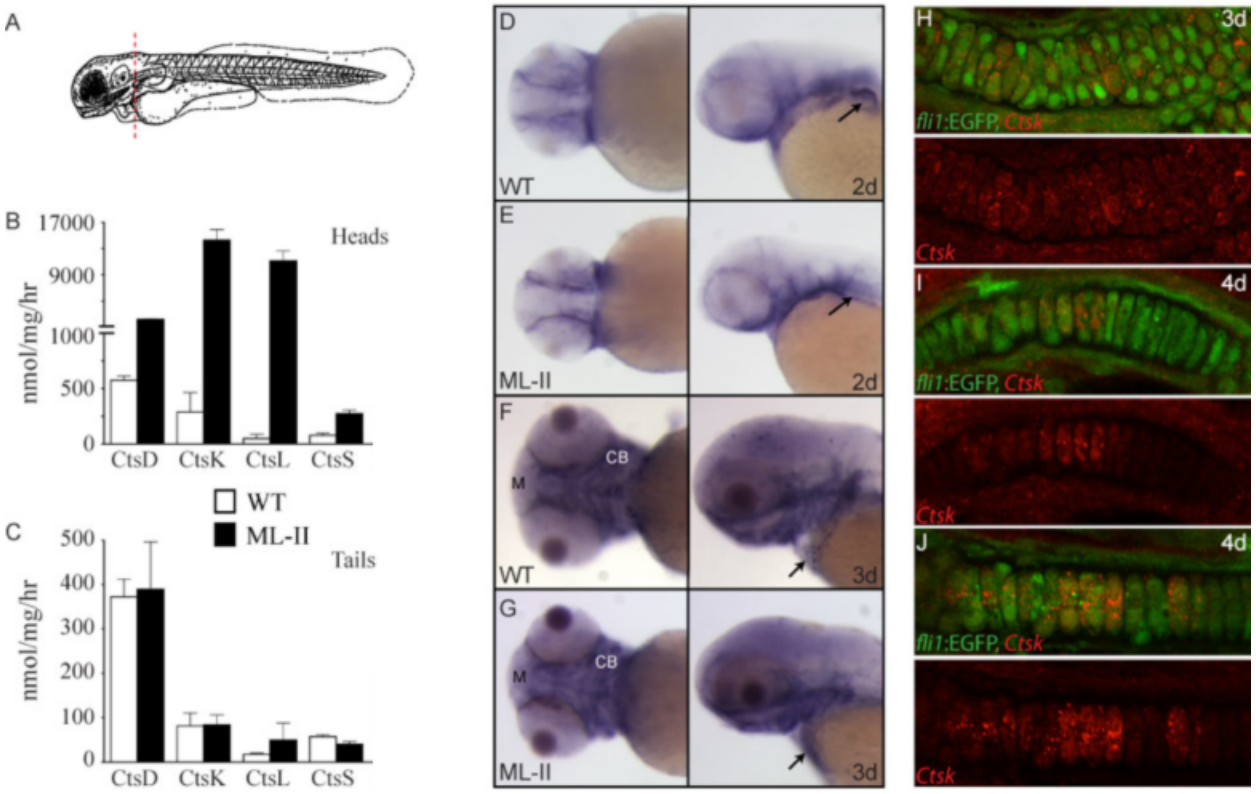

Figure 2.4. Cathepsin expression is enriched in the craniofacial skeleton of zebrafish embryos. Analysis of enzyme activities in lysates of 3 dpf WT and ML-II embryos separated into heads and tails, as diagrammed in (A, dashed line represents cut site) demonstrates that cathepsin activities are primarily increased in the head (B) compared to the tail (C), n=3. (D-G) *In situ* hybridization for cathepsin K expression shows mRNA is enriched in ventral tissues that generally correspond to the pharyngeal skeleton at 2d (D,E) and 3d (F,G) in WT and ML-II embryos. Arrows denote differences in the pattern of expression between WT and ML-II embryos. (H-J) Immunohistochemical stains for cathepsin K (red) on sections of 3d (H) and 4d (I,J) WT *fli1*:EGFP embryos show it is expressed in chondrocytes and peri-chondrial fibroblasts of the trabecular (H,J) and Meckel's cartilages (I). M, Meckel's cartilage; CB, Ceratobranchials.

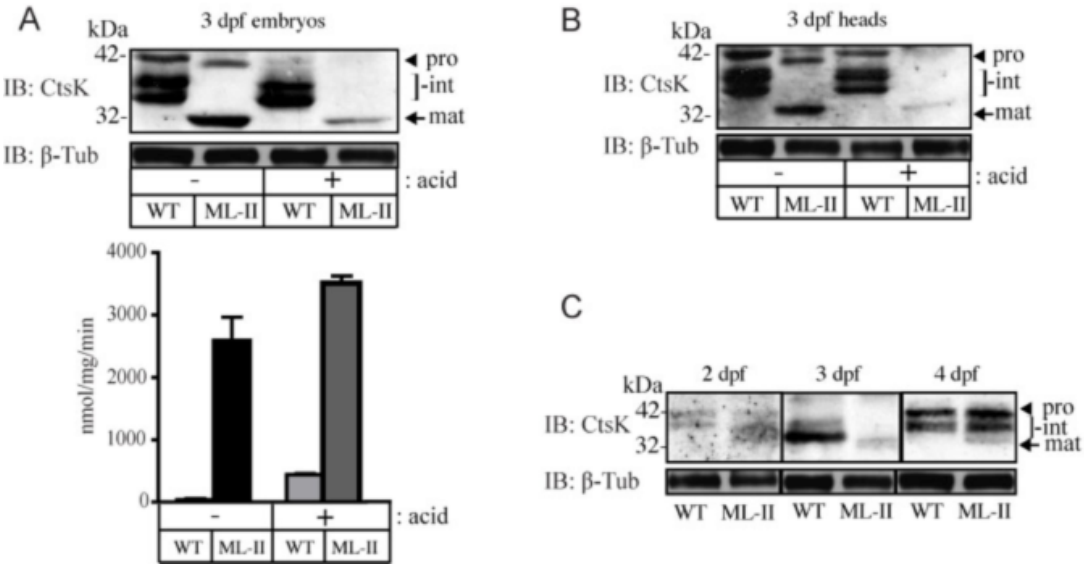

Figure 2.5. The mature form of cathepsin K is present early and persists in ML-II embryos.
(A) Western blot analysis and activity assays of whole embryo lysates with and without acid treatment. (B) Western blot analysis of 3 dpf zebrafish heads with and without acid treatment. (C) Western blot analysis of whole embryo lysates over a developmental time course spanning 2-4 dpf. Procathepsin K (*arrowhead*), intermediate forms (*bracket*), mature cathepsin K (*arrow*).

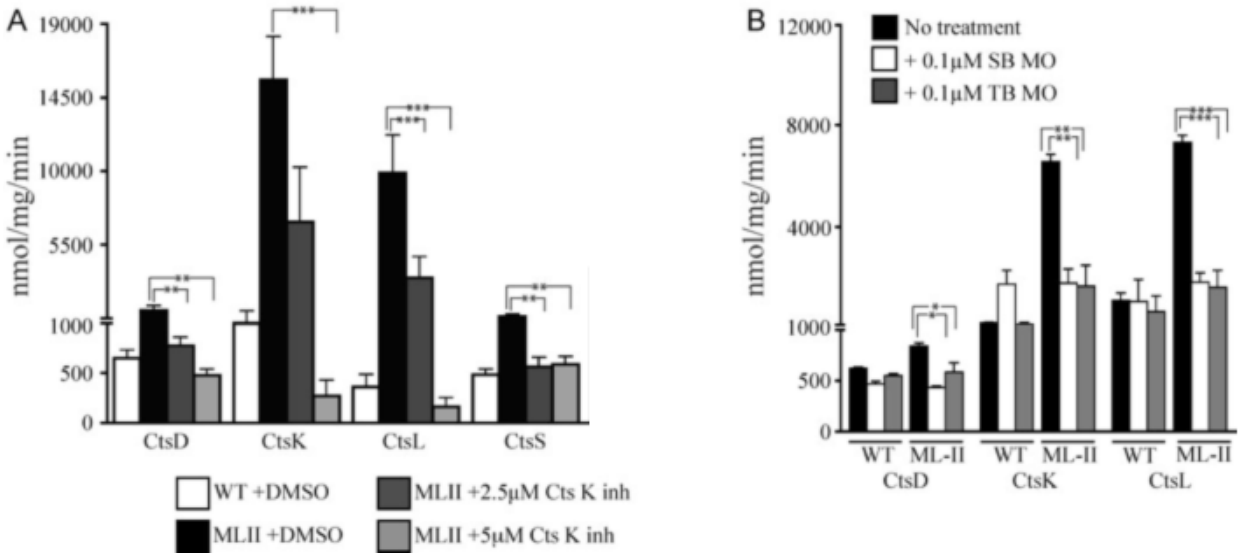

Figure 2.6. *In vivo* inhibition of cathepsin K reduces the activities of multiple cathepsins. (A) *in vivo* administration of a cathepsin K inhibitor at 2 dpf leads to reduced cathepsin activity levels measured at 4 dpf; for DMSO only treatment n=3, for samples treated with cathepsin K inhibitor n=6. (B) Inhibition of cathepsin K expression by morpholino knockdown also reduces the activity of multiple cathepsins and MMP; n=3 experiments per group with 45 embryos per experimental sample. (**P*<0.05, ***P*<0.01, ****P*<0.001, Student's *t*-test)

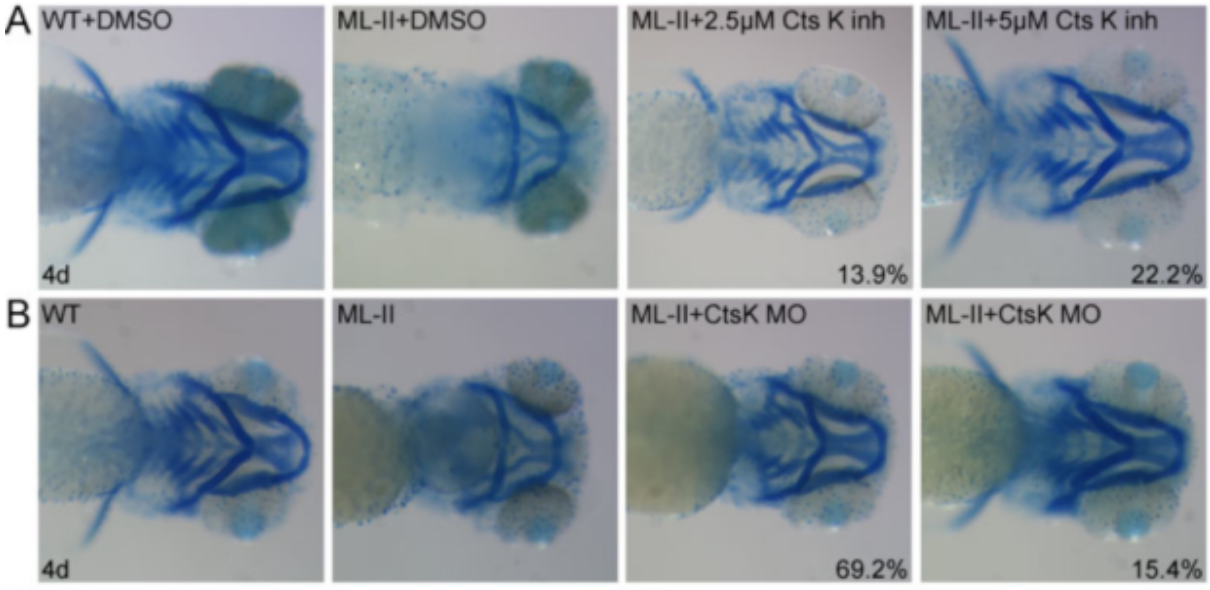

D

	1- Meckels meets Palate	2- PQ - PQ / M - CH	3- CH to CH angle	4- % with stained pectoral fins
WT (n=20)	100%	1.51	87±8°	100%
ML-II (n=23)	0.0%	1.97	152±2°	0.0%
ML-II/Cts K (n=40)	22.2%	1.76	106±10°	22.2%

E

	1- Meckels meets Palate	2- PQ - PQ / M - CH	3- CH to CH angle	4- % with stained pectoral fins
WT (n=22)	100%	1.57	85±8°	100%
ML-II (n=33)	0.0%	1.93	150±23°	0.0%
ML-II/Cts K (n=39)	48.7%	1.70	93±22°	76.3%

Figure 2.7. Inhibition of cathepsin K expression or activity results in correction of the ML-II cartilage morphogenesis defects. Alcian blue stains of embryos at 4 dpf showed that inhibition of either cathepsin K (A) activity using pharmacological agents or (B) expression by MO injection results in significant correction of multiple aspects of the craniofacial defects present in ML-II embryos. Percent values listed represent the number of embryos with these

phenotypes. For the drug treatments (A), n=160 embryos in 4 experiments, for MO experiments (B), n=100 embryos in 3 experiments. (C) The degree of correction was quantified as follows: 1-whether Meckels (M) cartilage meets the palate (P), 2- the “shape” of the jaw using the ratio of the distance between the palatoquadrate (PQ) bones over the distance from Meckels (M) cartilage to the ceratohyal (CH) bones, 3- the angle between the left and right ceratohyals (CH), and 4- whether the pectoral fins stained positively with Alcian blue. The quantitation of the degree of cartilage correction following pharmacological inhibition of cathepsin K activity (D) and SB MO-inhibition of cathepsin K expression (E) are presented.

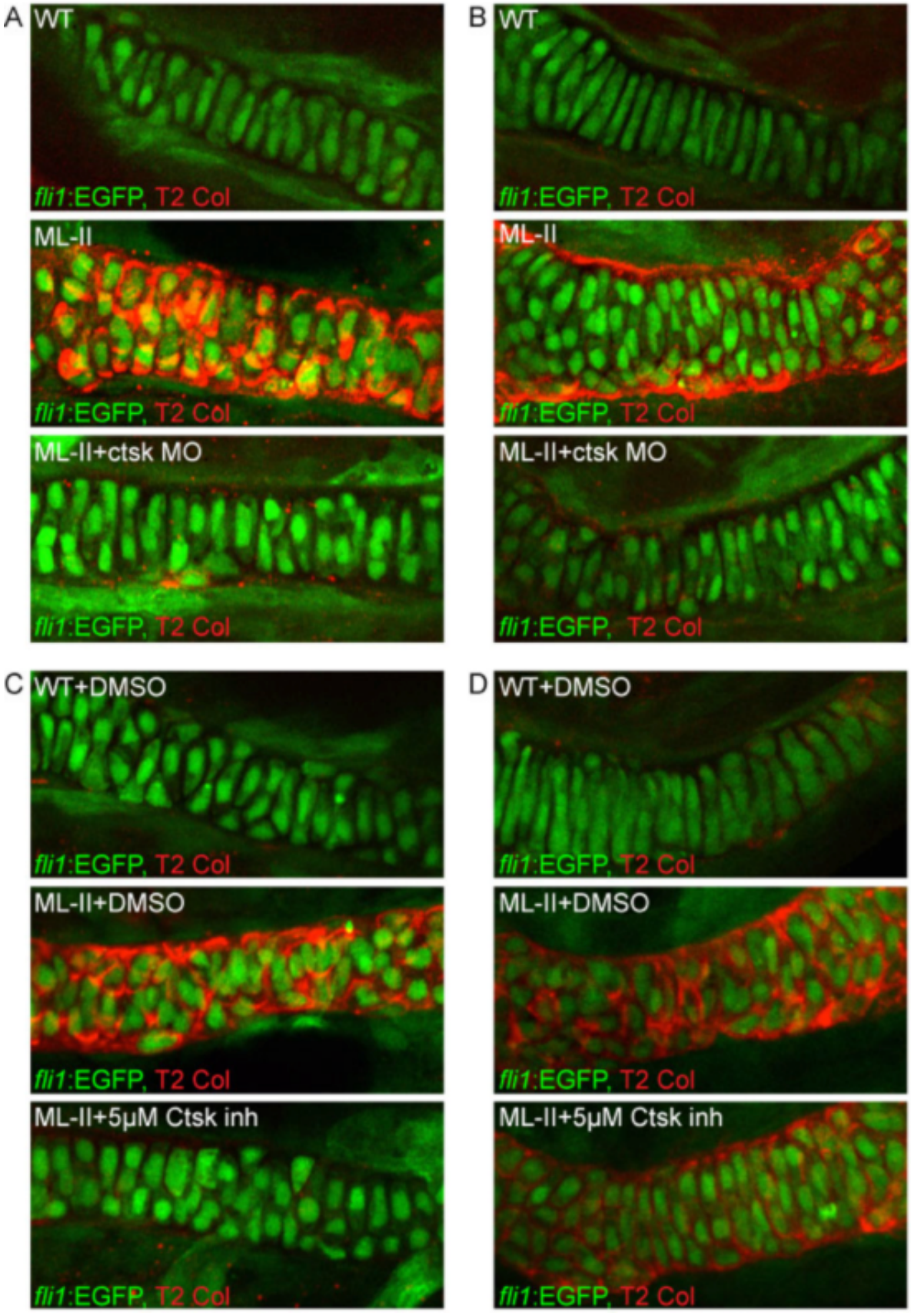
A
WT
fli1:EGFP, T2 Col
ML-II
fli1:EGFP, T2 Col
ML-II+ctsk MO
fli1:EGFP, T2 Col
B
WT
fli1:EGFP, T2 Col
ML-II
fli1:EGFP, T2 Col
ML-II+ctsk MO
fli1:EGFP, T2 Col
C
WT+DMSO
fli1:EGFP, T2 Col
ML-II+DMSO
fli1:EGFP, T2 Col
ML-II+5μM Ctsk inh
fli1:EGFP, T2 Col
D
WT+DMSO
fli1:EGFP, T2 Col
ML-II+DMSO
fli1:EGFP, T2 Col
ML-II+5μM Ctsk inh
fli1:EGFP, T2 Col

Figure 2.8. Inhibition of cathepsin K activity reduces type II collagen accumulation in ML-II morphant cartilages. Immunohistochemical analysis of type II collagen in the (A,C) trabecular and (B,D) Meckel's cartilages from (A,B) WT, ML-II, and ML-II/cts K MO-inhibited embryos, (C,D) WT, ML-II, and ML-II/cts K inhibitor-treated embryos reveal significant decreases in its expression following inhibition of cathepsin K.

CHAPTER 3: ALTERED ACTIVITY AND LOCALIZATION OF CATHEPSIN K UNDERLIES THE CARTILAGE DEFECTS IN A ZEBRAFISH MODEL OF MUCOLIPIDOSIS II[2]

[2] Petrey, A.C., et al. To be submitted to Journal of Biological Chemistry.

Abstract

The severe disorder, mucolipidosis II (ML-II; I-cell disease), is caused by defects in mannose 6-phosphate (M6P) biosynthesis. Patients exhibit multiple developmental defects including skeletal, craniofacial and joint abnormalities. Utilizing an ML-II zebrafish model, we previously showed that the cartilage defects are associated with altered chondrocyte differentiation, elevated levels of type II collagen, and increased and sustained activity of several proteases including cathepsin K (Ctsk). Inhibition of Ctsk by genetic and pharmacological means ameliorated multiple aspects of the craniofacial phenotypes. Further, we have demonstrated that the elevated activity of Ctsk is due to enhanced proteolytic processing of the enzyme proform into highly active mature forms. We hypothesize that this enhanced proteolytic processing correlates with the loss of M6P and Ctsk hypersecretion from cells. To test this hypothesis, we first analyzed the mannose phosphorylation status and activity of zebrafish cathepsins D (Ctsd) and K in WT and ML-II embryos. In WT embryos, Ctsd was only marginally M6P modified whereas Ctsk was extensively modified. In ML-II, the mannose phosphorylation of both cathepsins was reduced, with the majority of excessive Ctsk activity lacking M6P. To address whether unmodified Ctsk is in fact hypersecreted from the cell, we isolated WT and ML-II zebrafish chondrocytes and found that the intracellular

activity of Ctsk but not Ctsd is substantially reduced in ML-II cells, consistent with cathepsin-specific hypersecretion. Immunohistochemical staining for Ctsk and Ctsd confirmed a unique extracellular localization of Ctsk within ML-II cartilage. To assess the direct contribution of Ctsk to the pathology of ML-II, we overexpressed Ctsk in WT embryos, which was sufficient to enhance enzyme activation, lead to an increase in activity lacking M6P, and resulted in craniofacial abnormalities, each reminiscent of the biochemical and phenotypic aspects of ML-II. These findings further support a central role for Ctsk in the cartilage pathogenesis of this disease.

Introduction

Mannose-6-Phosphate (Man-6-P) mediated targeting of acid hydrolases to the lysosome serves as the primary mechanism by which many glycosyl hydrolases and proteases are diverted out of the secretory pathway and deposited within the lysosomal network. Biosynthesis of this key recognition marker is initiated by the enzyme UDP-*N*-acetylglucosamine:lysosomal enzyme *N*-acetylglucosamine-1-phosphotransferase (GlcNAc-1-phosphotransferase) which transfers a GlcNAc-1-phosphate to mannose residues of select oligomannosyl N-glycans within the *cis* Golgi. Removal of the GlcNAc monosaccharide by the enzyme GlcNAc-1 phosphodiester α-*N*-acetylglucosaminidase or “uncovering enzyme” reveals the Man-6-P monoester,

generating the lysosomal trafficking signal [1, 2]. These sugar-phosphates are the key recognition markers for sorting of newly synthesized lysosomal proteins by the cation-dependent and cation-independent mannose 6-phosphate receptors (CD-MPR; CI-MPR). Man-6-P residues are essential for receptor-mediated transport to lysosomes [3, 4]. Impaired biosynthesis of this recognition marker leads to the fatal lysosomal storage disorder Mucolipidosis II (ML-II; I-cell disease) and the less severe ML-III. Mutations in the gene encoding for GlcNAc-1-phosphotransferase (GNPTAB) alpha or beta subunits result in a failure to synthesize the Man-6-P trafficking signal and as a consequence lysosomal hydrolases are secreted from the cell [4-7]. The clinical manifestations of ML-II include pronounced skeletal and craniofacial defects, cardiac insufficiency, and recurrent lung infections, many of which are present at birth [8]. In recent years a clearer picture of the genetic basis for the disorder and the specific functions of the enzymes they encode has emerged. However, many of the molecular and cellular mechanisms driving the progressive nature of ML-II are still poorly understood.

To further investigate the developmental nature of this disease, we previously generated and characterized a mopholino-based knockdown model for ML-II using zebrafish. ML-II embryos exhibited defects in many of the same systems as patients including craniofacial cartilage abnormalities and cardiac defects. *GNPTAB* depletion led to decreased mannose phosphorylation of lysosomal hydrolases, striking changes in the timing and expression of type II collagen linked with the abnormal chondrogenesis of craniofacial cartilage [9].

These findings suggested that loss of Man-6-P biosynthesis impaired normal chondrocyte development in the ML-II zebrafish. We demonstrated that the expression and activity of several proteases are increased and sustained throughout early development in ML-II embryos. Further investigation revealed the elevated activity of the cathepsins and MMPs was primarily in the head, and cathepsin K was subject to abnormal processing in ML-II. Suppression of one lysosomal enzyme, cathepsin K, was shown to reduce the activity of other proteases and partially correct the craniofacial defects in these embryos [10].

Our previous studies suggest cathepsin K plays a key role in the cartilage pathogenesis of ML-II. In light of its known role in bone and cartilage homeostasis, we hypothesized that loss of Man-6-P dependent trafficking leads to enhanced activation and hypersecretion of cathepsin K. We propose that mislocalization or inappropriate expression of active cathepsin K leads to the craniofacial phenotypes observed in ML-II embryos. To address this question, we undertook biochemical analysis of cathepsin mannose phosphorylation and localization in zebrafish. Our results indicated that cathepsin K is enzymatically active at neutral pH, is extensively mannose phosphorylated on either or both of its two N-glycans, and is deficient in chondrocytes isolated from ML-II zebrafish. Our data further demonstrates that expression of forms of cathepsin K lacking N-glycans is sufficient to generate craniofacial cartilage defects analogous to those seen in ML-II embryos. Together, these data suggest that Man-6-P modification of cathepsin K is a regulatory mechanism of enzyme activity and inappropriate expression or localization of cathepsin K leads to cartilage defects in zebrafish.

Results

Zebrafish lyososmal cathepsin proteases S, and K but not D and L have residual activity at neutral pH.

To determine which cathepsins may be active following hypersecretion, we performed in vitro enzyme assays to profile their activity between acidic and neutral conditions. The activity of cathepsin proteases was initially reported under very acidic conditions, but recent reports have shown that some retain substantial activity at neutral pH [11-14]. For all enzymes tested, the normalized activity values represent only the activity that could be specifically inhibited. As shown in Fig. 3.1, the pH optimum for the zebrafish cathepsins lies under acidic conditions. The aspartyl protease cathepsin D, exhibits peak activity at pH 5.5, and activity decreases to less than 25% activity under neutral conditions. The cysteine proteases cathepsins K, L, and S all are shown have distinct profiles. Cathepsin L has a more narrow distribution, with an optimum at pH 5.0 and rapidly diminishing activity in either more acidic or neutral conditions. Both cathepsins S and K share an optimum of pH 6.0, and contain appreciable levels of residual activity at pH 7.0. This observation was most striking in the case of cathepsin S, which retains ~70% of its activity at pH 7.0. Cathepsin K has been reported to be significantly more stable and active at neutral conditions upon binding to chondroitin sulfate. In the environment of the ECM it is likely cathepsins S and K function as potent matrix-degrading enzymes.

Zebrafish cathepsins K, L, and S are extensively Man-6-P modified.

To quantify the relative amount of cathepsin enzymatic activity that contains Man-6-P glycans, we subjected zebrafish embryos and adult brains to affinity chromatography using an immobilized CI-MPR column. Brain contains very high levels of M6P-modified proteins, presumably because the acid phosphatase responsible for removing the trafficking marker is present at low levels. Lysates were fractionated over the column and the protease activity of each fraction was measured. As shown in Table 3.1, the vast majority of the activity corresponding to cathepsins K, L, and S bound to the CI-MPR column, indicating that one or more of their glycans contains Man-6-P residues. By contrast, only a fraction of the activity corresponding to cathepsin D (24% of brain and 16% of embryos) bound the column. Similar results were obtained in all cases, but Man-6-P levels appeared at their highest in zebrafish brain. Interaction with the CI-MPR column was Man-6-P mediated as treatment of lysates with alkaline phosphatase prior to fractionation effectively abolished all column binding. To address whether the poor binding of cathepsin D might represent loss of Man-6-P within the lysosome, we performed a similar approach using a concanavalin A (conA) column to determine the relative level of high mannose oligosaccharides. As shown in Table 3.2, only 27% of cathepsin D activity from brain bound to the conA column, indicating that the major glycoform is not capable of mannose phosphorylation by phosphotransferase. These data are consistent with the observation that cathepsin D is poorly mannose phosphorylated when compared to cathepsins K, L, and S [15].

Sequence comparison of zebrafish and human cathepsins D and K.

Cathepsin proteases are well studied in humans and other mammals, but have been investigated to a lesser extent in zebrafish. Comparison of the zebrafish and human cathepsin K amino acid sequence (Fig 3.2A) revealed 62% sequence identity and 77% similarity between species. The coding region of zebrafish cathepsin K is 999 bp in length and encodes an 18-residue pre-peptide, a 99-residue pro-peptide, and a 216-amino acid mature enzyme. Both species contain a single N-glycan site in their pro- and mature forms, though at different locations within the primary sequence. Autoactivation is believed to occur in a step-wise fashion and the putative sites are conserved in zebrafish. Alignment of human and zebrafish cathepsin D sequences revealed 67% identity, 80% similarity. The coding region for cathepsin D is 1197bp in length and encodes an 18-residue pre-peptide, a 46-residue pro-peptide, and the resulting product is further cleaved to form a 97-amino acid light chain and 244-residue heavy chain mature forms. Studies of human cathepsin D have shown a key c-terminal oligosaccharide is required for efficient Man-6-P modification [16]. The c-terminal N-glycan sequon present is absent in the zebrafish enzyme and likely explains its poor mannose phosphorylation. However, cathepsin D is capable of reaching the lysosome independent of the Man-6-P receptor pathway through interaction with sortilin, and it is unlikely lysosomal targeting is disrupted.

***Cathepsins K and L are deficient within enriched chondrocyte populations isolated from ML-II zebrafish*.**

Several studies have shown that the Man-6-P pathway is a requirement for lysosomal biogenesis and efficient trafficking of cathepsin proteases [17, 18]. The above experiments suggest that loss of Man-6-P residues on cathepsins K, L, and S may result in impaired lysosomal targeting and subsequent hypersecretion into the extracellular space. To determine if these proteases are secreted in cell types relevant to the craniofacial defects in our ML-II model, we generated morphants in a transgenic line to enrich for either chondrocytes. *Tg(fli1a*:EGFP) embryos express EGFP in endothelial cells, certain hematopoietic cells, and neural crest-derived cells which give rise to chondrocytes and craniofacial cartilage [19]. To further explore the hypersecretion of cathepsin proteases in these cell populations, GFP-positive (GFP+) and GFP-negative (GFP-) cells were isolated by fluorescence activated cell sorting (FACS) from dissociated WT and ML-II transgenic embryos and then compared cell-associated protease activity. The results of this analysis is shown figure 3.3. Cathepsin D is present at normal levels in GFP+ and GFP- cells at both time points. By contrast, cathepsin K was significantly deficient within ML-II GFP+ enriched chondrocytes at both days, and reduced to a lesser extent in GFP- cells at 3dpf (Fig. 3.3B). Cathepsin S, however, appeared to be present at elevated levels in ML-II GFP+ cells, particularly at 2dpf (figure 3.3D). Unlike any of the other cathepsins, L appeared deficient within GFP+ and GFP- ML-II chondrocytes at both days (Fig. 3.3C). Surprisingly, cathepsin S was found at

normal or elevated levels within these cells (Fig 3.3D). These findings suggest that cathepsins L and K are targeted to the lysosome primarily by the Man-6-P pathway, unlike cathepsin D. In an effort to further determine the selectivity of lysosomal hydrolase trafficking within these cells, we analyzed the intracellular contents of several glycosyl hydrolases as shown in figure 3.4A. We did not detect any substantial reduction in activity within sorted cells, suggesting that the consequences of impaired Man-6-P biosynthesis is protein and cell-type specific.

To further confirm that cathepsin K is deficient within sorted ML-II chondrocytes, cathepsin K protein was analyzed by western blot in isolated cells. Although the procathepsin K band was present in both lysates, the mature form was absent within ML-II cells. Highly similar results were obtained from ML-II GFP- cells, as seen in figure 3.4B. Because the mature, active form is absent within these cells, it is likely that the measured intracellular activity in ML-II results from weak catalytic activity of procathepsin K or from residual mature form beneath the limit of detection. Collectively, these observations suggest that cathepsin K is activated and retained within the lysosome of WT cells, but the active form is hypersecreted from ML-II chondrocytes. Loss of Man-6-P alters the intracellular content of some, but not all, lysosomal hydrolases.

Cathepsin K expressed in CHO cells is not mannose phosphorylated and is secreted into media.

The prior experiments establish that cathepsin K is likely hypersecreted from ML-II cells in the absence of mannose phosphorylation. In order to closely

investigate relationship between mannose phosphorylation and hypersecretion of cathepsin K, we generated several glycan-deleted cathepsin K mutants. These mutants were expressed in CHO cells and subject to CI-MPR affinity chromatography of media and cell lysates. All forms of cathepsin K expressed in CHO cells were absent within the cell lysates and present at high levels in media (figure 3.5A). Analysis of media revealed that no form of zebrafish cathepsin K was capable of mannose phosphorylation, but retained high-mannose glycans as shown in Table 3.3. This data is consistent with other reports that cathepsin K is not Man-6-P modified in some cell types [11, 20, 21].

Loss of mannose phosphorylation of cathepsin K results in increased activity.

Cathepsin K is processed into its active form after reaching the low pH environment of the lysosome [22]. Despite disruption of lysosomal trafficking in ML-II, cathepsin K appears to be subject to enhanced processing and activation [10, 18]. To determine the consequence of reduced mannose phosphorylation of cathepsin K in an *in vivo* context, cathepsin K and glycan-deleted forms were expressed in WT embryos. Man-6-P binding activity was measured by CI-MPR column fractionation at 3dpf. Interestingly, overexpression of cathepsin K alone marginally reduced binding, possibly saturating or escaping GlcNAc-1-phosphotransferase. The results of this analysis, shown in figure 3.6A, clearly demonstrate that loss of a single glycan is sufficient to alter the mannose phosphorylation of cathepsin K and leads to increased activity. Expression of the

single mutants, N23Q or N216Q revealed differences in their ability to bind the column. Binding is drastically reduced in the single mutant N216Q (39%) compared to wt ctsk (71%) or N23Q (74%), suggesting that the relative utilization of these two glycans is not uniform. In the case of the double mutant N23/216Q column binding was reduced to levels similar to that observed in ML-II embryos (27%). In light of the fact that upon activation, mature cathepsin K will only contain its c-terminal glycan, we next addressed whether loss of both glycans had an effect on the activation of cathepsin K. Glycoforms of cathepsin K were expressed in embryos and whole embryo lysates were measured at 3dpf. Whereas the N23Q glycoform was present at activity levels comparable to WT cathepsin K, the activities of N216Q and N23/216Q mutants were substantially elevated (Fig 3.6B). Loss of mannose phosphorylation correlated positively with an increase in activity suggesting that cathepsin K activation is enhanced upon loss of Man-6-P.

Overexpression of cathepsin K leads to elevated cathepsin L activity in zebrafish heads.

Our prior studies showed that the majority of the elevated protease activity in the zebrafish model for ML-II was regionally increased in the head, but not tail. To address if this was consistent upon overexpression of cathepsin K we separated embryos at 3dpf into head and tail sections and assayed each of these pools for protease activity. The results of this analysis (Fig. 3.7) revealed that overexpression of either cathepsin K or glycan deleted forms lead to an increase

in activity the head and tail of embryos. Overexpression of cathepsin K was similar to that of N23Q, but the activity of the c-terminal mutant N216Q and the double mutant were substantially higher possibly due to enhanced activation of the pro-enzyme. Surprisingly, expression of cathepsin K also led to a substantial increase cathepsin L activity in heads, but only modestly in tails. This finding is similar to observations in the zebrafish ML-II model, and further establishes a relationship between cathepsins K and L. Additionally, these data suggest that mRNA injection of cathepsin K leads to ectopic expression in cell types that may not be relevant to ML-II such as the tail.

Overexpression of glycan-deleted forms of cathepsin K generates craniofacial defects in zebrafish.

Previous characterization of the zebrafish ML-II model revealed pronounced disruption of chondrocytes within trabecular and Meckels cartilages that correlated with increased spatial and temporal protease activity [9]. The above experiments establish that cathepsin K is highly M6P-modified, and loss of mannose phosphorylation leads to enhanced activation. We next tested whether increased activity of cathepsin K in a wild-type background is capable of generating craniofacial defects similar to the zebrafish model of ML-II. For these experiments, WT embryos were injected with either wt-ctsk mRNA, single glycan deleted forms, or double glycan deleted. Analysis of embryos stained with Alcian blue at 4dpf (Figure 3.8) revealed striking cartilage defects when the c-terminal glycan, but not the n-terminal, is deleted. The degree of cartilage

dysmorphogenesis was quantified using multiple parameters, shown schematically in Fig. 3.8B and detailed in Table 3.3. Measurements scored included: 1) a standard length of the embryo, 2) whether Meckels cartilage reached the palate, 3) the shape of the anterior jaw, 4) the angle of the two ceratohyal (CH) cartilages, 5) the presence of Alcian-blue-positive cartilage in pectoral fins, and 6) the presence of cardiac edema. Overexpression of wt ctsk or N23Q led to mild phenotypes in a proportion of embryos, with 14% and 17% of animals exhibiting craniofacial cartilage defects. Surprisingly, overexpression of either form of cathepsin K lacking the c-terminal glycan (N216Q or N23/216Q) led to significantly more severe phenotypes, with 46% and 41% of animals affected respectively. Unlike the ML-II morphants, pectoral fins retained alcian blue staining in all but the most severely affected embryos. Craniofacial cartilage structures were either severely disrupted or unaffected, likely due to differences in systemic expression of cathepsin K. Because a reduction in the overall size of the embryo could distort comparative measurements, we normalized measurements to a standard length and found no statistically significant difference. To further link the generation of these phenotypes to the activity of cathepsin K, we generated a catalytic site mutant that also lacked both glycans (C139S/N23/216Q). This mutant was confirmed to be catalytically inactive and overexpression generated no observable phenotypes (Fig. 3.9). Previous studies showed that inhibition of cathepsin K reduces the abnormal deposition and expression of type II collagen characteristic of ML-II chondrocytes. We

investigated whether overexpression of cathepsin K led to persistent type II collagen expression but found no clear alterations in deposition (data not shown).

Discussion

Animal models for lysosomal storage disorders have proven invaluable tools for investigation of pathological mechanisms underlying these diseases [23-29]. External development and optical clarity throughout embryogenesis make use of zebrafish as a model system well suited to developmental, genetic, and biochemical analysis. Previous investigation of a zebrafish model for ML-II revealed the craniofacial cartilage phenotypes are linked to the elevated activity of cathepsin proteases. These studies uncovered a key role for excessive cathepsin K activity underlying the cartilage defects observed in ML-II embryos [9, 10]. To further explore the role of cathepsin proteases as a molecular basis for these phenotypes, the pH dependent activity of these lysosomal enzymes were characterized. Cathepsins D and L exhibited similar profiles with strongly acidic pH optimums while K and S exhibit optimal activity close to pH 6.0. Cathepsins K and S were further distinguished by the presence of residual activity at neutral pH, while cathepsins D and L strictly require acidic conditions. There are several reports that cathepsins S and K can function in the slightly alkaline environment of the ECM [14, 30-32]. The activity of cathepsin K within the ECM is regulated by its conformational stability, autoproteolysis, and degradation by other proteases including cathepsin S [33, 34]. Binding of sulfated glycosaminoglycans (GAGs) function as allosteric regulators of cathepsin K,

enhancing its stability at neutral pH [34, 35]. Interactions with GAGs have also been shown to facilitate autocatalytic conversion of pro-cathepsins B and S into their mature forms [36, 37].

Most cathepsin proteases utilize the Man-6-P pathway to reach the lysosome, but cathepsins D and H have been shown to make use of independent pathways [38]. Our results indicate that Man-6-P modification of cathepsins is protein-specific. Cathepsins K, L, and S are extensively modified, but cathepsin D is not. Sequence analysis revealed a key N-glycosylation site in human cathepsin D is missing from the zebrafish sequence. Loss of Man-6-P biosynthesis in cells enriched for chondrocytes revealed cathepsins D and S at normal or elevated levels, but cathepsins K and L were largely deficient. To further explore the consequences of impaired Man-6-P trafficking of cathepsin K, mutant glycoforms were expressed in zebrafish and analyzed for CI-MPR column binding and activity. These analyses revealed that utilization of the two N-glycan sites of cathepsin K is not uniform as mutation of N216Q significantly affected Man-6-P mediated column binding. Activity of either the N216Q mutant, or the N23/216Q double mutant was significantly elevated with respect to WT or N23Q cathepsin K. These data suggest that loss of Man-6-P leads to enhanced activation of cathepsin K in zebrafish. Overexpression of mutants lacking the c-terminal glycan exhibited craniofacial cartilage defects, severe cardiac edema, a kinked tail, and an elevation in the activity of cathepsin L. Expression of a catalytic mutant of cathepsin K lacking both glycosylation sites had no

observable phenotype, indicating that these phenotypes are due to the elevated activity and mislocalization of cathepsin K.

The mechanistic basis for increased activity of cathepsin K upon loss of Man-6-P warrants further investigation as the activation of cathepsin K in physiological conditions is still somewhat unclear. Autocatalytic activation *in vitro* requires low pH and mature enzyme for efficient activation, typically occurring within the lysosome [22]. Recent studies from osteoclasts isolated from *GNPTAB-/-* mice have shown cathepsin K is deficient within secretory lysosomes while the localization of cathepsin D is unaffected [18]. These data are consistent with our observations and supports the hypothesis that upon loss of Man-6-P modifications cathepsin K enters constitutive secretory vesicles and is activated by an undefined mechanism, potentially within abnormally acidified vesicles in the secretory pathway. Processing may also result from contact with proteases within the secretory pathway or with cell-surface proteases within the extracellular space. There are several reports of cathepsins functioning to activate other proteases, such as L and S activating C [39]. Investigating the mechanisms that control enzyme secretion and activation are necessary understanding the ML-II disease process.

The craniofacial phenotypes generated upon overexpression of cathepsin K are consistent with those observed in the zebrafish model for ML-II [9]. However, ectopic expression of cathepsin K has led to a significantly more severe cardiac edema as well as a kinked tail phenotype not seen in ML-II animals. It is worth nothing that there are also biochemical aspects of this

approach that are distinct from the characteristics observed in ML-II; cathepsin K is secreted from ML-II cells leading to extracellular activity and a deficient lysosome. This approach addresses only the inappropriate secretion and extracellular activity of cathepsin K, while the lysosome retains normal intracellular cathepsin K content. Restricted expression of cathepsin K, driven by the *fli1* promoter would directly assess the consequence of loss of Man-6-P modified cathepsin K in chondrocytes and whether generation of cartilage defects is cell autonomous.

The basis for the increased activity of cathepsin L upon overexpression of cathepsin K is unclear. The mechanistic basis for this interaction may arise from transcriptional elevation, or enhanced activation due to cathepsin K in compartments it is not normally present. Intralysosomal collagen degradation depends upon the activity of cathepsin L, thus it may be possible collagen fragments stimulate expression of L in a fashion similar to that of K [40, 41]. These results support a relationship between these collagenolytic lysosomal proteases and warrants further study.

In summary, our results demonstrate that loss of mannose phosphorylation of cathepsin K is sufficient to generate craniofacial cartilage defects in zebrafish. These phenotypes resemble those observed in a zebrafish model for ML-II, and also correspond with increased activity of cathepsin L. These results highlight the key regulatory role of mannose phosphorylation of cathepsin K during development and the contribution of specific glycans to Man-6-P dependent trafficking. Further studies are necessary to identify cell-type

specific effects of cathepsin K hypersecretion and the mechanism underlying ML-II phenotypes.

Materials and Methods

Fish strains

Wild-type zebrafish were obtained from Fish 2U (Gibsonton, FL) and maintained using standard protocols. Embryos were staged according to the criteria established by Kimmel (Kimmel et al., 1995). In some cases, 0.003% 1-phenyl-2-thiourea was added to the growth medium to block pigmentation. All MO-generated phenotypes were tested in several genetic backgrounds, including a wild-type strain from a commercial source (Fish 2U). Analyses of craniofacial phenotypes were performed in both the F2U wild-type strain and Tg (*fli1a*:EGFP)*y1* transgenic line (Lawson and Weinstein, 2002). Handling and euthanasia of fish for all experiments were carried out in compliance with University of Georgia's policies. This protocol was approved by the University of Georgia Institutional Animal Care and Use Committee (permit number: A2009 8-144).

Anti-sense morpholino injection and mRNA expression

Expression of N-acetylglucosamine-1-phosphotransferase (αβ subunit, *GNPTAB*) was inhibited by injection of morpholino oligonucleotides (MO) as previously described (Flanagan-Steet et al., 2009). Experiments involving mRNA rescue in

the morphant background were performed following injection of full-length phosphotransferase mRNA as previously described (Flanagan-Steet et al., 2009).

Cathepsin K Cloning, Mutagenesis and mRNA expression

The full-length coding region of *ctsK* was cloned by PCR from a cDNA construct generated by the Zebrafish Genome Collection using the following primers: (5' – CGGGATCCCGCAGAATGGGTA – 3' and 3' – GCTCTAGAGCTCACATGACGGGA – 5') (Thermo Scientific, Waltham, MA.) The resulting product was subcloned into pCSII+ using BamHI and XbaI sites. pCSII-ctsk plasmid DNA was linearized with NotI and full length mRNA was generated with Message Machine SP6 kit (Roche Applied Science, Indianapolis, IN.) Optimal expression of ctsk was determined by ctsk enzyme assays and western blot. Injection of 150pg of purified *ctsk* mRNA at the 1-2 cell stage led to detectable activity without any phenotypic affects. *N*-glycosylation sequon sites were mutated using the QuickChange XL site-directed mutagenesis kit (Agilent Technology, Santa Clara, CA). The N-terminal glycan was mutated using the following primers: (5' – GCTCACTCTCTGGACCAACTCTCTCTGGATGA – 3' and 5' - TCATCCAGAGAGAGTTGGTCCAGAGAGTGAGC – 3') and the c-terminal using (5' – GCAGTGTGCCTACCAGACTTCAGGAGTAGCAG – 3' and 5' – CTGCTACTCCTGAAGTCTGGTAGGCACACTGC - 3'). The active site cysteine of cathepsin K was changed to serine using the following primers: (5' -

CAAGGATCATGCGGCTCCTCTTGGGCGTTCAGCTCTGTTG - 3' reverse: 5' - CAACAGAGCTGAACGCCCAAGAGGAGCCGCATGATCCTTG - 3').

Embryo dissociation and cell sorting

Wild-type and morphant *fli1*:EGFP embryos were collected at the indicated stages, dechorionated and deyolked then dissociated and sorted by Flourescence Activated Cell Scanning (FACS) as previously described (Petrey, et al., 2011).

Protease activity assays

For the protease activity assays, wild-type and morphant embryos were dechorionated, deyolked (as described in embryo dissociation and cell sorting section above), and homogenized on ice by sonication in 10mM Tris pH 6.5, 1% Triton X-100, centrifuged at 15,000 rpm for 10 min at 4C, and the protein concentration determined by Micro-BCA protein assay (Thermo Scientific). Assay kits for Cathepsins D and S were obtained from Anaspec (San Jose, Ca) and assays were performed according to manufacturer's specifications.The activity of Cathepsin K was determined from the rate of hydrolysis of $(Z\text{-Leu-Arg})_2$-Rhodamine 110 purchased from Calbiochem (San Diego, Ca). Substate was dissolved in DMSO at 1mM and stored at -20C prior to use. The activity of Cathepsin L was determined from the rate of hydrolysis of $(Z\text{-Phe-Arg})_2$-R110, purchased from Abbiotec (San Diego, Ca). The substrate was dissolved in distilled water at 1mM and stored at -20C prior to use. All inhibitors were

obtained from Calbiochem and were used at the following final concentrations. EDTA chelates metals inhibiting MMPs, (10 mM); pepstatin A inhibits cathepsin D (1 μM); Cathepsin L inhibitor IV, 1-Naphthalenesulfonyl-Ile-Trp-CHO, selective and reversible, inhibits Cathepsin L (1 μM); Cathepsin K inhibitor II, Boc-Phe-Leu-NHNH-CO-NHNH-Leu-Z, a selective, and reversible inhibitor of cathepsin K (1 μM). The cysteine protease inhibitor E-64 inhibits Cathepsin S (1 μM). For cathepsins K and L, a rhodamine 110 standard was used. Enzyme activity was measured as previously described (Petrey, et al. 2012).

Generation and transfection of glycan-deleted cathepsin K mutants

Wild-type cathepsin K, N23Q, N216Q, or N23/216Q constructs were transfected into CHO cells and media or cell lysates were subjected to CI-MPR lectin chromatography to assess levels of mannose phosphorylation or enzyme activity assays were performed. For secretion assays, transiently transfected CtsK mutants were incubated for 48hrs in serum-free media, collected, concentrated, and subjected to Western blot analysis. Media samples and cell lysates were normalized to total secreted protein using micro BCA protein assay.

M6P receptor affinity column and glycosidase assays

Wild-type and morphant embryo extracts were fractionated using an M6P receptor affinity column as described previously. Activity of lysosomal enzymes was measured in each column fraction using fluorescent substrates: 4 methylumbelliferyl galactoside (for β-galactosidase activity), 4-methylumbelliferyl

glucuronide (for β-glucuronidase activity), and 4-methylumbelliferyl β-*N*-acetylglucosaminide (for β-hexosaminidase activity). Reactions were performed in 50 mmol/L citrate buffer (pH 4.5) and 0.5% Triton X-100 containing 3 mmol/L of the respective substrates. Column fractions were measured for protease activity as described above. The percentage of bound activity relative to total activity recovered from three or more independent experiments.

Embryo extract preparation and immunoblot analysis of cathepsin K

For analysis of cathepsin K in wild-type and morphant embryos, whole animal lysates were prepared by incubation overnight in 3% SDS, 10mM Tris pH 7.4, with sigma protease inhibitor cocktail (Sigma, St. Louis, MO). Lysates were homogenized on ice by sonication, centrifuged at 15,000 rpm for 10 min at 4C, and the protein concentration determined by Micro-BCA protein assay (Thermo Scientific). 100µg of lysate was run on a SDS-PAGE gel and protein was transferred to a nitrocellulose membrane (Bio-rad) and probed with either polyclonal anti-cathepsin K antibody (cat# 19027, Abcam). Immunodetection of β-tubulin was used as a loading control. Secondary goat anti-rabbit antibodies tagged with HRP were used to detect protein by chemiluminesence (GE Healthcare, Piscataway, NJ).

Alcian blue staining and quantification of craniofacial phenotypes

Embryos were stained with Alcian blue as decribed previously. Analysis of craniofacial structures was performed using the morphometric parameters

outlined in the results section. Stained embryos were photographed on an Olympus SZ-16 dissecting scope outfitted with Q-capture software and a Retiga 2000R color camera.

References

1. Do, H., et al., *Human mannose 6-phosphate-uncovering enzyme is synthesized as a proenzyme that is activated by the endoprotease furin.* J Biol Chem, 2002. **277**(33): p. 29737-44.

2. Rohrer, J. and R. Kornfeld, *Lysosomal hydrolase mannose 6-phosphate uncovering enzyme resides in the trans-Golgi network.* Mol Biol Cell, 2001. **12**(6): p. 1623-31.

3. Dahms, N.M., L.J. Olson, and J.J. Kim, *Strategies for carbohydrate recognition by the mannose 6-phosphate receptors.* Glycobiology, 2008. **18**(9): p. 664-78.

4. Kornfeld, S., *Trafficking of lysosomal enzymes.* Faseb J, 1987. **1**(6): p. 462-8.

5. Raas-Rothschild, A., et al., *Molecular basis of variant pseudo-hurler polydystrophy (mucolipidosis IIIC).* J Clin Invest, 2000. **105**(5): p. 673-81.

6. Reitman, M.L. and S. Kornfeld, *Lysosomal enzyme targeting. N-Acetylglucosaminylphosphotransferase selectively phosphorylates native lysosomal enzymes.* J Biol Chem, 1981. **256**(23): p. 11977-80.

7. Reitman, M.L. and S. Kornfeld, *UDP-N-acetylglucosamine:glycoprotein N-acetylglucosamine-1-phosphotransferase. Proposed enzyme for the phosphorylation of the high mannose oligosaccharide units of lysosomal enzymes.* J Biol Chem, 1981. **256**(9): p. 4275-81.

8. Cathey, S.S., et al., *Phenotype and genotype in mucolipidoses II and III alpha/beta: a study of 61 probands.* J Med Genet, 2010. **47**(1): p. 38-48.

9. Flanagan-Steet, H., C. Sias, and R. Steet, *Altered chondrocyte differentiation and extracellular matrix homeostasis in a zebrafish model for mucolipidosis II.* Am J Pathol, 2009. **175**(5): p. 2063-75.

10. Petrey, A.C., et al., *Excessive activity of cathepsin K is associated with cartilage defects in a zebrafish model of mucolipidosis II.* Dis Model Mech, 2012. **5**(2): p. 177-90.

11. Bromme, D., et al., *Human cathepsin O2, a matrix protein-degrading cysteine protease expressed in osteoclasts. Functional expression of human cathepsin O2 in Spodoptera frugiperda and characterization of the enzyme.* J Biol Chem, 1996. **271**(4): p. 2126-32.

12. Bromme, D., et al., *The specificity of bovine spleen cathepsin S. A comparison with rat liver cathepsins L and B.* Biochem J, 1989. **264**(2): p. 475-81.

13. Burleigh, M.C., A.J. Barrett, and G.S. Lazarus, *Cathepsin B1. A lysosomal enzyme that degrades native collagen.* Biochem J, 1974. **137**(2): p. 387-98.

14. Kirschke, H., et al., *Cathepsin S from bovine spleen. Purification, distribution, intracellular localization and action on proteins.* Biochem J, 1989. **264**(2): p. 467-73.

15. Qian, Y., et al., *Functions of the alpha, beta, and gamma subunits of UDP-GlcNAc:lysosomal enzyme N-acetylglucosamine-1-phosphotransferase.* J Biol Chem, 2010. **285**(5): p. 3360-70.

16. Cantor, A.B. and S. Kornfeld, *Phosphorylation of Asn-linked oligosaccharides located at novel sites on the lysosomal enzyme cathepsin D.* J Biol Chem, 1992. **267**(32): p. 23357-63.

17. Marschner, K., et al., *A key enzyme in the biogenesis of lysosomes is a protease that regulates cholesterol metabolism.* Science, 2011. **333**(6038): p. 87-90.

18. van Meel, E., et al., *Disruption of the Man-6-P targeting pathway in mice impairs osteoclast secretory lysosome biogenesis.* Traffic, 2011. **12**(7): p. 912-24.

19. Covassin, L., et al., *Global analysis of hematopoietic and vascular endothelial gene expression by tissue specific microarray profiling in zebrafish.* Dev Biol, 2006. **299**(2): p. 551-62.

20. Gottesman, M.M., *Transformation-dependent secretion of a low molecular weight protein by murine fibroblasts.* Proc Natl Acad Sci U S A, 1978. **75**(6): p. 2767-71.

21. Bromme, D. and K. Okamoto, *Human cathepsin O2, a novel cysteine protease highly expressed in osteoclastomas and ovary molecular cloning, sequencing and tissue distribution.* Biol Chem Hoppe Seyler, 1995. **376**(6): p. 379-84.

22. McQueney, M.S., et al., *Autocatalytic activation of human cathepsin K.* J Biol Chem, 1997. **272**(21): p. 13955-60.

23. Hubler, M., et al., *Mucolipidosis type II in a domestic shorthair cat.* J Small Anim Pract, 1996. **37**(9): p. 435-41.

24. Gelfman, C.M., et al., *Mice lacking alpha/beta subunits of GlcNAc-1-phosphotransferase exhibit growth retardation, retinal degeneration, and secretory cell lesions.* Invest Ophthalmol Vis Sci, 2007. **48**(11): p. 5221-8.

25. Haskins, M.E., *Animal models for mucopolysaccharidosis disorders and their clinical relevance.* Acta Paediatr Suppl, 2007. **96**(455): p. 56-62.

26. Simonaro, C.M., et al., *Mechanism of glycosaminoglycan-mediated bone and joint disease: implications for the mucopolysaccharidoses and other connective tissue diseases.* Am J Pathol, 2008. **172**(1): p. 112-22.

27. Metcalf, J.A., et al., *Upregulation of elastase activity in aorta in mucopolysaccharidosis I and VII dogs may be due to increased cytokine expression.* Mol Genet Metab, 2009.

28. Boonen, M., et al., *Mice lacking mannose 6-phosphate uncovering enzyme activity have a milder phenotype than mice deficient for N-acetylglucosamine-1-phosphotransferase activity.* Mol Biol Cell, 2009. **20**(20): p. 4381-9.

29. Vogel, P., et al., *Comparative pathology of murine mucolipidosis types II and IIIC.* Vet Pathol, 2009. **46**(2): p. 313-24.

30. Scott, P.G. and C.H. Pearson, *Cathepsin D: cleavage of soluble collagen and crosslinked peptides.* FEBS Lett, 1978. **88**(1): p. 41-5.

31. Ishidoh, K. and E. Kominami, *Procathepsin L degrades extracellular matrix proteins in the presence of glycosaminoglycans in vitro.* Biochem Biophys Res Commun, 1995. **217**(2): p. 624-31.

32. Konttinen, Y.T., et al., *Acidic cysteine endoproteinase cathepsin K in the degeneration of the superficial articular hyaline cartilage in osteoarthritis.* Arthritis Rheum, 2002. **46**(4): p. 953-60.

33. Barry, Z.T. and M.O. Platt, *Cathepsin S cannibalism of cathepsin K as a mechanism to reduce type I collagen degradation.* J Biol Chem, 2012. **287**(33): p. 27723-30.

34. Novinec, M., et al., *Conformational flexibility and allosteric regulation of cathepsin K.* Biochem J, 2010. **429**(2): p. 379-89.

35. Cherney, M.M., et al., *Structure-activity analysis of cathepsin K/chondroitin 4-sulfate interactions.* J Biol Chem, 2011. **286**(11): p. 8988-98.

36. Caglic, D., et al., *Glycosaminoglycans facilitate procathepsin B activation through disruption of propeptide-mature enzyme interactions.* J Biol Chem, 2007. **282**(45): p. 33076-85.

37. Vasiljeva, O., et al., *Recombinant human procathepsin S is capable of autocatalytic processing at neutral pH in the presence of glycosaminoglycans.* FEBS Lett, 2005. **579**(5): p. 1285-90.

38. Canuel, M., et al., *Sortilin mediates the lysosomal targeting of cathepsins D and H.* Biochem Biophys Res Commun, 2008. **373**(2): p. 292-7.

39. Dahl, S.W., et al., *Human recombinant pro-dipeptidyl peptidase I (cathepsin C) can be activated by cathepsins L and S but not by autocatalytic processing.* Biochemistry, 2001. **40**(6): p. 1671-8.

40. Robinson, M.W., et al., *Collagenolytic activities of the major secreted cathepsin L peptidases involved in the virulence of the helminth pathogen, Fasciola hepatica.* PLoS Negl Trop Dis, 2011. **5**(4): p. e1012.

41. Gruber, H.E., et al., *Constitutive expression of cathepsin K in the human intervertebral disc: new insight into disc extracellular matrix remodeling via cathepsin K and receptor activator of nuclear factor-kappaB ligand.* Arthritis Res Ther, 2011. **13**(4): p. R140.

Figures

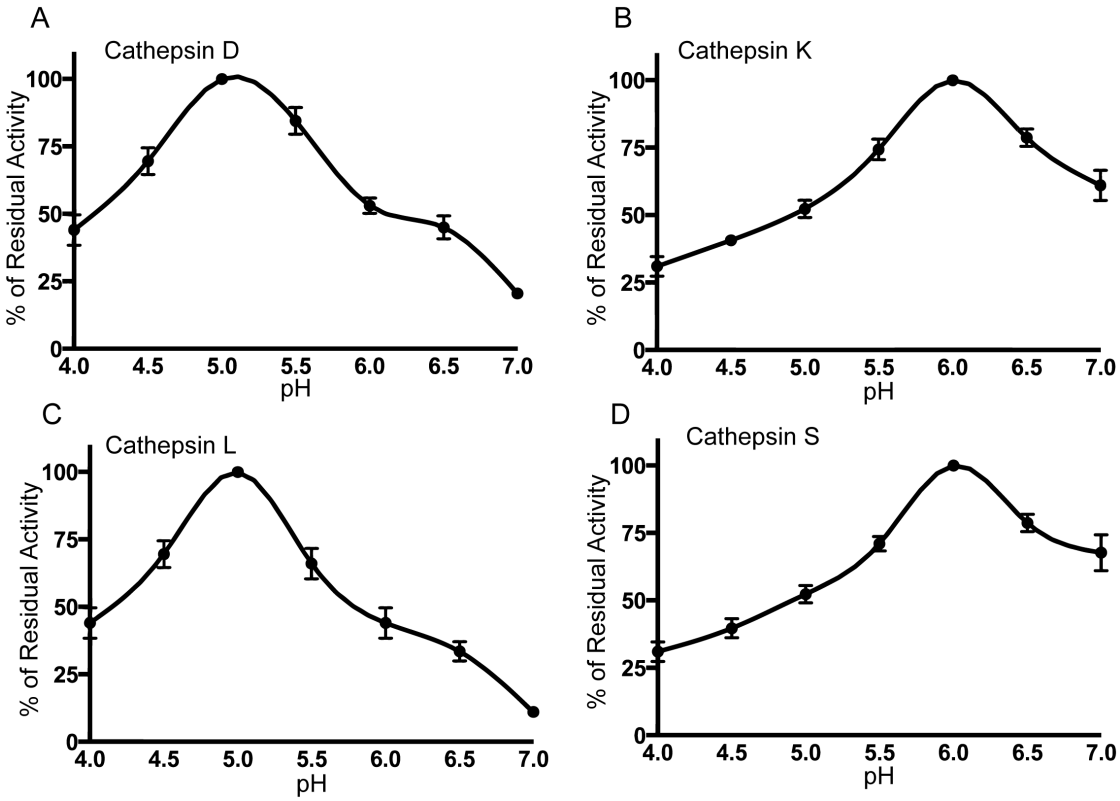

Figure 3.1. Enzymatic activity profile of zebrafish cathepsins. Cathepsin activity was measured at 2dpf from WT detergent lysates and is plotted as percent of peak activity. Activity values are based on the rate of hydrolysis of cathepsin-specific fluorogenic peptide substrates.

Table 3.1. Mannose phosphorylation of zebrafish cathepsins. Detergent extracts from adult brain or 3dpf wild-type and morphant embryos were fractionated over the CI-MPR column. Bound activity relative to total activity was determined. For embryos, n represents the number of independent assays of 20 fish.

	% of activity bound to CI-MPR column		
Lysosomal hydrolase	WT Brain (n=10)	WT Embryos (n=7)	ML-II Embryos (n=7)
β-Hexosaminidase	23.3 ± 3.2	18.3 ± 5.4	9.4 ± 2.8
Cathepsin D	24.2 ± 8.4	16.4 ± 4.8	5.0 ± 2.1
Cathepsin K	93.1 ± 4.0	86.2 ± 5.5	17.2 ± 3.7
Cathepsin L	88.8± 3.6	82.6 ± 3.9	23.7 ± 8.8
Cathepsin S	70.7 ± 15.9	65.8 ± 11.2	30.1 ± 15.5

Table 3.2. Concanavalin A binding of Cathepsin D. Detergent extracts from adult brain were fractionated over a ConA column. Bound activity relative to total activity was determined as a measure of oligomannosyl glycans. Endo Hf treatment was used as a control.

	% of activity bound to ConA column	
Lysosomal hydrolase	- Endo Hf (n=3)	+ Endo Hf (n=3)
Cathepsin D	27 ± 5	5 ± 4

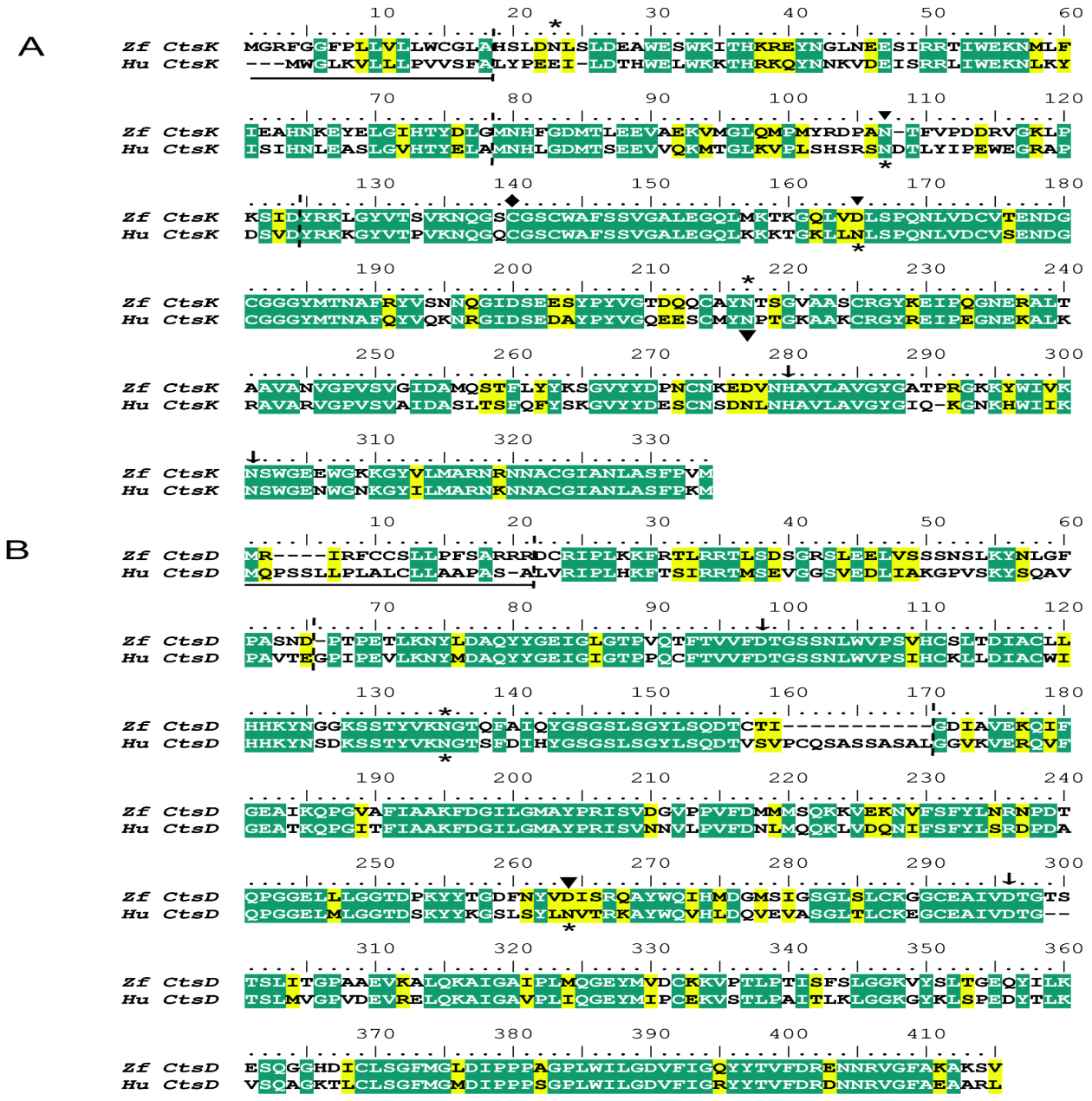

Figure 3.2. Amino acid alignment of zebrafish cathepsins D and K with their human homologues. Sequence identity is highlighted in blue and similarity in yellow. Numbering is based on the zebrafish sequence with the initial methionine assigned as 1. The underline indicates the pre-petide, and the vertical dashed line denotes regions of known proteolytic processing of the human enzymes. N-glycosylation sequons are indicated by the presence of an adjacent asterisk and a triangle denotes the absence of a sequon in the corresponding homologue. Arrows indicate catalytic residues, and the diamond denotes the position of a catalytic site mutant described later in the text. Sequence data from the NCBI protein database were aligned using ClustalW.

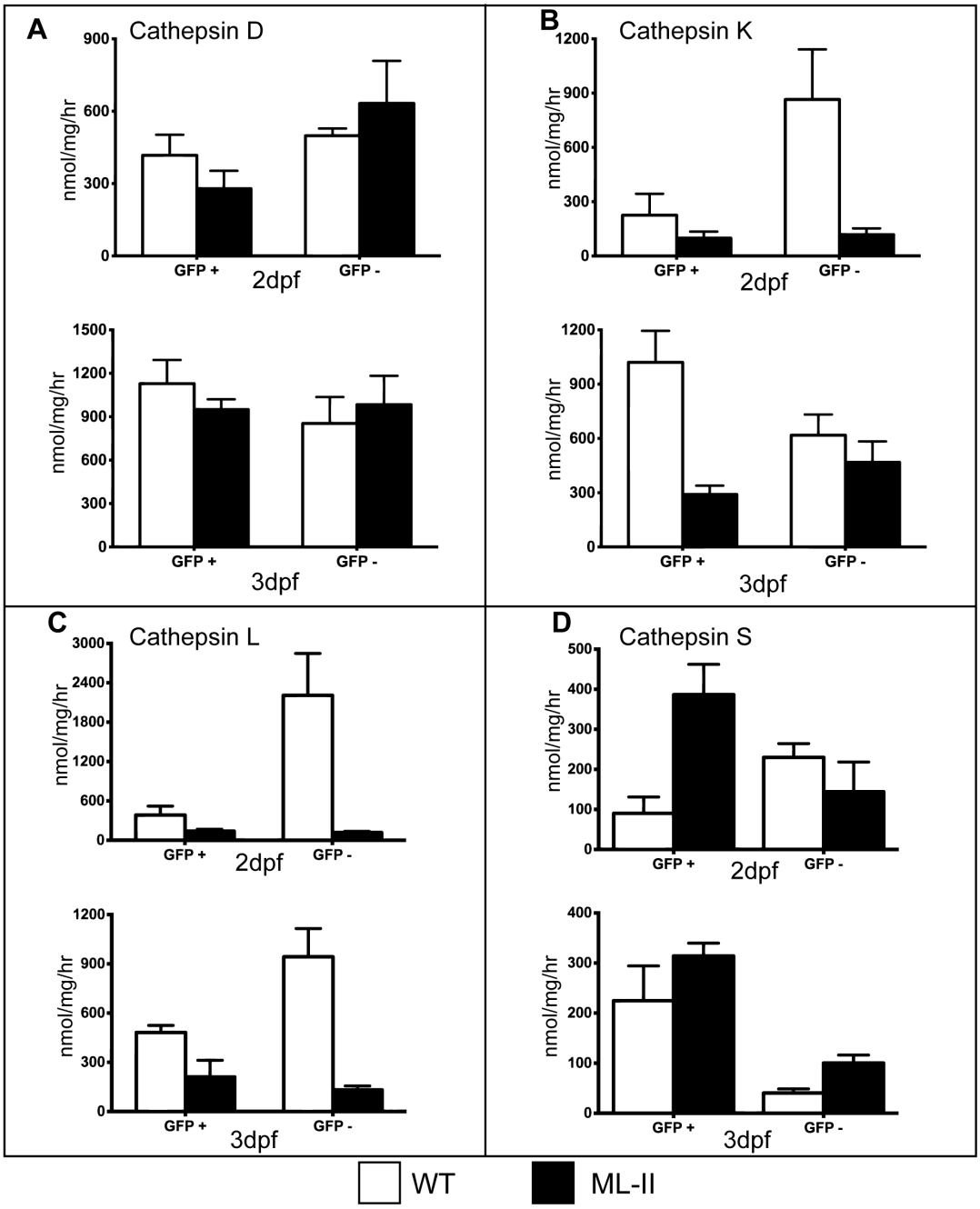

Figure 3.3. Cathepsins K and L are deficient within isolated chondrocyte cell populations. WT and ML-II *fli1a*:EGFP embryos were dissociated and enriched for chondrocytes by FACS at 2 and 3dpf. Cell lysates were assayed for intracellular cathepsin protease activity using specific fluorogenic substrates. Activity measurements were performed on three independent cellular isolations.

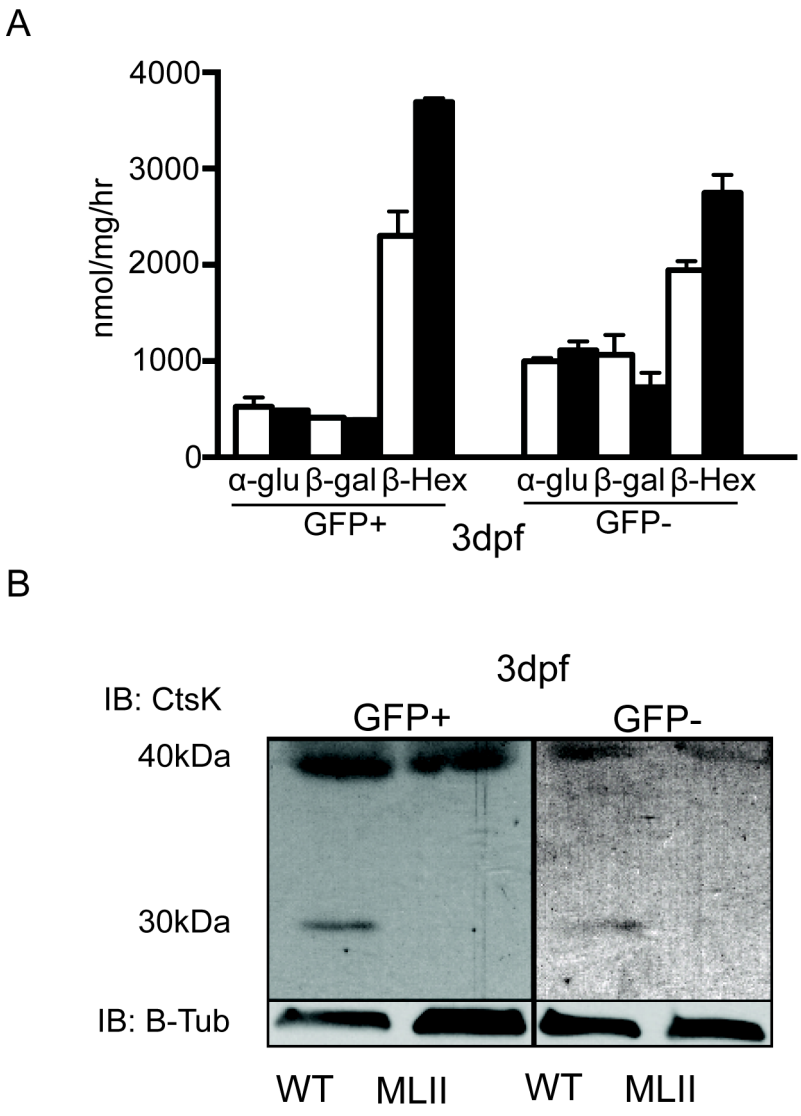

Figure 3.4. Selective hypersecretion in isolated ML-II chondrocytes. Isolated GFP+ and GFP- cells were collected from WT and ML-II embryos at 3dpf. (A) Intracellular glycosyl hydrolase activity was measured and normalized to total protein. (B) Cathepsin K immunoblots show intracellular loss of mature enzyme at steady state within GFP+ and GFP- ML-II cells. β-tubulin was used as a loading control.

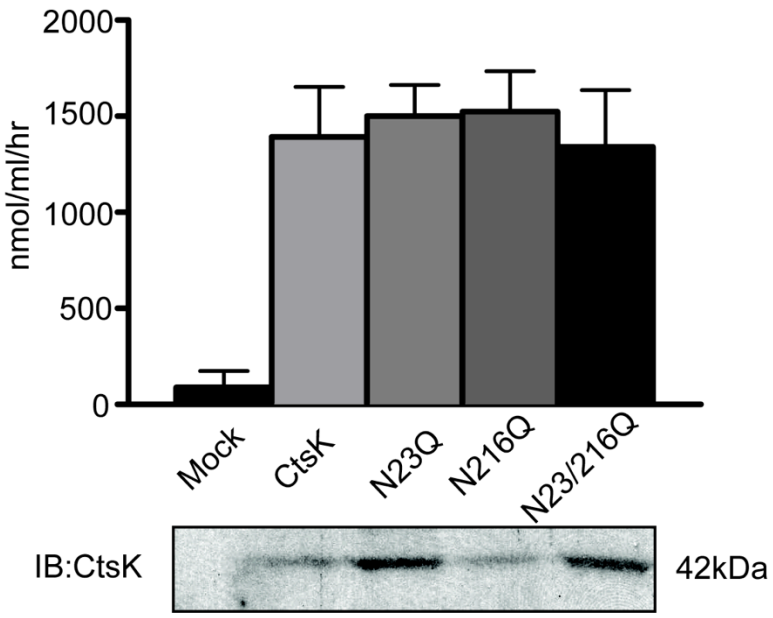

Figure 3.5. Heterologously expressed zebrafish cathepsin K is secreted into the media of cultured cells. Forms of cathepsin K were transiently transfected into CHO cells. Media was collected after 48 hours, concentrated, and then assayed for cathepsin activity and immunoblotted for the presence of cathepsin K.

Table 3.3. Concanavalin A binding of zebrafish cathepsin K. Detergent lysates of zebrafish brain or concentrated media from transfected CHO cells were fractionated over a ConA column. Bound activity relative to total activity was determined as a measure of oligomannosyl glycans.

	% of activity bound to ConA column	
Lysosomal hydrolase	Zebrafish Brain (n=3)	CHO Media (n=3)
Cathepsin K	88 ±7	79± 11

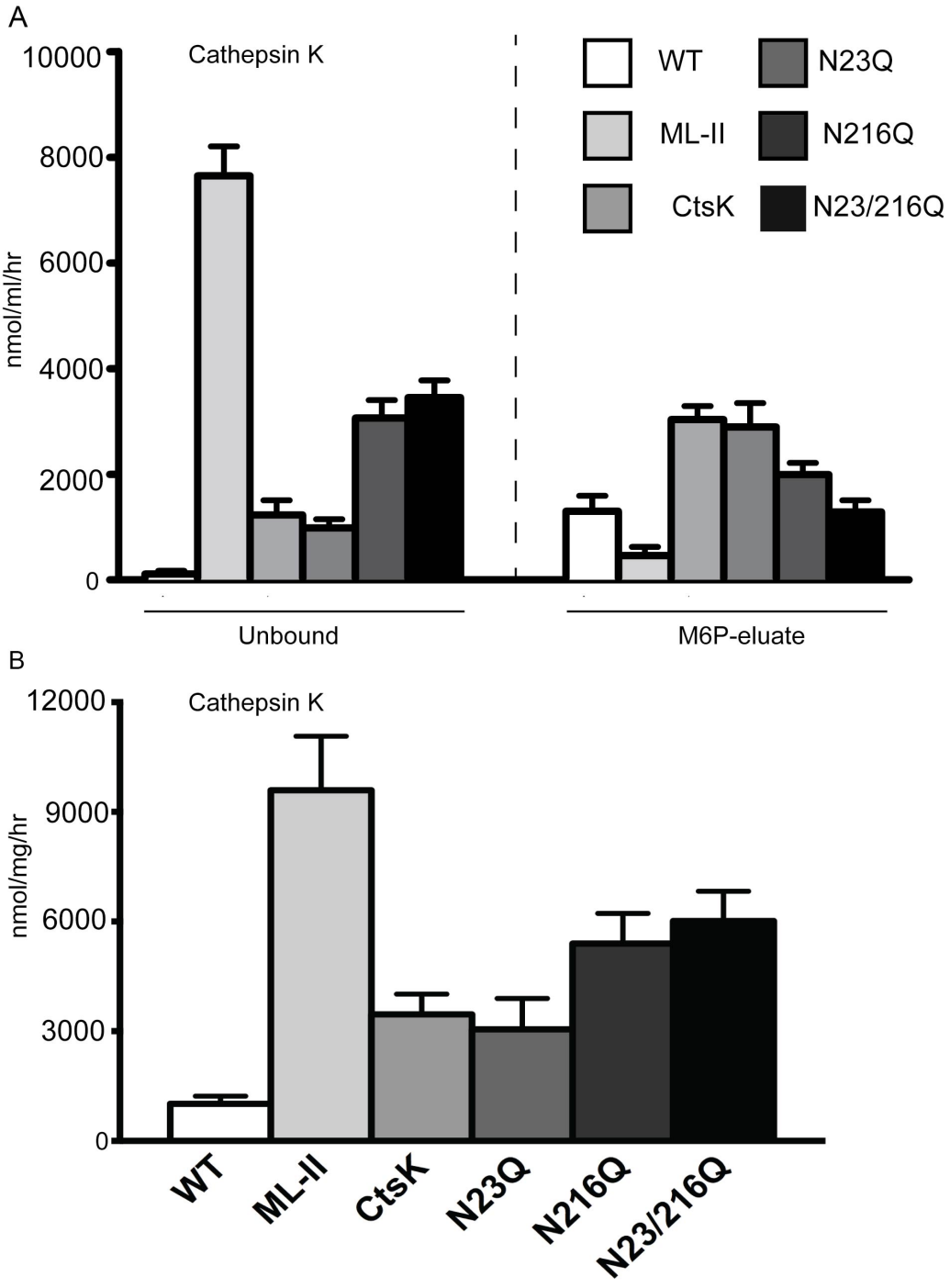

Figure 3.6. Loss of Man-6-P modification of cathepsin K corresponds with increased activity. Cathepsin K activity was measured in WT, ML-II, CtsK, N23Q, N216Q, and N23/216Q embryos. (A) Detergent extracts from 3dpf embryos were normalized for total protein, fractionated over the CI-MPR column, and assayed for cathepsin K activity. The binding profile indicates that loss of the c-terminal glycan reduces CI-MPR binding. (B) Cathepsin K activity measured at 3dpf from whole embryo lysates shows that the N216Q mutation leads to increased activity.

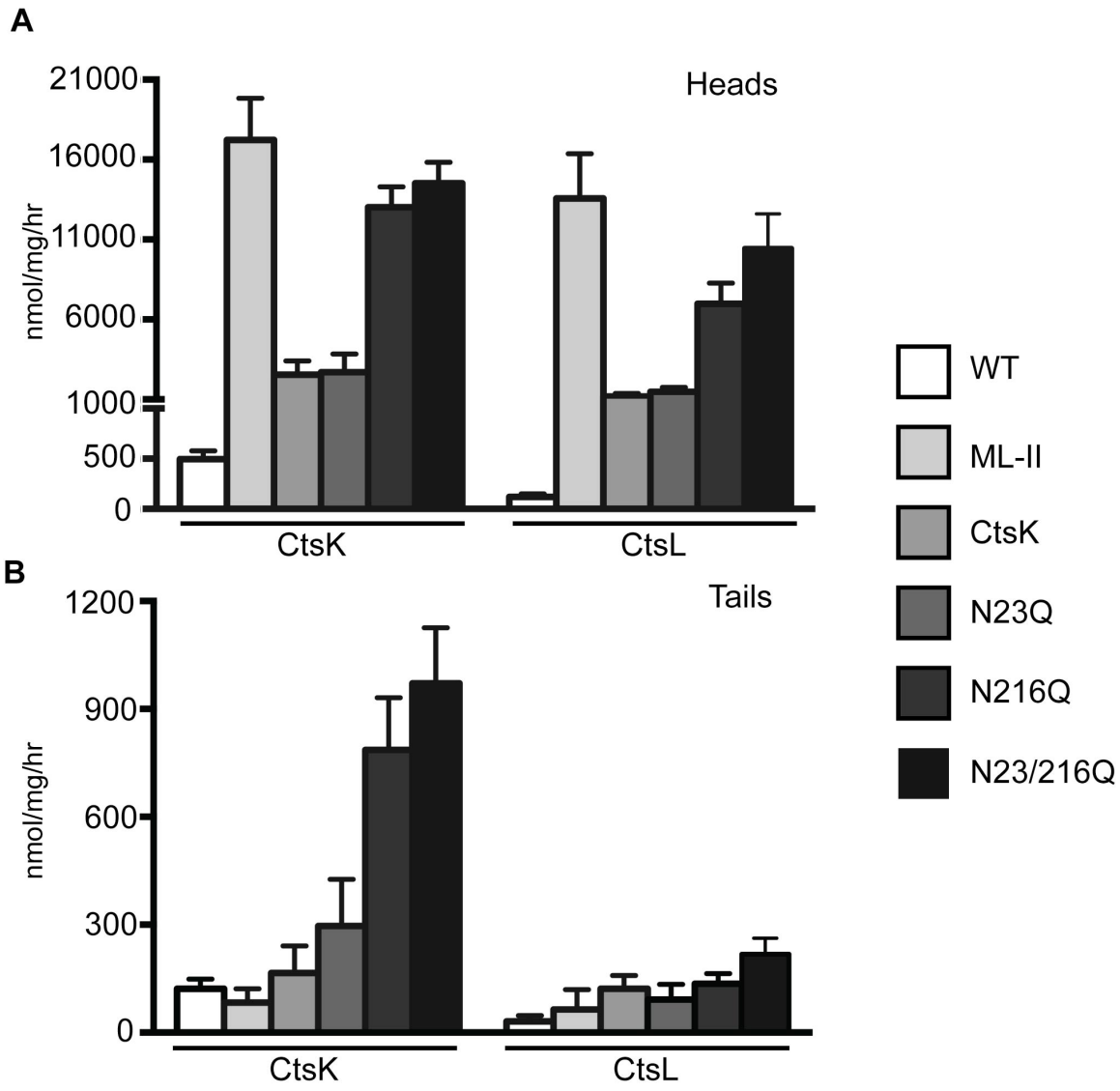

Figure 3.7. Cathepsin K and L activity is elevated in zebrafish heads and tails upon loss of Man-6-P. Analysis of cathepsin K and L activity in 3dpf lysates from WT, ML-II, CtsK, N23Q, N216Q, and N23/216Q embryos. (A) mRNA expression of forms of cathepsin K leads to elevated cathepsin L activitiy in the head. (B) mRNA expression of cathepsin K leads to a dramatic increase in activity localized within tails.

A

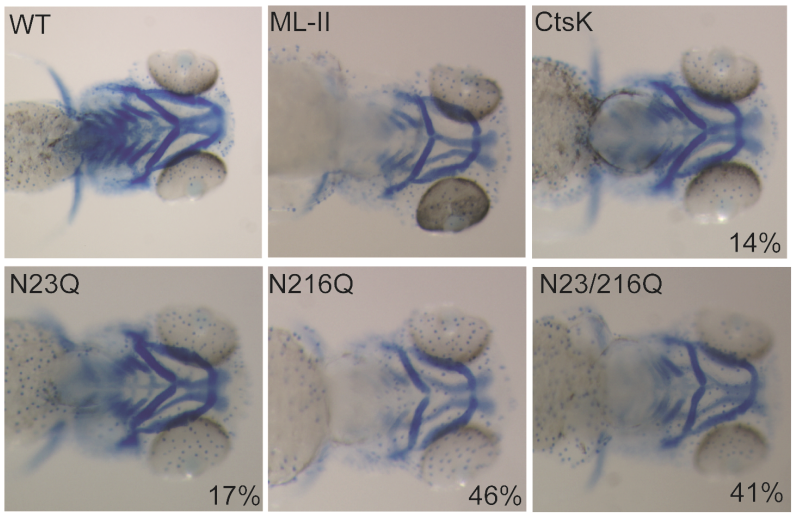

B

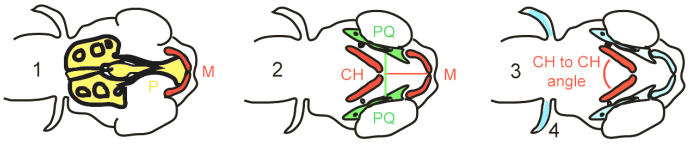

C

	WT (n=30)	ML-II (n=72)	CtsK (n=76)	N23Q (n=60)	N216Q (n=65)	N23/216Q (n=76)
Standard Length	231.13	225.24	228.31	229.67	230.62	231.87
Meckels	126.05	90.19	114.13	118.37	99.40	103.08
Ceratohyal	160.30	115.11	149.10	153.45	126.61	134.08
(1) Meckels meets Palate	100%	0.0%	86.5%	83.7%	54.3%	59.6%
(2) PQ - PQ / M - CH	1.37	1.79	1.42	1.44	1.56	1.51
(3) CH to CH angle	87±4°	144±5°	95±14°	92±13°	122±19°	110±21°
(4) % stained pectoral fins	100%	0.0%	100%	100%	96%	97%

Figure 3.8. Overexpression of cathepsin K leads to craniofacial cartilage defects. mRNA forms of CtsK, N23Q, N216Q, and N23/216Q were expressed in embryos and (A) analyzed by alcian blue staining. (B) Several cartilage elements were measured and the degree of craniofacial disruption was measured using the following: (1) whether Meckels cartilage (M) meets the palate, (2) the "shape" of the jaw using the ratio of the distance between the palatoquadrate (PQ) bones over the distance from Meckels (M) cartilage to the ceratohyal (CH) bones, (3) the angle between the left and right ceratohyals (CH), and (4) whether the pectoral fins stained positively with Alcian blue.

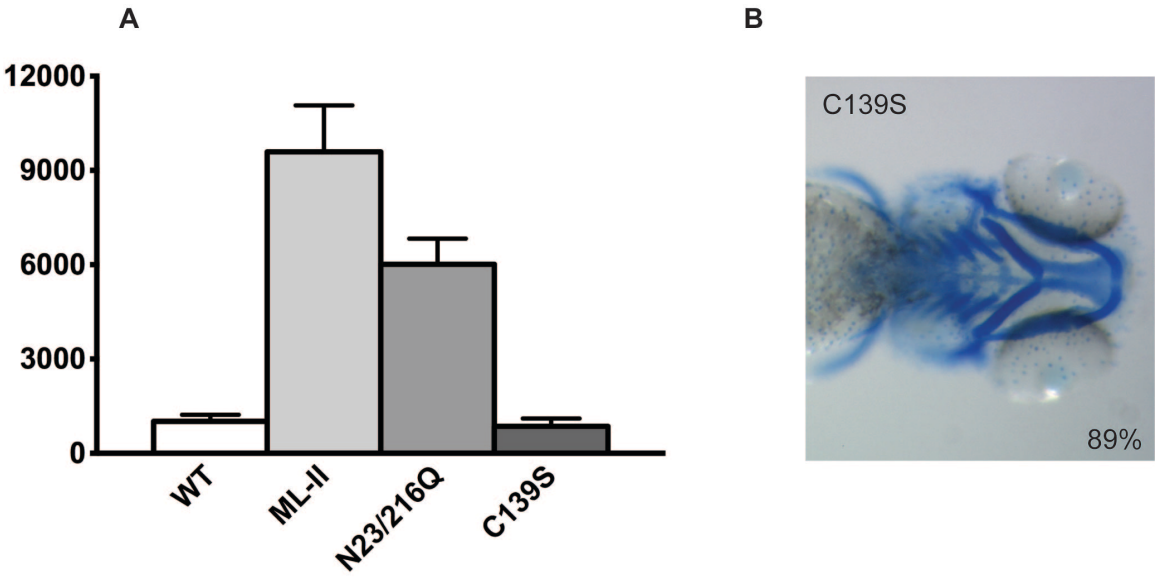

Figure 3.9. Overexpression of catalytically inactive cathepsin K lacking N-glycans does not alter craniofacial cartilage morphology. mRNA forms of cathepsin K with both glycans deleted (N23/216Q), and also with an inactive catalytic site (C139S) were expressed in embryos and assayed for activity. (A) The C139S mutant effectively abolishes catalytic activity of cathepsin K. (B) Several cartilage elements were assessed following expression of the catalytically inactive form of cathepsin K lacking both glycans (C139S). Expression of this form of cathepsin K generated no phenotypes, suggesting the dysmorphogenesis previously shown is a consequence of cathepsin K activity.

CHAPTER 4: INCREASED MATRIX METALLOPROTEINASE ACTIVITY IS A GENERAL FEATURE OF MUCOLIPIDOSIS II[3]

[3] Petrey, A.C., et al. To be submitted to the Journal of Biological Chemistry.

Abstract

Lysosomal storage disorders (LSDs) are inherited metabolic disorders resulting from the defective catabolism of material destined for degradation within the lysosome. Mucolipidosis II (ML-II; I-cell disease), is recognized as one of the most clinically severe LSDs and is caused by defects in mannose 6-phosphate (M6P) biosynthesis. Patients exhibit multiple developmental defects including skeletal, craniofacial and joint abnormalities. Utilizing an ML-II zebrafish model, we previously showed that the cartilage defects are associated with altered chondrocyte differentiation, elevated levels of type II collagen, and increased transcripts of matrix metalloproteinases (MMPs). In this report, we find that the activity of MMPs are elevated at early developmental time points in an ML-II zebrafish model. This elevated activity was localized to the head, enriched within chondrocytes and osteoblasts, and largely due to the increased level of MMP-13. Further, this activity was rescued upon suppression of cathepsin K and is also present within a feline model for ML-II, suggesting it is a general feature of the disease. We further investigated potential mechanisms underlying the increased expression of these proteases and found elevated transcripts in cDNA isolated from ML-II fibroblast-like synoviocytes. These data identify several proinflammatory cytokines as novel therapeutic targets for the treatment of bone and join pathologies in ML-II.

Introduction

Lysosomal storage disorders (LSDs) are a group of rare, progressive disorders that affect multiple organ systems. A hallmark of these diseases is the progressive deterioration of bone and joints, leading to significant health impact [1-4]. Mucolipidosis II (ML-II) is a severe LSD with patients exhibiting skeletal dysplasia, coarsening of the face, and joint abnormalities, present at birth [5-9]. Although the primary genetic defect in ML-II is well characterized, it is not understood how loss of mannose-6-phosphate (M6P) lysosomal targeting leads to the underlying symptoms. Recent advances have highlighted the contribution of the extracellular matrix (ECM) in the pathology of the mucopolysaccharidoses (MPS), a class of related storage disorders [10-14]. In both ML-II and the MPSs, lysosomal dysfunction is believed to lead to disruption or activation of secondary molecular pathways that contribute to the bone and cartilage abnormalities.

Identification of these secondary pathways is important as it provides a therapeutic approach designed to reduce symptoms without having to replace defective enzymes or genes. Insights into the cartilage pathology of ML-II have been hampered in part due to the lack of a genetically accessible, early developmental model of the disease. In a zebrafish model for ML-II, our lab has demonstrated that the cartilage defects in fish embryos are accompanied by changes in the expression profile of several classes of proteases and ECM proteins including collagens, lamanin, aggrecan, and matrix degrading enzymes including cathepsins and matrix metalloproteinases (MMPs) [15, 16]. Loss of

ECM homeostasis can lead to abnormal release of growth factors stored within the matrix, abnormal initiation of signal transduction, and affect the development and differentiation of cartilage precursors. Matrix degrading enzymes including cathepsins, a disintegrin and metalloproteinase with thrombospondin motifs (ADAMTS), and MMPs can be stimulated by the presence of cytokines and growth factors generated as a result of matrix degradation [17-19]. Several studies utilizing animal models of MPS disorders have identified increases in the transcript abundance of MMPs and inflammatory cytokines as a consequence of lysosomal dysfunction and storage [10-12, 14, 20].

Taking advantage of early developmental methods amenable to the zebrafish system, in combination with a feline model representing the later stages of ML-II, we investigated the role of lysosomal dysfunction in impaired ECM homeostasis. The aim of this study was to characterize the involvement of MMPs in these two models of ML-II with a long-term goal of using these findings to explore the mechanistic basis of LSDs. Our results show that the transcript abundance of MMPs reported in Chapter 2 corresponds with elevated MMP activity. This abnormal protease activity is elevated and sustained throughout early development in zebrafish ML-II embryos. We further demonstrate that the MMPs are present in their active form, and this elevated activity is specific to the loss of GlcNAc-1-phosphotransferase activity. The activity and steady-state level of MMPs, in particular MMP-13, are elevated in zebrafish and in a feline ML-II model, suggesting it is a general feature of the disease. Further, elevated MMP activity is rescued to normal levels upon ablation of cathepsin K activity in ML-II

zebrafish. Analysis of feline fibroblast-like synoviocytes (FLSs) from both ML-II and Maroteaux–Lamy syndrome (MPS VI) reveal the increased transcript abundance of several pro-inflammatory cytokines and effector proteins, suggesting these molecules may be the molecular basis for increased expression of the MMPs. Together, these data suggest that MMPs play a role in the pathology of ML-II in development and at later stages of the disease.

Results

Matrix Metalloproteinase activity is sustained and elevated in zebrafish ML-II embryos.

Transcript abundance profiling of isolated populations of zebrafish cells enriched for chondrocytes revealed that the transcripts for *MMP-13* and other MMPs were elevated in both GFP+ and GFP- cells isolated from a *Tg(fli1a*:EGFP) zebrafish model for ML-II [16]. To explore whether MMP activity was increased in ML-II embryos, total MMP activity was measured by hydrolysis of a FRET-based peptide substrate with broad specificity for this class of proteases. This increase was particularly evident at later developmental stages (5dpf). As shown in Figure 4.1A, general MMP activity in WT embryos was high at 1 and 2 dpf but decreased in later stages. In ML-II embryos, activity was increased and sustained; mirroring the profile previously reported for cathepsins K and L. MMP activity was largely abated in mRNA rescued embryos, suggesting that increased expression of MMPs is a result of lysosomal dysfunction due to

loss of Man-6-P targeting (Fig 4.1B). Because MMPs are synthesized as inactive zymogens that require proteolytic processing of their inhibitory pro-petide for activation, we examined whether the MMPs detected existed as a mature enzyme or weakly catalytic proenzymes. Treatment of embryo lysates with 4-amino phenylmercuric acetate (APMA) a general activator of MMPs, resulted in a 26% increase in MMP activity in both WT and ML-II embryos (Fig. 4.1C). The modest degree of APMA-stimulated activation suggests that the MMPs assayed in both WT and ML-II embryos were already processed to their mature forms. Consistent with their dependence on zinc ions, general MMP activity in embryo lysates could be effectively inhibited in the presence of EDTA. Taken together, these data show that MMPs are present at high levels in ML-II embryos at developmental stages that correspond to the maturation and formation of craniofacial cartilage, and are processed into their active forms.

Matrix Metalloproteinases are elevated in the head, and cell populations enriched for chondrocytes, but not osteoblasts in ML-II zebrafish.

We next explored whether MMP activity was elevated in the head and in specific cell types relevant to the craniofacial defects in our ML-II model. WT and ML-II embryos were separated into head and tail sections and each of these pools was assayed for MMP activity. The results of this analysis clearly demonstrated that the vast majority of MMP activity is present in the heads of ML-II embryos (Fig. 4.2A). Activity was also elevated in the tail relative to WT but represents only a fraction of total activity, suggesting that these enzymes might

be upregulated in cell types that are enriched within the head. We next generated ML-II morphants in *Tg(fli1a*:EGFP) or *Tg(osx:*EGFP) embryos and sorted cells by FACS to enrich for either chondrocytes or osteoblasts. *Tg(fli1a*:EGFP) embryos express EGFP in endothelial cells, certain hematopoietic cells, and neural crest-derived cells which give rise to chondrocytes and craniofacial cartilage, while *Tg(osx*:EGFP) embryos express EGFP in osteoblasts, a subset of the mesenchyme associated with bone development [21, 22]. To determine if either population of cells may contribute to the cartilage phenotypes seen in ML-II, embryos were dissociated and subject to FACS sorting to enrich for either chondrocytes or osteoblasts in GFP+ cells from *fli1a* or *osx* embryos, respectively. Analysis of these cell populations revealed elevated MMP activity in GFP+ cells isolated from *Tg(fli1a*:EGFP) ML-II embryos at 2 and 3dpf (Fig. 4.2B), while the activity in GFP- cells was relatively normal. This finding was reversed within the *Tg(osx:*EGFP) embryos at 3dpf, as MMP activity was slightly reduced within GFP+ osteoblasts, and substantially increased in GFP- cells (Fig. 4.2D). These data suggest that MMP activity is elevated within chondrocytes, but not osteoblasts in ML-II animals, suggesting that alterations in protease activity is cell-type specific possibly due to the nature of ECM molecules expressed by these cells.

MMP-13 activity and steady-state levels are significantly increased in ML-II embryos.

In light of the broad specificity of the MMP substrate used in our initial experiments and the redundant substrate specificity of MMPs, the source of increased MMP activity was investigated further by using a substrate with high specificity for MMP-12 and MMP-13. As shown in Figure 4.3A, increases in MMP-12/13 activity comparable to those detected with the general MMP substrate were observed in ML-II embryos. This suggests that one or both of these proteases account for the elevated MMP activity observed with the general substrate. Using an MMP-13 specific antibody, western blot analysis of detergent lysates was performed (Fig. 4.3B). Not only were total MMP-13 levels increased in ML-II embryos, but also that the enzyme was primarily present in its mature, activated form, confirming both the APMA-mediated activation experiment (Fig 4.1C) and the MMP-12/13 substrate results presented above. This data is consistent with the expression profile of these proteases, as MMP-12 is primarily expressed within macrophages and likely represents a fraction of total MMP activity while MMP-13 is more ubiquitously expressed.

MMP activity is reduced upon suppression of cathepsin K in ML-II embryos.

Our previous studies showed that suppression of cathepsin K by pharmacological or genetic means recovered the elevated activity of other cathepsins to relatively normal levels [16]. To address whether this relationship also existed between cathepsin K and the MMPs, activity was analyzed after

cathepsin K suppression. As shown in Figure 4.4A and 4.4B, reduction in the activity of cathepsin K by either method results in a decrease of general MMP activity, though not to the same degree seen with the cathepsins (Fig. 2.6).

Inhibition of MMP-13 does not reduce the activity of cathepsin proteases in a ML-II zebrafish model.

As mentioned above, inhibition or suppression of cathepsin K led to reduced activity of other cathepsins and MMPs as well as correction of several craniofacial defects observed in our zebrafish ML-II model [16]. In light of these findings, and the significantly increased presence of MMP-13 (Figs. 4.3B,C) we addressed whether inhibition of MMP-13 could also correct these biochemical and phenotypic characteristics. Administration of a MMP-13 specific inhibitor led to no significant reduction in the activity associated with either cathepsin K or L (Figure 4.5). Further, no correction of craniofacial cartilage was observed (data not shown). Inhibition of MMP-13 by this method suggests that the relationship between cathepsin K and MMP-13 is not bi-directional.

MMP activity is elevated in a feline model of ML-II and is a general feature of the disease.

Increased ECM disruption and MMP activity has been noted in several tissues from animal models of lysosomal storage disorders, including MPS I, VI, and VII [10-14, 23]. Because the elevated MMP activity in ML-II embryos could represent a zebrafish-specific phenomenon, this activity was investigated in

fibroblast-like synoviocytes and from feline models of ML-II and MPS-VI. As shown in figure 4.6, the level of cell-associated MMP activity was significantly higher in ML-II synoviocytes relative to WT. Further, as noted in the zebrafish model, activity was fully inhibited by EDTA and treatment with APMA revealed these MMPs are also present as mature enzymes. General MMP activity was also elevated in MPS-VI cells, but to a lesser extent compared with ML-II cells. We further investigated the level of the MMPs in tissues isolated from the feline model of ML-II, as it represents a later time point in the progression of the disease.

Proinflammatory cytokine transcripts are elevated in feline ML-II and MPS VI synovial fibroblasts.

Pathological inflammation and cartilage destruction relies upon the inflamed synovial tissue to activate catabolic pathways within surrounding cells. In RA and MPS disorders, the synovial membrane is infiltrated by proinflammatory cytokine-producing macrophages, resulting in a state of chronic inflammation leading to cartilage, bone loss, and osteopenia [11, 18, 24-26]. Several studies have shown that inflammation is a consequence of GAG storage, and that GAGs can stimulate the inflammatory pathway via mechanisms similar to lipopolysaccharide (LPS) [14]. To explore whether the mechanistic basis of MMP expression might stem from the expression of inflammatory cytokines, RT-PCR was performed in synovial tissue isolated from ML-II and MPS VI feline joints. As shown in Figure 4.7, the several genes involved in inflammation are

transcriptionally elevated in synovium from ML-II and MPS VI animals. Pro-inflammatory cytokines TNF-α, IL-1β, and TGF-β are elevated in ML-II and MPS VI FLSs, and could explain the increased activity and transcription of MMP-13. Toll-like receptors 2 and 4 (TLR4), are a well studied components of the innate immune response and recognize the presence of pathogen-related molecules, including LPS [14, 27-30]. Consistent with observations in other MPS models, TLR4 and the related TLR2 were found significantly elevated in MPS VI, and surprisingly, in ML-II [14]. Additionally, the transcription factor EB (TFEB), known to function as a regulator of lysosomal biogenesis and autophagy, was found at elevated levels in both ML-II and MPS VI [31]. Phosphorylation of TFEB, by extracellular-signal related kinase (ERK) prevents TFEB nuclear translocation and transcriptional induction [32]. Immunoblotting revealed that the expression of ERK1/2 was reduced in ML-II, but present at relatively normal levels in MPS VI FLSs, suggesting that TFEB-mediated signaling could be initiated in ML-II, but not MPS VI. These findings support the hypothesis that storage of GAGs leads to an inflammatory response in MPS disorders and suggest that a similar mechanism may be present in ML-II synovium.

Discussion

Accumulation of undigested material within lysosomes is viewed as the primary pathological defect in LSDs including ML-II and MPS VI. However, the mechanism by which storage leads to defects in cartilage and bone are still not

well understood. GAG accumulation in the MPS disorders and RA has been shown to promote the proliferation of macrophages and other immune cells, resulting in inflammation and bone destruction [17, 26, 33-36]. Animal models have proven useful tools for uncovering the molecular mechanisms as a consequence of lysosomal storage, implicating inflammation as an attractive therapeutic target [13, 23]. Interestingly, no signs of lysosomal storage have been observed in a zebrafish model of ML-II despite significant developmental defects, suggesting that multiple mechanisms are likely involved in the progression of ML-II [15].

Chapter 2 highlighted the role of cathepsin proteases in a zebrafish model of ML-II and transcriptional analysis of cells enriched for chondrocytes implicated a role for MMPs in cartilage defects. To further explore the role of MMPs in these phenotypes, their activity was measured over a developmental timeline corresponding to cartilage differentiation and development in zebrafish. General MMP activity is elevated in ML-II animals, and the recovered upon reintroduction of GlcNAc-1-phosphotransferase. Analysis of the MMPs revealed they are present in active, mature forms and the elevated activity is primarily localized within the regions of craniofacial defects observed in ML-II. Chondrocyte development depends upon the regulated expression and remodeling of several matrix components including aggrecans and collagens, the primary substrates of MMPs. Isolation and analysis of chondrocytes and osteoblasts from ML-II animals revealed that MMPs are expressed at elevated levels in chondrocytes, and at reduced levels in osteoblasts relative to control cells. These data suggest

that abnormal expression in cells enriched for chondrocytes, which were previously shown to be deficient in cathepsin K (Fig. 3.3) express elevated levels of several matrix-degrading enzymes. Further analysis of MMPs revealed that the majority of the activity observed in ML-II embryos corresponds to MMP-13, which at steady state is primarily present as a mature enzyme. Suppression of cathepsin K activity was shown to reduce the activity of other proteases and recover several of the ML-II craniofacial phenotypes in chapter 2. Reduction in cathepsin K activity in ML-II embryos also corresponded with decreased activity of general MMP activity, although to a lesser extent than seen with the cathepsins. However, inhibition of MMP-13 led to no improvement of the cartilage phenotypes and did not reduce the activity of the cathepsin proteases in ML-II zebrafish. These findings suggest a unidirectional relationship between these potent collagenases cathepsin K and the MMPs, and that pathological degradation of the ECM mediated by cathepsin K and MMPs is an underlying mechanism of the cartilage defects observed in ML-II zebrafish.

Analysis of fibroblast-like synoviocytes isolated from the joints of ML-II and MPS VI cats revealed MMP activities are also elevated in these tissues, supporting the hypothesis that increased MMPs are a general feature of LSDs. Further, both general and MMP-13 specific activity was elevated in MPS VI FLSs and to a greater extent in ML-II. Transcript analysis of a genes involved in inflammation demonstrated that several MMP-stimulating cytokines were strikingly elevated. Increased expression of TNF-α, IL-1β, or TGF-β, has been shown to stimulate MMP expression and lead to pathological degradation of

cartilage and bone. The increased transcript levels of TLR2 and TLR4 may implicate a molecular pathway of recognition of lysosomal storage and impaired glycoconjugates metabolism, which, in turn leads to pathological inflammation. These data are consistent with analysis of synovial fluid from MPS rats, cats, and dogs, all of which exhibit increased levels of inflammatory molecules and MMPs. It is important to note however, that TLR4 in zebrafish is not capable of LPS recognition, suggesting this mechanism relies upon different effectors or is not present in the zebrafish ML-II model [37].

In this report we have further defined the pathological characteristics of ML-II using zebrafish and feline models, illustrating that increased MMP activity is a hallmark of this disease. Our data suggests that some shared pathology likely exists between ML-II and the MPS disorders, as several characteristics appear highly similar. Importantly, we provide data that a relationship between impaired lysosomal targeting of cathepsin K and the MMPs exists and suppression of cathepsin K activity in ML-II reduces the abnormal elevation of MMPs. However, the pathological mechanism linking lysosomal dysfunction to increases in inflammatory cytokines and MMP activity remains unclear and further studies are needed to better define how these pathways are intertwined.

Materials and Methods

Fish strains

Wild-type zebrafish were obtained from Fish 2U (Gibsonton, FL) and maintained using standard protocols. Embryos were staged according to the criteria

established by Kimmel (Kimmel et al., 1995). In some cases, 0.003% 1-phenyl-2-thiourea was added to the growth medium to block pigmentation. All MO-generated phenotypes were tested in several genetic backgrounds, including a wild-type strain from a commercial source (Fish 2U). Analyses of craniofacial phenotypes were performed in both the F2U wild-type strain and Tg (*fli1a*:EGFP)*y1* transgenic line (Lawson and Weinstein, 2002). Handling and euthanasia of fish for all experiments were carried out in compliance with University of Georgia's policies. This protocol was approved by the University of Georgia Institutional Animal Care and Use Committee (permit number: A2009 8-144).

Anti-sense morpholino injection and mRNA expression

Expression of N-acetylglucosamine-1-phosphotransferase (αβ subunit, *GNPTAB*) was inhibited by injection of morpholino oligonucleotides (MO) as previously described (Flanagan-Steet et al., 2009). Experiments involving mRNA rescue in the morphant background were performed following injection of full-length phosphotransferase mRNA as previously described (Flanagan-Steet et al., 2009).

Embryo dissociation and cell sorting

Wild-type and morphant *fli1*:EGFP embryos were collected at the indicated stages, dechorionated and deyolked then dissociated and sorted by Flourescence Activated Cell Scanning (FACS) as previously described (Petrey, et al., 2011).

Protease activity assays

For the protease activity assays, WT and morphant embryos were dechorionated, deyolked (as described in embryo dissociation and cell sorting section above), and homogenized on ice by sonication in 10mM Tris pH 6.5, 1% Triton X-100. Embryo lysates were centrifuged at 15,000 rpm for 10 min at 4˚C and the protein concentration determined by Micro-BCA protein assay (Thermo Scientific). To gauge enzyme-specific substrate hydrolysis, equivalent samples were incubated with respective inhibitors or vehicle for 15 min at 4˚C before starting the assay. The enzymatic activity of the MMPs was determined from the rate of hydrolysis of a general MMP substrate, QXL520 -γ-Abu-Pro-Cha-Abu-Smc-His-Ala-Dab (5-FAM)-Ala-Lys-NH_2, (cat# 60581-01) from Anaspec. According to the manufacturer, the substrate is cleaved by MMP-1, 2, 3, 7, 9, 12, and 13. MMPs were activated using *p*-aminophenylmercuric acetate (APMA). The metal ion chelator, EDTA, was used as an inhibitor. Fluorescence units were measured at various time intervals with a SpectraMax Genesis microplate fluorimeter from Molecular Devices (Sunnyvale, Ca) with excitation at 485nm and emission at 538nm. Reference standards were supplied with the assay reagents the MMPs.

Small molecule in vivo inhibition of cathepsin K activity

At 24 hpf embryos were collected, dechorionated and 20-30 embryos placed per well into 6-well tissue culture plates. At 48 hpf embryos were treated with either 2.5 μM or 5.0 μM Cts K inhibitor, or control treated with 0.3% DMSO (which

represents the highest amount present with the inhibitor). After two days of continuous drug treatment, embryos were subsequently collected (96 hpf) and processed for either Alcian blue staining or cathepsin enzyme assays.

Preparation of feline fibroblast-like synoviocytes

After removal of any excess tissue, synovial membranes were washed twice with PBS (supplemented with Pen/Strep) and minced into small pieces with a scalpel. Diced membranes were digested in RPMI-1640 media containing 0.5 mg/mL sterilized collagenase type IA (Sigma; C9891) at 37˚C for 3 hours in a 15 mL conical tube. After incubation, suspended cells were pipetted through a sterile 100µm nylon mesh into a new centrifuge tube. Cells were washed twice in complete RPMI-1640 media containing 15% heat-inactivated FBS and plated in a T-25 culture flask. After 6 hrs to allow attachment, fresh media was placed on the cell monolayer to remove any residual tissue or debris. MMP activity assays in cell lysates was performed as described earlier.

References

1. Fratantoni, J.C., C.W. Hall, and E.F. Neufeld, *The defect in Hurler's and Hunter's syndromes: faulty degradation of mucopolysaccharide.* Proc Natl Acad Sci U S A, 1968. **60**(2): p. 699-706.

2. Neufeld, E.F., T.W. Lim, and L.J. Shapiro, *Inherited disorders of lysosomal metabolism.* Annu Rev Biochem, 1975. **44**: p. 357-76.

3. Beutler, E., *Lysosomal storage diseases: natural history and ethical and economic aspects.* Mol Genet Metab, 2006. **88**(3): p. 208-15.

4. Meikle, P.J. and J.J. Hopwood, *Lysosomal storage disorders: emerging therapeutic options require early diagnosis.* Eur J Pediatr, 2003. **162 Suppl 1**: p. S34-7.

5. Babcock, D.S., et al., *Fetal mucolipidosis II (I-cell disease): radiologic and pathologic correlation.* Pediatr Radiol, 1986. **16**(1): p. 32-9.

6. Cathey, S.S., et al., *Molecular order in mucolipidosis II and III nomenclature.* Am J Med Genet A, 2008. **146A**(4): p. 512-3.

7. Kabra, M., et al., *I-cell disease (Mucolipidosis II).* Indian J Pediatr, 2000. **67**(9): p. 683-7.

8. Leroy, J.G., S. Cathey, and M.J. Friez, *Mucolipidosis II*, in *GeneReviews*, R.A. Pagon, et al., Editors. 1993: Seattle (WA).

9. Pazzaglia, U.E., et al., *Bone changes of mucolipidosis II at different ages. Postmortem study of three cases.* Clin Orthop Relat Res, 1992(276): p. 283-90.

10. Ma, X., et al., *Upregulation of elastase proteins results in aortic dilatation in mucopolysaccharidosis I mice.* Mol Genet Metab, 2008. **94**(3): p. 298-304.

11. Metcalf, J.A., et al., *Upregulation of elastase activity in aorta in mucopolysaccharidosis I and VII dogs may be due to increased cytokine expression.* Mol Genet Metab, 2009.

12. Simonaro, C.M., et al., *Joint and bone disease in mucopolysaccharidoses VI and VII: identification of new therapeutic targets and biomarkers using animal models.* Pediatr Res, 2005. **57**(5 Pt 1): p. 701-7.

13. Simonaro, C.M., et al., *Mechanism of glycosaminoglycan-mediated bone and joint disease: implications for the mucopolysaccharidoses and other connective tissue diseases.* Am J Pathol, 2008. **172**(1): p. 112-22.

14. Simonaro, C.M., et al., *Involvement of the Toll-like receptor 4 pathway and use of TNF-alpha antagonists for treatment of the mucopolysaccharidoses.* Proc Natl Acad Sci U S A, 2010. **107**(1): p. 222-7.

15. Flanagan-Steet, H., C. Sias, and R. Steet, *Altered chondrocyte differentiation and extracellular matrix homeostasis in a zebrafish model for mucolipidosis II.* Am J Pathol, 2009. **175**(5): p. 2063-75.

16. Petrey, A.C., et al., *Excessive activity of cathepsin K is associated with cartilage defects in a zebrafish model of mucolipidosis II.* Dis Model Mech, 2012. **5**(2): p. 177-90.

17. Burrage, P.S., K.S. Mix, and C.E. Brinckerhoff, *Matrix metalloproteinases: role in arthritis.* Front Biosci, 2006. **11**: p. 529-43.

18. Fernandes, J.C., J. Martel-Pelletier, and J.P. Pelletier, *The role of cytokines in osteoarthritis pathophysiology.* Biorheology, 2002. **39**(1-2): p. 237-46.

19. Hornebeck, W., et al., *[Proteolysis directed by the extracellular matrix].* J Soc Biol, 2003. **197**(1): p. 25-30.

20. Dangelo, M., et al., *Activation of transforming growth factor beta in chondrocytes undergoing endochondral ossification.* J Bone Miner Res, 2001. **16**(12): p. 2339-47.

21. Covassin, L., et al., *Global analysis of hematopoietic and vascular endothelial gene expression by tissue specific microarray profiling in zebrafish.* Dev Biol, 2006. **299**(2): p. 551-62.

22. DeLaurier, A., et al., *Zebrafish sp7:EGFP: a transgenic for studying otic vesicle formation, skeletogenesis, and bone regeneration.* Genesis, 2010. **48**(8): p. 505-11.

23. Eliyahu, E., et al., *Anti-TNF-alpha therapy enhances the effects of enzyme replacement therapy in rats with mucopolysaccharidosis type VI.* PLoS One, 2011. **6**(8): p. e22447.

24. Buckwalter, J.A. and H.J. Mankin, *Articular cartilage: tissue design and chondrocyte-matrix interactions.* Instr Course Lect, 1998. **47**: p. 477-86.

25. Homandberg, G.A. and F. Hui, *Association of proteoglycan degradation with catabolic cytokine and stromelysin release from cartilage cultured with fibronectin fragments.* Arch Biochem Biophys, 1996. **334**(2): p. 325-31.

26. Yasuda, T., *Cartilage destruction by matrix degradation products.* Mod Rheumatol, 2006. **16**(4): p. 197-205.

27. Berthet, J., et al., *Human platelets can discriminate between various bacterial LPS isoforms via TLR4 signaling and differential cytokine secretion.* Clin Immunol, 2012. **145**(3): p. 189-200.

28. Visintin, A., et al., *Secreted MD-2 is a large polymeric protein that efficiently confers lipopolysaccharide sensitivity to Toll-like receptor 4.* Proc Natl Acad Sci U S A, 2001. **98**(21): p. 12156-61.

29. Guha, M. and N. Mackman, *LPS induction of gene expression in human monocytes.* Cell Signal, 2001. **13**(2): p. 85-94.

30. Kirschning, C.J., et al., *Human toll-like receptor 2 confers responsiveness to bacterial lipopolysaccharide.* J Exp Med, 1998. **188**(11): p. 2091-7.

31. Sardiello, M., et al., *A gene network regulating lysosomal biogenesis and function.* Science, 2009. **325**(5939): p. 473-7.

32. Settembre, C., et al., *TFEB links autophagy to lysosomal biogenesis.* Science, 2011. **332**(6036): p. 1429-33.

33. Wilson, S., et al., *Glycosaminoglycan-mediated loss of cathepsin K collagenolytic activity in MPS I contributes to osteoclast and growth plate abnormalities.* Am J Pathol, 2009. **175**(5): p. 2053-62.

34. Li, Z., et al., *Regulation of collagenase activities of human cathepsins by glycosaminoglycans.* J Biol Chem, 2004. **279**(7): p. 5470-9.

35. Nagase, H. and M. Kashiwagi, *Aggrecanases and cartilage matrix degradation.* Arthritis Res Ther, 2003. **5**(2): p. 94-103.

36. Wang, J.Y. and M.H. Roehrl, *Glycosaminoglycans are a potential cause of rheumatoid arthritis.* Proc Natl Acad Sci U S A, 2002. **99**(22): p. 14362-7.

37. Sepulcre, M.P., et al., *Evolution of lipopolysaccharide (LPS) recognition and signaling: fish TLR4 does not recognize LPS and negatively regulates NF-kappaB activation.* J Immunol, 2009. **182**(4): p. 1836-45.

Figures

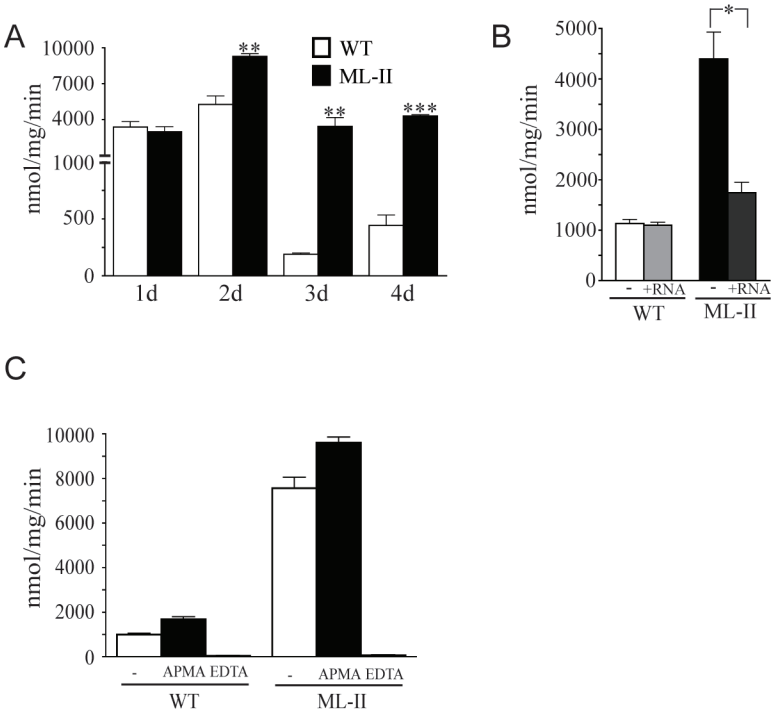

Figure 4.1. MMP activity is increased in ML-II embryos. (A-C) General MMP activity was measured in WT and ML-II embryo lysates, across a developmental timecourse (1-4 dpf; *panel A*), following introduction of GlcNAc-1-phosphotransferase mRNA (3 dpf; *panel B*), and after incubation with EDTA (inhibits MMPs) or APMA (activates MMPs) for 2 h (3 dpf; *panel C*).

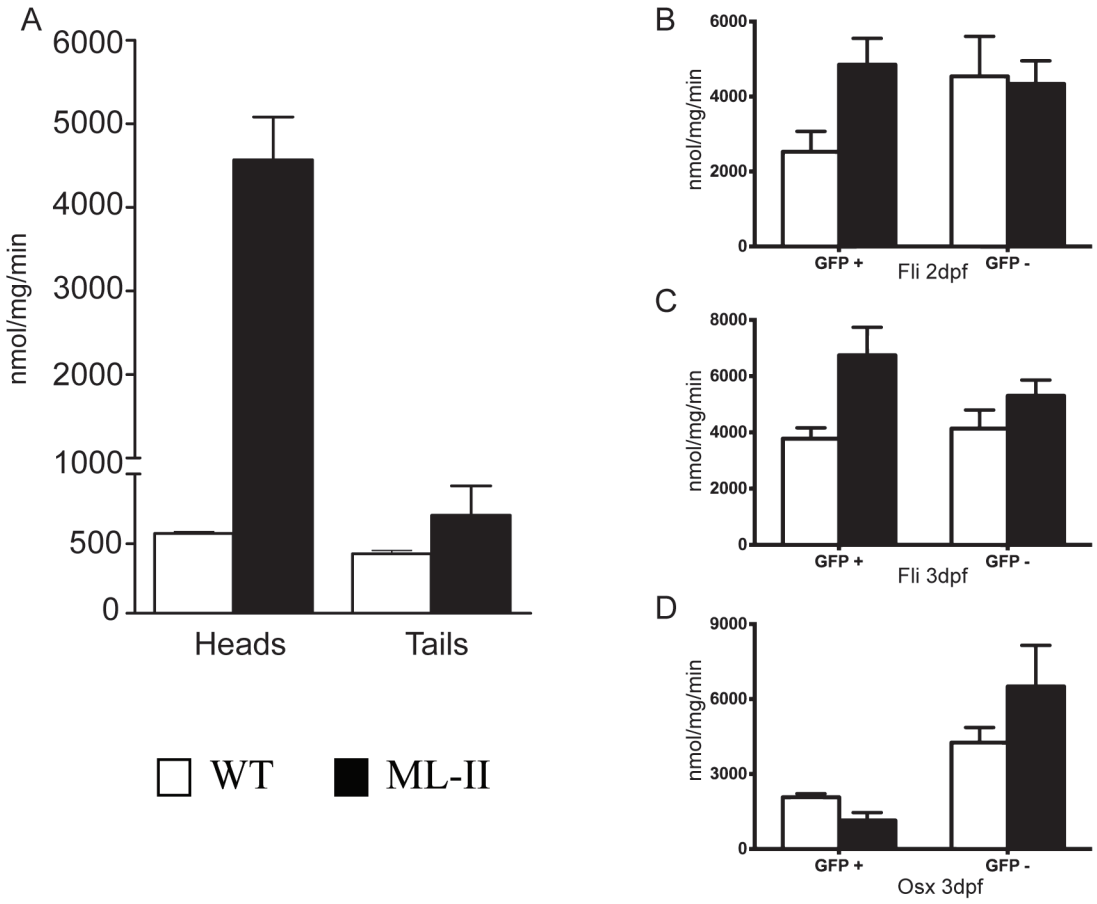

Figure 4.2. MMP activity is elevated in the head and cartilage of ML-II embryos. (A) General MMP activity was measured in WT and ML-II embryo heads and tails at 3dpf. (B,C) WT and ML-II *fli1a*:EGFP embryos were dissociated and enriched for chondrocytes by FACS at 2 and 3dpf. (D) WT and ML-II *osx*:EGFP embryos were dissociated and enriched for osteoblasts by FACS at 3dpf. Cell lysates were assayed for intracellular MMP activity using specific fluorogenic substrates.

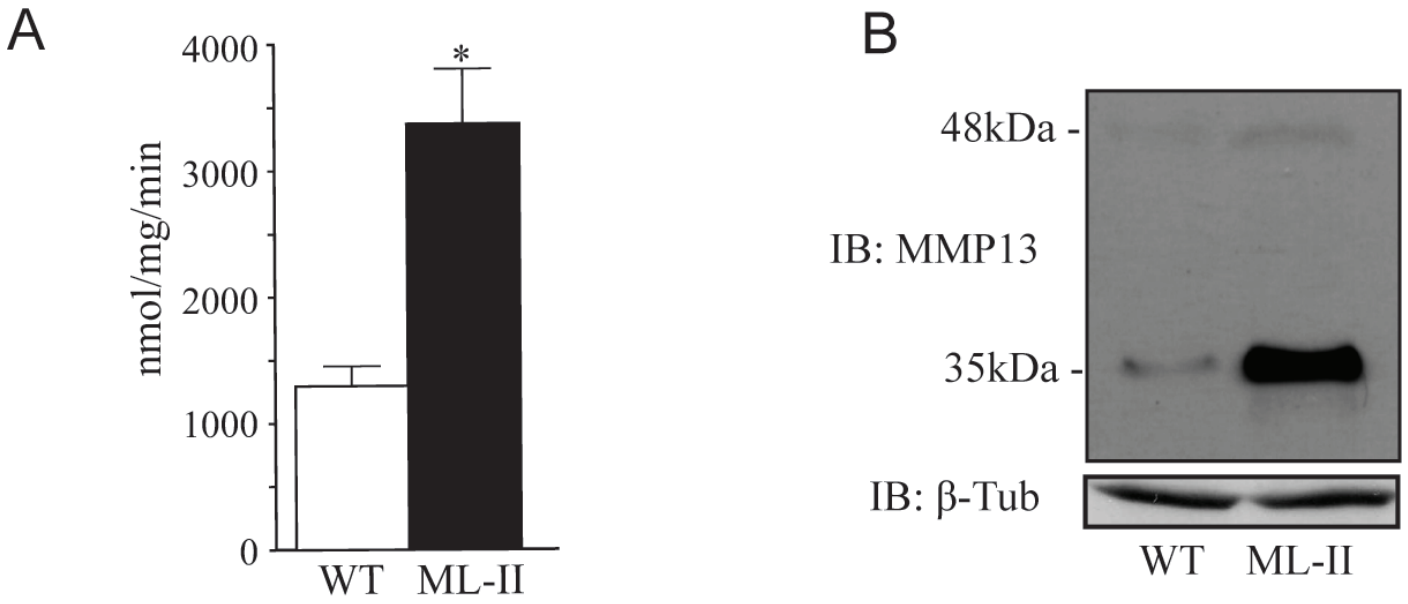

Figure 4.3. MMP-13 is significantly elevated in ML-II. (A) Activity of MMP-12/13 in 3 dpf WT and ML-II embryos measured using specific fluorogenic substrate. (B) MMP-13 immunoblots show increased steady-state levels of both the MMP13 precursor (48kDa) and the mature active (35kDa) forms in 3dpf ML-II embryo lysates. ß-Tubulin was used as a loading control.

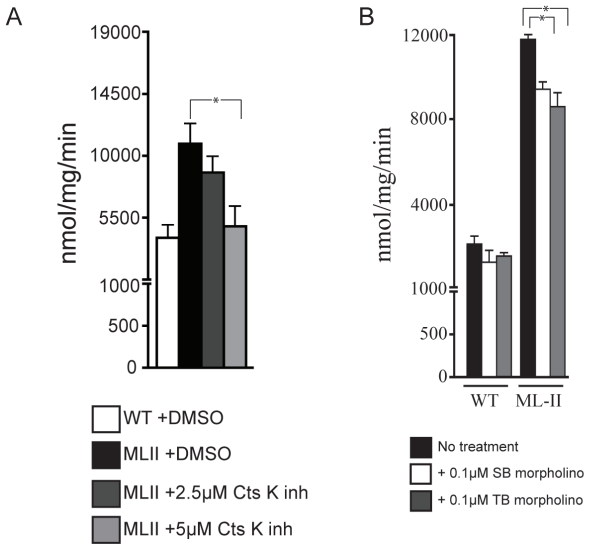

Figure 4.4. *In vivo* inhibition of cathepsin K reduces MMP activity in ML-II embryos. (A) *in vivo* administration of a cathepsin K inhibitor at 2 dpf leads to reduced cathepsin and MMP activity levels measured at 4 dpf; for DMSO only treatment n=3, for samples treated with cathepsin K inhibitor n=6. (B) Inhibition of cathepsin K expression by morpholino knockdown also reduces the activity of

multiple cathepsins and MMP; n=3 experiments per group with 45 embryos per experimental sample. (*P<0.05, **P<0.01, ***P<0.001, Student's t-test)

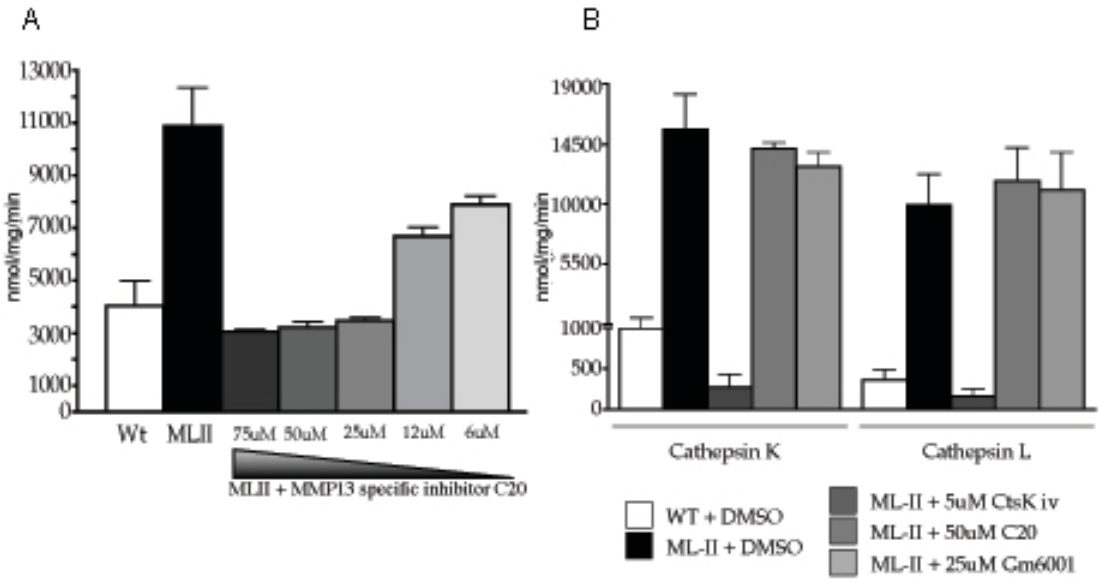

Figure 4.5. Inhibition of MMP-13 is unable to reduce the activity of Cathepsins K and L in ML-II zebrafish. (A) Embryos were treated with various concentrations of a MMP-13 specific inhibitor at 2dpf, then assayed for MMP-13 activity at 4dpf. (B) Following inhibition of MMP-13, or administration of a general MMP inhibitor, embryos were assayed for cathepsin K or L activity at 4dpf. Inhibition by either method did not affect the activity of either cathepsin.

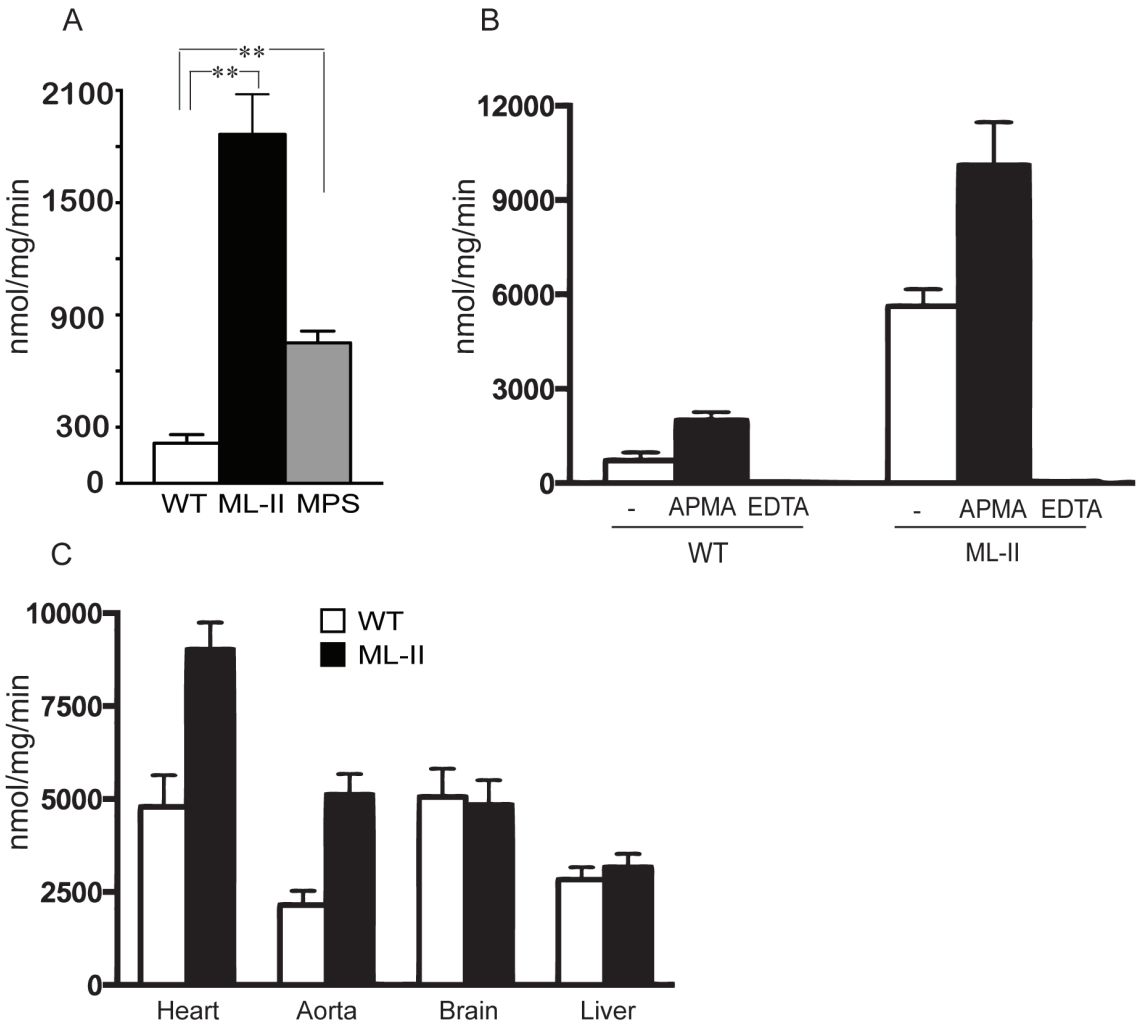

Figure 4.6. Matrix Metalloproteinase activity is elevated in a feline ML-II model. (A) Fibrobliast-like synoviocytes were isolated from WT, ML-II, and MPS VI cats and cell-associated MMP activity was measured. (B) Activity was measured after incubation with EDTA (inhibits MMPs) or APMA (activates MMPs) for 2h. (C) Tissues isolated from a feline model of ML-II reveal elevated MMP activity in the heart and aorta. (**P*<0.05, ***P*<0.01, ****P*<0.001, Student's *t*-test)

A

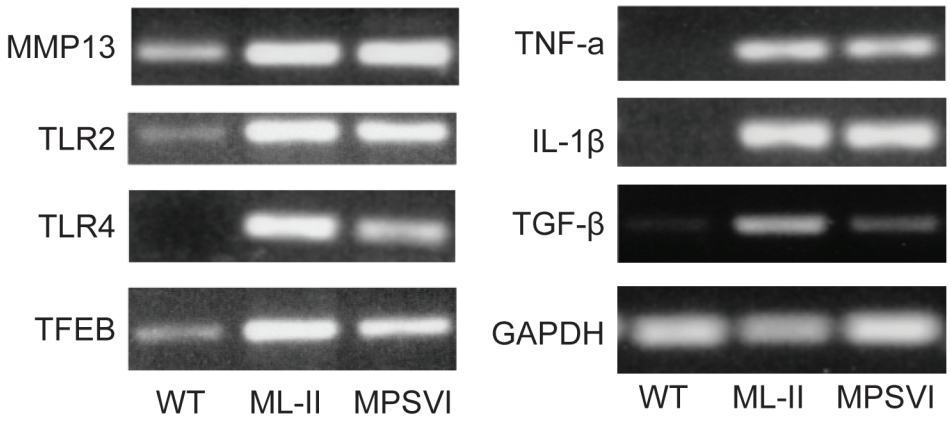

B

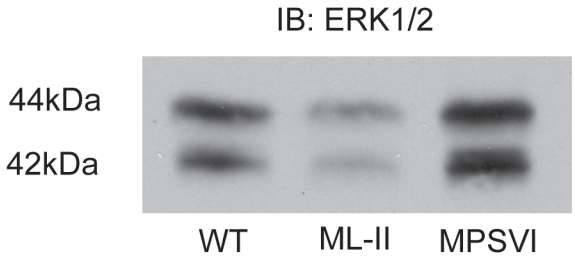

Figure 4.7. Genes involved in inflammation are elevated in feline lysosomal storage disorders including ML-II. (A) Fibroblast-like synoviocytes were isolated from WT, ML-II, and MPS VI cats and analyzed for expression of inflammation-related genes revealing elevated transcripts in ML-II and MPS VI cells. (B) Immunoblot analysis of fibroblast-like synoviocytes show reduced steady-state levels of ERK1/2.

CHAPTER 5: DISCUSSION AND FUTURE PERSPECTIVES

The Contribution of Proteases to the Pathophysiology of Mucolipidosis II.

Cathepsin proteases have long been known to be integral components of the lysosome with enormous disruptive potential once activated as their concentration within lysosomes is reported to exceed 1 mM [1]. The majority of cathepsin proteases require Man-6-P modification to reach the lysosome, and the consequences of disrupted localization of these proteases are demonstrated in Chapters 2 and 3. We further investigated the role of Man-6-P biosynthesis through use of a GlcNAc-1-Phosphotransferase gamma-subunit null zebrafish line. Studies using this model revealed changes in the mannose phosphorylation of some lysosomal hydrolases, but no overt phenotypes (data presented in Appendix A, supplemental figures). Cathepsin gene knockouts have revealed that intralysosomal protein degradation is not exclusively dependent on any single cathepsin as lysosomal storage is not present in these animals [2]. Thus it is highly likely that many of the pathological defects observed in ML-II are due to impaired localization and inappropriate protease activity in compartments in which they are not normally present. Cathepsin proteases are expressed either ubiquitously or tissue and cell-type specifically and are regulated at the level of transcription, activation, localization, and inhibition by cystatins. Cystatins are

non-selective 1:1 stoichoimetric inhibitors of cathepsins and enter into the constitutive secretory pathway to control the inappropriate activity of cathepsins within the ECM. Disturbance of the normal balance of cathepsin regulation is associated with a number of pathological conditions including RA, OA, cancer, neurological disorders, osteoporosis, and as this work has shown, lysosomal storage disorders such as ML-II [3-6].

This work also establishes a role for the matrix metalloproteinases in the pathology of ML-II. Using two ML-II animal models, we have established that MMPs are elevated in craniofacial regions and isolated osteoblasts from zebrafish as well as fibroblast-like synoviocytes and cardiac tissues from the feline model. The latter is perhaps particularly relevant as patients suffer from valve thickening and cardiac failure [7]. MMPs occupy a central role in several normal physiological conditions despite the fact that the biological roles of MMPs have traditionally been associated with unregulated degradation and turnover of ECM components. Matrix degradation, as with many biological processes, is a precise event relying upon the on demand production and secretion of MMPs from activated cells through interaction of cell surface receptors and specific matrix components [8]. While MMPs are primarily responsible for the homeostasis of the extracellular matrix, when the balance between transcription, activation, stability, and inhibition is altered, MMPs contribute to its destruction under disease conditions [9-11].

Disrupted Lysosomal Targeting Leads to Hypersecretion of Cathepsins and ECM Degradation.

With the exception of cathepsins D and H, which may also reach the lysosome through interactions with sortilin, most cathepsins rely exclusively upon Man-6-P mediated lysosomal targeting [12, 13]. Loss of this regulatory mechanism leads to hypersecretion of lysosomal hydrolases from the cell into the ECM and serum. Though cathepsin proteases are most commonly associated with the slightly acidic, reducing environment of the lysosome, several have been shown to retain substantial residual activity at neutral pH [1, 2]. Enzyme stability, inhibition by cystatins, and oxidation of catalytic thiol residues function as regulatory mechanisms of cathepsins within the environment of the ECM. However, these safeguards can be overcome by pericellular acidification, reduced cystatin concentrations, and increased cathepsin transcription or activation [14]. Data presented in Chapter 3 highlights that not all cathepsins have a strict acidic pH optimum, as both cathepsin K and S retain potent activity at neutral pH values. Observations from diseases of pathological bone and cartilage degradation have revealed pericellular acidification, redistribution of lysosomes to the cell surface, and secretion of lysosomal proteases into the ECM. Extracellular acidification is also observed under physiological conditions of bone remodeling. Bone-resorbing osteoclasts form a sealed, acidified space between the osteoclast and the bone surface leading to the demineralization of bone and the degradation of collagens [15]. Triple helical type I and II collagens have been shown to be highly resistant to proteolysis and few collagenases are

capable of hydrolyze peptide bonds within this domain. The MMPs contain a specific structural motif, called the hemopexin domain, to facilitate partial unfolding of the triple helix and cleave at a single site [16]. However, cathepsin K has been shown to be the predominant collagenase within osteoclasts and is the only cathepsin known to cleave the collagen triple helix in a GAG-mediated mechanism that does not disrupt its ability to degrade other substrates [4, 17].

The data presented in Chapter 2 highlights the role of cathepsin K in the craniofacial cartilage phenotypes observed in ML-II zebrafish. The data presented demonstrates that substantial cathepsin K activity is required in WT embryos at 2dpf and this enzyme is subject to strict regulation via proteolytic processing. It is possible that the activity of this collagenase is needed during specific developmental time points to assist in the remodeling of collagens during embryonic development. *In situ* analysis of cathepsin K expression revealed significant levels of transcripts throughout the craniofacial region and immunostaining confirms the presence of cathepsin K in chondrocytes. As osteoclasts are not yet present at these early stages in development, it is likely that the majority of inappropriate activity observed in ML-II may arise from chondrocytes and surrounding cells. The specific mechanism underlying the sustained activation of cathepsin K shown in Figure 2.5 is not known, but the finding that mutation of the C-terminal glycan N216Q of cathepsin K led loss of M6P-binding and an increase in activity (Fig. 3.6) supports the hypothesis that abnormal activation is due to hypersecretion of the enzyme. It is possible then that cathepsin K may be activated by the activity of another protease within the

secretory pathway, or through contact with cell surface proteases within the extracellular space. Cathepsin K has been shown to interact with several GAGs and it is possible this interaction may facilitate autocatalytic activation within the ECM, as has been shown for cathepsins, B, S, and D. However, only the endopeptidases are likely to be autoactivated, as the exopeptidase cathepsins X and C have been shown to require the activity of cathepsins L and S for their activation [1].

The Role of Cathepsin K and Type II Collagen in ML-II.

Although the present studies have established the involvement of cathepsin K in the craniofacial cartilage pathologies seen in a zebrafish model of ML-II, there are several questions that should be addressed in future studies in regard to the activation of cathepsin K, the substrates it acts upon, details of its localization, and perhaps most importantly, how suppression of cathepsin K activity leads to a reduction in the activity of other proteases. Although cathepsin K is deficient within sorted ML-II chondrocytes and appears present in the ECM of these animals by immunostaining, a more direct assessment of hypersecretion would allow for a better understanding of how the trafficking of K is affected upon loss of Man-6-P. We attempted to address several of these questions with the generation of mutant forms of cathepsin K lacking either or both N-glycans. While these studies further implicate that the enhanced activation of cathepsin K is a consequence of the loss of Man-6-P, without an epitope tagged form it was not possible to distinguish these constructs from endogenous cathepsin K in whole

embryos. Generation of epitope-tagged forms of cathepsin K has been completed and we believe expression of these forms will answer a key question: whether the phenotypes observed upon mRNA injection of N216Q cathepsin K are a result of extracellular localization and enhanced activation. Additional data in our laboratory supports the observation that cathepsin K and cathepsin D are targeted to different lysosomal compartments within the cell, and the targeting of K but not D is affected in ML-II. It is possible that under normal conditions cathepsin K is targeted to a secretory lysosome and remains in its pro-form until activation, acidification, and secretion of lysosomal contents into the ECM. It is of importance to address the mechanism and localization of cathepsin K activation. Subcellular fractionation experiments to isolate components of the secretory pathway combined with immunostaining for cathepsin K would allow for detailed investigation into what forms of cathepsin K are present. Pulse-chase labeling of cathepsin K in a cell-culture system would shed light on the activation and trafficking of cathepsin K upon loss of specific glycans, leading to a better understanding of where and how the enzyme becomes activated.

The ultimate goal of the cathepsin K project is to determine how genetic suppression or pharmacological inhibition of cathepsin K leads to a decrease in the activities of other cathepsins and MMPs. The data in Chapter 3 supports, at least partially, the hypothesis that extracellular activity of cathepsin K (not lysosomal deficiency) is responsible for the elevated activity of these proteases. These findings merit further consideration as to whether proteases other than cathepsin L are elevated, such as the MMPs, and if these changes in activity are

due to altered processing or represent changes in transcription. Several possible mechanisms by which these proteases are transcriptionally elevated exist.

Disruption of growth factor signaling as a result of increased protease activity has been a long-standing hypothesis in our laboratory and could impact several pathways including FGFs, IGF, TGF-β, or others. Several observations from our zebrafish model suggest that TGF-β signaling is altered in ML-II. Disruption of TGF-β signaling is associated with skeletal and cardiac abnormalities in humans [18-20]. Further, several TGF-βs have been shown to regulate chondrocyte development and cartilage ECM deposition, including the expression of type II collagen [21]. Our previous findings showed Sox9 and phosphorylated Smad2 was altered throughout the craniofacial region of ML-II animals. As shown in chapter 2, the accumulation of type II collagen was reversed in ML-II animals treated with cathepsin K inhibitors. This finding supports the hypothesis that extracellular protease activity may liberate latent TGF-β, leading to enhanced signal transduction and increased type II collagen transcription. The mechanism underlying how the increased activity of a protease known to degrade type II collagen leads to more type II collagen is not clear. Overexpression of cathepsin K was not sufficient to recapitulate the accumulation of type II collagen, despite generating craniofacial phenotypes. It is possible that these mechanisms are distinct, or that systemic expression of cathepsin K is capable of generating phenotypes independent of any affect on type II collagen. Although collagen is present at elevated levels, a clear picture of whether it is intact or fragmented remains an open question and would address whether

cathepsin K is degrading collagen. It is plausible that despite the increased levels of both cathepsin K and type II collagen, that cathepsin K is unable to degrade collagen or is acting on other substrates. Preliminary studies in our laboratory suggest that cystatins, the endogenous inhibitors of cathepsins, are present at normal levels in ML-II zebrafish. It is possible that increased cathepsin K activity leads to enhanced biosynthesis of type II collagen and is not directly degrading that particular component of the ECM, possibly due to substrate level inhibition of cathepsin K, inhibition within the ECM, or other mechanisms. The development of cartilage structures is highly dependent upon ECM biosynthesis and remodeling of matrix proteins and may be uniquely sensitive to potent collagenases such as cathepsin K. The state of the ECM in the zebrafish ML-II model still remains to be fully characterized. To further address these questions, transgenic animals that express forms of cathepsin K in specific tissues, such as chondrocytes, are necessary to understand the contribution of individual cell types in the craniofacial cartilage pathogenesis.

Future Perspectives – The Role of Other Cathepsins in ML-II.

As discussed in Chapter 1, Lysosomal cathepsins have been shown to have specific and individual functions that are important to normal biological functions, often related with the restricted tissue expression of these proteases. This work has detailed a specific role for cathepsin K in the cartilage pathogenesis of ML-II, but it does not preclude similar or different roles for the other cathepsins. Initial *in vivo* inhibition experiments suggested that similar

affects to those observed with the cathepsin K inhibitor are seen with inhibition of cathepsin L. However, inhibitor specificity experiments revealed that the L inhibitor could also inhibit cathepsin K. Use of a highly specific cathepsin L inhibitor, or morpholino knock down, would address whether correction of craniofacial phenotypes are a result in the reduced activity of cathepsin L following cathepsin K suppression. The possibility that cathepsin K acts to activate cathepsin L is an attractive one, as similar relationships have been shown to exist between several of the cathepsin proteases and the activity of L increases as a result of overexpression of cathepsin K.

Though correction of the cardiac edema was observed upon suppression of cathepsin K, it is highly possible this phenotype is a consequence of the direct activity of another cathepsin protease. Several cathepsins have been shown to be present in the heart, though the specific functions of most have yet to be elucidated. Cathepsin L has been shown to function in cardiac repair and is present at elevated levels in myocardium following infarction. Other cysteine cathepsins, including S and B are highly abundant in the ventricular myocardium of patients with hypertensive heart failure, and have been implicated in ECM turnover and cardiac remodeling. It is possible that dysregulation of cathepsin activity or localization can result in the cardiac phenotypes seen in ML-II animals and patients.

Matrix Metalloproteinases and ECM Turnover.

Investigation into several animal models of lysosomal storage disorders has revealed profound disruption of matrix components and an increase in the activity of matrix metalloproteinases [22, 23]. Our findings in the feline ML-II model are consistent with observations from MPS animals, indicating that the increase in MMP activity corresponds with an increase in the expression of TNF-α. This cytokine has been shown to promote cartilage degradation through stimulation and release of several MMPs [24-26]. A picture is beginning to emerge that the presence of pro-inflammatory cytokines is a hallmark of the mucopolysaccharidoses and are present at elevated levels in bone, joints, and tissues of affected animals.

However, the contribution of the MMPs to the cartilage phenotypes seen in ML-II is not clearly defined. Cathepsin K is, under the right conditions, the most potent collagenase known and may have more impact upon ECM disruption than the MMPs [27]. Analysis of collagens would provide insight into the function of these proteases *in vivo.* MMP collagenases cleave a specific, single peptide bond in type I and type II collagens leading to a very well defined 1/4 C-terminal and 3/4 N-terminal fragments [16, 28]. Cathepsin K, by contrast, cleaves collagen at multiple locations, resulting in more complete degradation [17, 29]. Immunodetection experiments of matrix soluble and insoluble fractions would allow for direct investigation of how what state the type II collagen is present in. This analysis should be further extended to other structural components of the

ECM such as aggrecan, fibronectin, and fibrillins, all of which are likely subject to fragmentation.

Directly addressing the contribution of MMPs to the phenotypes observed in ML-II holds significant value. However, inhibition of MMPs as a therapy for OA or RA has proven ineffective, perhaps due to insufficient specificities of inhibitors or possibly because MMPs primarily function in highly regulated processing of extracellular proteins and the cathepsins are the causative proteases underlying matrix destruction in disease [11, 30]. Recent studies have shown MMPs function in the activation or inactivation of various growth factors at the cell surface, indicating these proteases likely play a key regulatory role in ECM metabolism. It is plausible then, that the contribution of MMPs to ML-II lies not in direct disruption of the ECM, but altered signaling, perhaps leading to induction of cathepsin K [31, 32]. MMP-13 is an attractive target as it appears elevated in both models, is present in an activated form, and has been shown to be elevated in cartilage and cardiac tissue in disease. Genetic manipulation of the MMPs, either through siRNA in culture or morpholinos in zebrafish, would allow for suppression of specific proteases and the ability to assess their role in ML-II pathogenesis.

Future Perspectives – Mechanisms of Elevated Protease Transcription.

Future investigation into the mechanisms underlying the pathophysiology of ML-II will depend upon a clear understanding of the molecular basis of increased protease activity. The data presented suggests several possible

pathways by which this might occur and a model is shown in Figure 5.1. As previously mentioned, the activity of proteases within the ECM has been shown to release latent growth factors including TNF-α shedding, FGF release, IGF and IGF binding protein, TGF-β, and other bone morphogenic proteins [33-35]. Additional data generated in our laboratory supports a role for increased deposition of TGF-β into the ECM of ML-II fibroblasts, and a decrease in downstream signaling. The particular mechanism underlying this observation is an area of current investigation.

Release of latent growth factors within the ECM would depend upon disruption and degradation of the matrix itself, and byproducts of ECM degradation can function as modulators of signal transduction. The cysteine-rich (CR) domain found in many ECM proteins (including type I and type II collagens) has been shown to function as a potent BMP-agonist and regulates BMP-family signaling at sufficient concentrations. The CR domain from type II collagen has been shown to interact directly with BMP and TGF-β and act as a sink for TGF-β family members. In this context, TGF-β signaling may be disrupted by either the overproduction of type II collagen, or released by the activity of proteases in ML-II [36, 37]. Further investigation is necessary to determine how these pathways are affected in ML-II.

The presence of inflammatory cytokines is one possible source responsible for increased protease levels. To date, the source of proinflammatory cytokines found in MPS disorders, and reported here in a feline ML-II model, remains unknown. A number of mechanisms are possible, including

accumulation of GAGs as activators of the TLR-mediated inflammation [24]. Disruption of ECM components may also lead to increased levels of proteases in bone and joint disease, as fibronectin fragments and collagen peptides are capable of stimulating proinflammatory cytokine transcription [38, 39]. Though these cytokines were noted in feline FLSs and in chondrocytes (data not shown), we have not found the presence of proinflammatory cytokines or increased TLRs in zebrafish. Further, although inclusions are noted in cultured cells, presently there are no signs of storage within our zebrafish model as accumulation of storage materials may be a later consequence of the disease. Zebrafish are also notably resistant to the presence of LPS, requiring significantly higher levels to elicit the same response seen in mammals [40]. It is possible that these parameters are not present in zebrafish, represent a chronic condition later in the disease, or function through an alternate mechanism in lower vertebrates.

Work over the past decade illustrates that the lysosome is a highly dynamic organelle with multiple functions beyond rote degradation of materials. This is evidenced by the presence of specialized lysosomes including secretory lysosomes and autophagic lysosomes. In a number of storage disorders, including MPS, ML-II, Gaucher, Niemann Pick, Parkinson, Alzheimer, and Huntington disease there are reports of elevated levels of cathepsin proteases in specific cell types and tissues [22, 41-46]. Though these studies have not comprehensively evaluated the cathepsins, they have nevertheless, identified specific cathepsins involved in disease pathology as a consequence of storage of material within cells or lysosomes. It is plausible that within the cell there exists a

regulatory network capable of sensing lysosomal “burden” and responds by increased lysosomal biogenesis in an attempt to reconcile storage. The transcription factor EB (TFEB) is likely one element of such a network and has been shown to increase the transcription of several lysosomal proteins and enzymes including glycosyl hydrolases, cathepsin proteases, as well as autophagy-related proteins and both M6PRs [47]. TFEB-mediated lysosomal biogenesis requires nuclear translocation, and has been shown to be localized within the nucleus of MPS II and III cells, as well as cells treated with high levels of sucrose. Phosphorylation of TFEB prevents nuclear translocation, thus it is likely that a protein, or a protein complex, with phosphatase-containing activity is capable of sensing lysosomal storage within the cell [48, 49]. Expression of TFEB was capable of clearing storage within a cell-culture system with huntingtin storage, and it is possible enhancement of genes containing the TFEB promoter may assist in clearance of storage material in certain diseases [49]. However, the consequences of continued and prolonged stimulation of lysosomal transcription are not known and, in contexts such as ML-II, may be deleterious. Suppression of TFEB directly, or its nuclear translocation, may lead to a global reduction in lysosomal protease transcription in ML-II and represent a novel therapeutic approach. TFEB is silenced by the microRNA miR-128, which is significantly elevated in Alzheimer’s disease [50]. The function of TFEB in ML-II, and other storage disorders, remains an important area for future investigation.

References

1. Turk, V., et al., *Cysteine cathepsins: from structure, function and regulation to new frontiers.* Biochim Biophys Acta, 2012. **1824**(1): p. 68-88.

2. Chapman, H.A., R.J. Riese, and G.P. Shi, *Emerging roles for cysteine proteases in human biology.* Annu Rev Physiol, 1997. **59**: p. 63-88.

3. Petrey, A.C., et al., *Excessive activity of cathepsin K is associated with cartilage defects in a zebrafish model of mucolipidosis II.* Dis Model Mech, 2012. **5**(2): p. 177-90.

4. Konttinen, Y.T., et al., *Acidic cysteine endoproteinase cathepsin K in the degeneration of the superficial articular hyaline cartilage in osteoarthritis.* Arthritis Rheum, 2002. **46**(4): p. 953-60.

5. Martel-Pelletier, J., J.M. Cloutier, and J.P. Pelletier, *Cathepsin B and cysteine protease inhibitors in human osteoarthritis.* J Orthop Res, 1990. **8**(3): p. 336-44.

6. Takahashi, D., et al., *Down-regulation of cathepsin K in synovium leads to progression of osteoarthritis in rabbits.* Arthritis Rheum, 2009. **60**(8): p. 2372-80.

7. Kobayashi, H., et al., *Pathology of the first autopsy case diagnosed as mucolipidosis type III alpha/beta suggesting autophagic dysfunction.* Mol Genet Metab, 2011. **102**(2): p. 170-5.

8. Murphy, G. and H. Nagase, *Localizing matrix metalloproteinase activities in the pericellular environment.* FEBS J, 2011. **278**(1): p. 2-15.

9. Hsu, C.C. and S.C. Lai, *Matrix metalloproteinase-2, -9 and -13 are involved in fibronectin degradation of rat lung granulomatous fibrosis caused by Angiostrongylus cantonensis.* Int J Exp Pathol, 2007. **88**(6): p. 437-43.

10. Mauch, S., et al., *Matrix metalloproteinase-19 is expressed in myeloid cells in an adhesion-dependent manner and associates with the cell surface.* J Immunol, 2002. **168**(3): p. 1244-51.

11. Burrage, P.S., K.S. Mix, and C.E. Brinckerhoff, *Matrix metalloproteinases: role in arthritis.* Front Biosci, 2006. **11**: p. 529-43.

12. Coutinho, M.F., M.J. Prata, and S. Alves, *A shortcut to the lysosome: The mannose-6-phosphate-independent pathway.* Mol Genet Metab, 2012.

13. Canuel, M., et al., *Sortilin mediates the lysosomal targeting of cathepsins D and H.* Biochem Biophys Res Commun, 2008. **373**(2): p. 292-7.

14. Zeeuwen, P.L., et al., *The cystatin M/E-cathepsin L balance is essential for tissue homeostasis in epidermis, hair follicles, and cornea.* FASEB J, 2010. **24**(10): p. 3744-55.

15. Yavropoulou, M.P. and J.G. Yovos, *Osteoclastogenesis - Current knowledge and future perspectives.* J Musculoskelet Neuronal Interact, 2008. **8**(3): p. 204-16.

16. Overall, C.M., *Molecular determinants of metalloproteinase substrate specificity: matrix metalloproteinase substrate binding domains, modules, and exosites.* Mol Biotechnol, 2002. **22**(1): p. 51-86.

17. Li, Z., W.S. Hou, and D. Bromme, *Collagenolytic activity of cathepsin K is specifically modulated by cartilage-resident chondroitin sulfates.* Biochemistry, 2000. **39**(3): p. 529-36.

18. Yang, Z., et al., *Absence of integrin-mediated TGFbeta1 activation in vivo recapitulates the phenotype of TGFbeta1-null mice.* J Cell Biol, 2007. **176**(6): p. 787-93.

19. Maeda, S., et al., *Activation of latent transforming growth factor beta1 by stromelysin 1 in extracts of growth plate chondrocyte-derived matrix vesicles.* J Bone Miner Res, 2001. **16**(7): p. 1281-90.

20. Janssens, K., et al., *Transforming growth factor-beta1 to the bone.* Endocr Rev, 2005. **26**(6): p. 743-74.

21. Yang, X., et al., *TGF-beta/Smad3 signals repress chondrocyte hypertrophic differentiation and are required for maintaining articular cartilage.* J Cell Biol, 2001. **153**(1): p. 35-46.

22. Ma, X., et al., *Upregulation of elastase proteins results in aortic dilatation in mucopolysaccharidosis I mice.* Mol Genet Metab, 2008. **94**(3): p. 298-304.

23. Metcalf, J.A., et al., *Upregulation of elastase activity in aorta in mucopolysaccharidosis I and VII dogs may be due to increased cytokine expression.* Mol Genet Metab, 2009.

24. Simonaro, C.M., et al., *Involvement of the Toll-like receptor 4 pathway and use of TNF-alpha antagonists for treatment of the mucopolysaccharidoses.* Proc Natl Acad Sci U S A, 2010. **107**(1): p. 222-7.

25. Rucavado, A., et al., *Increments in cytokines and matrix metalloproteinases in skeletal muscle after injection of tissue-damaging toxins from the venom of the snake Bothrops asper.* Mediators Inflamm, 2002. **11**(2): p. 121-8.

26. Eliyahu, E., et al., *Anti-TNF-alpha therapy enhances the effects of enzyme replacement therapy in rats with mucopolysaccharidosis type VI.* PLoS One, 2011. **6**(8): p. e22447.

27. Bromme, D. and K. Okamoto, *Human cathepsin O2, a novel cysteine protease highly expressed in osteoclastomas and ovary molecular cloning, sequencing and tissue distribution.* Biol Chem Hoppe Seyler, 1995. **376**(6): p. 379-84.

28. Overall, C.M., *Matrix metalloproteinase substrate binding domains, modules and exosites. Overview and experimental strategies.* Methods Mol Biol, 2001. **151**: p. 79-120.

29. Li, Z., et al., *Collagenase activity of cathepsin K depends on complex formation with chondroitin sulfate.* J Biol Chem, 2002. **277**(32): p. 28669-76.

30. Morrison, C.J., et al., *Matrix metalloproteinase proteomics: substrates, targets, and therapy.* Curr Opin Cell Biol, 2009. **21**(5): p. 645-53.

31. Butler, G.S. and C.M. Overall, *Updated biological roles for matrix metalloproteinases and new "intracellular" substrates revealed by degradomics.* Biochemistry, 2009. **48**(46): p. 10830-45.

32. Butler, G.S., et al., *Membrane protease degradomics: proteomic identification and quantification of cell surface protease substrates.* Methods Mol Biol, 2009. **528**: p. 159-76.

33. Jenkins, G., *The role of proteases in transforming growth factor-beta activation.* Int J Biochem Cell Biol, 2008. **40**(6-7): p. 1068-78.

34. Hornebeck, W., et al., *[Proteolysis directed by the extracellular matrix].* J Soc Biol, 2003. **197**(1): p. 25-30.

35. Zegarska, J., et al., *Extracellular matrix proteins, proteolytic enzymes, and TGF-beta1 in the renal arterial wall of chronically rejected renal allografts.* Transplant Proc, 2003. **35**(6): p. 2193-5.

36. Larrain, J., et al., *BMP-binding modules in chordin: a model for signalling regulation in the extracellular space.* Development, 2000. **127**(4): p. 821-30.

37. Furthauer, M., et al., *Fgf signalling controls the dorsoventral patterning of the zebrafish embryo.* Development, 2004. **131**(12): p. 2853-64.

38. Homandberg, G.A., R. Meyers, and D.L. Xie, *Fibronectin fragments cause chondrolysis of bovine articular cartilage slices in culture.* J Biol Chem, 1992. **267**(6): p. 3597-604.

39. Xie, D., F. Hui, and G.A. Homandberg, *Fibronectin fragments alter matrix protein synthesis in cartilage tissue cultured in vitro.* Arch Biochem Biophys, 1993. **307**(1): p. 110-8.

40. Sepulcre, M.P., et al., *Evolution of lipopolysaccharide (LPS) recognition and signaling: fish TLR4 does not recognize LPS and negatively regulates NF-kappaB activation.* J Immunol, 2009. **182**(4): p. 1836-45.

41. Gruber, H.E., et al., *Constitutive expression of cathepsin K in the human intervertebral disc: new insight into disc extracellular matrix remodeling via cathepsin K and receptor activator of nuclear factor-kappaB ligand.* Arthritis Res Ther, 2011. **13**(4): p. R140.

42. Kegel, K.B., et al., *Huntingtin expression stimulates endosomal-lysosomal activity, endosome tubulation, and autophagy.* J Neurosci, 2000. **20**(19): p. 7268-78.

43. Moles, A., et al., *Cathepsin B overexpression due to acid sphingomyelinase ablation promotes liver fibrosis in Niemann-Pick disease.* J Biol Chem, 2012. **287**(2): p. 1178-88.

44. Amritraj, A., et al., *Increased activity and altered subcellular distribution of lysosomal enzymes determine neuronal vulnerability in Niemann-Pick type C1-deficient mice.* Am J Pathol, 2009. **175**(6): p. 2540-56.

45. Vitner, E.B., et al., *Altered expression and distribution of cathepsins in neuronopathic forms of Gaucher disease and in other sphingolipidoses.* Hum Mol Genet, 2010. **19**(18): p. 3583-90.

46. Li, L., et al., *Parkinson's disease involves autophagy and abnormal distribution of cathepsin L.* Neurosci Lett, 2011. **489**(1): p. 62-7.

47. Sardiello, M., et al., *A gene network regulating lysosomal biogenesis and function.* Science, 2009. **325**(5939): p. 473-7.

48. Settembre, C., et al., *TFEB links autophagy to lysosomal biogenesis.* Science, 2011. **332**(6036): p. 1429-33.

49. Sardiello, M. and A. Ballabio, *Lysosomal enhancement: a CLEAR answer to cellular degradative needs.* Cell Cycle, 2009. **8**(24): p. 4021-2.

50. Gennarino, V.A., et al., *MicroRNA target prediction by expression analysis of host genes.* Genome Res, 2009. **19**(3): p. 481-90.

Figures

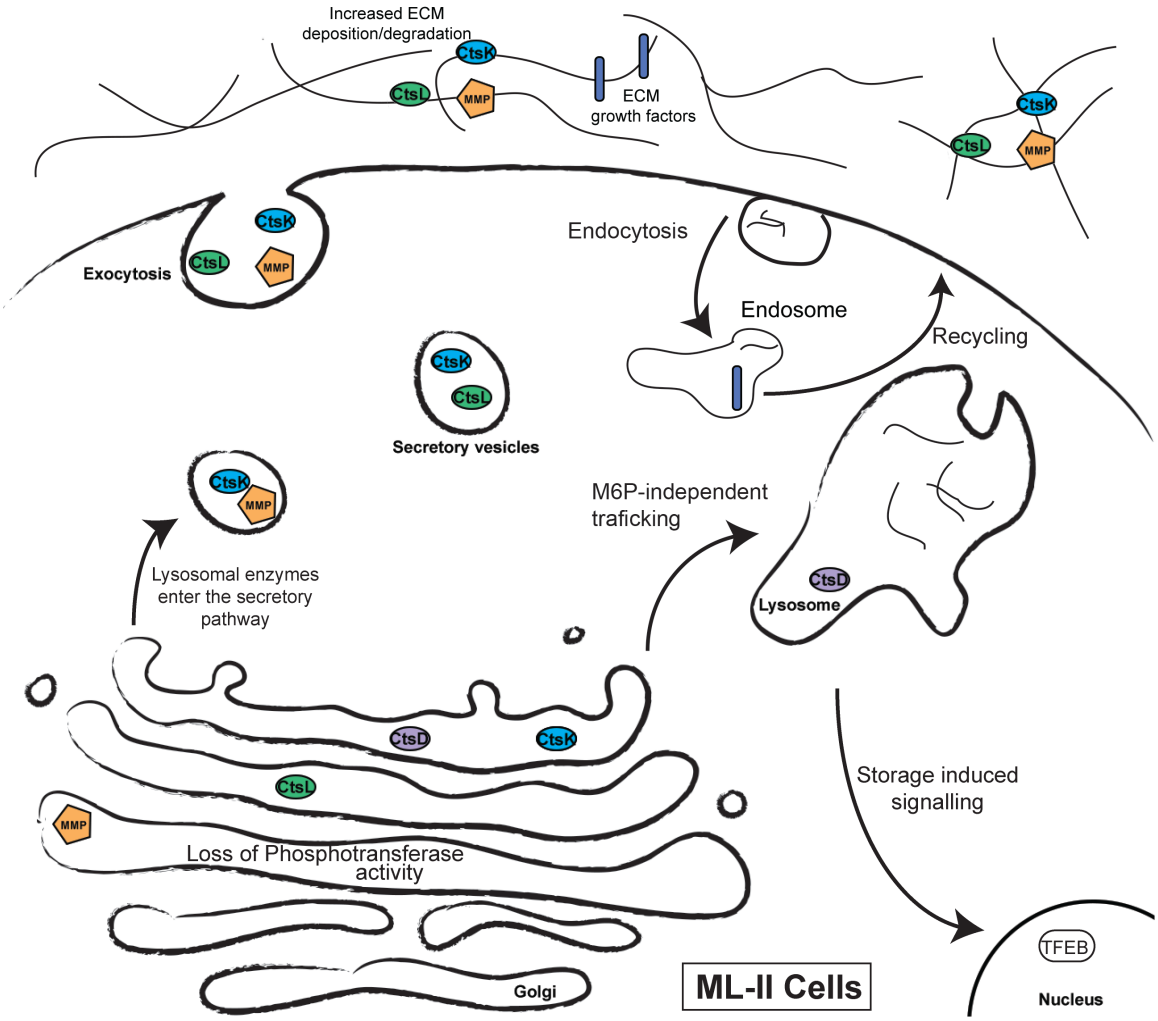

Figure 5.1. Schematic representation of implicated pathological mechanisms underlying the disease process in ML-II. Several disease mechanisms are likely involved in the progression of ML-II and implicated pathways are represented here. Without GlcNAc-1-Phosphotransferase activity, spatial regulation of cathepsin proteases is impaired and they enter into the secretory pathway where they may become activated and in contact with substrates they normally do not encounter. Growth factors, receptors, and ECM components may be degraded within the late secretory pathway and lead to impaired function and altered signaling events. Cathepsins D and H are likely exceptions, reaching the lysosome through an alternate pathway. Within the

ECM, cathepsins and MMPs function together to degrade the matrix, possibly liberating latent growth factors and altering BMP-family member signaling. Protease disruption of the ECM may alter morphogen gradients during development, affecting differentiation of chondrocytes. Degraded matrix fragments including collagens, aggrecans, and glycosaminoglycans are internalized and are not able to be properly turned over within the lysosome. Increased transcription of lysosomal machinery as a consequence of storage may occur either from an unknown mechanism of sensing storage within the endo/lysosomal network, or possibly in response to alternate pathways, such as secretion of lysosomal contents into the ECM. Accumulation of matrix fragments could induce an inflammatory response at later stages and lead to increased cathepsin and MMP transcription.

APPENDIX: SUPPLEMENTAL FIGURES

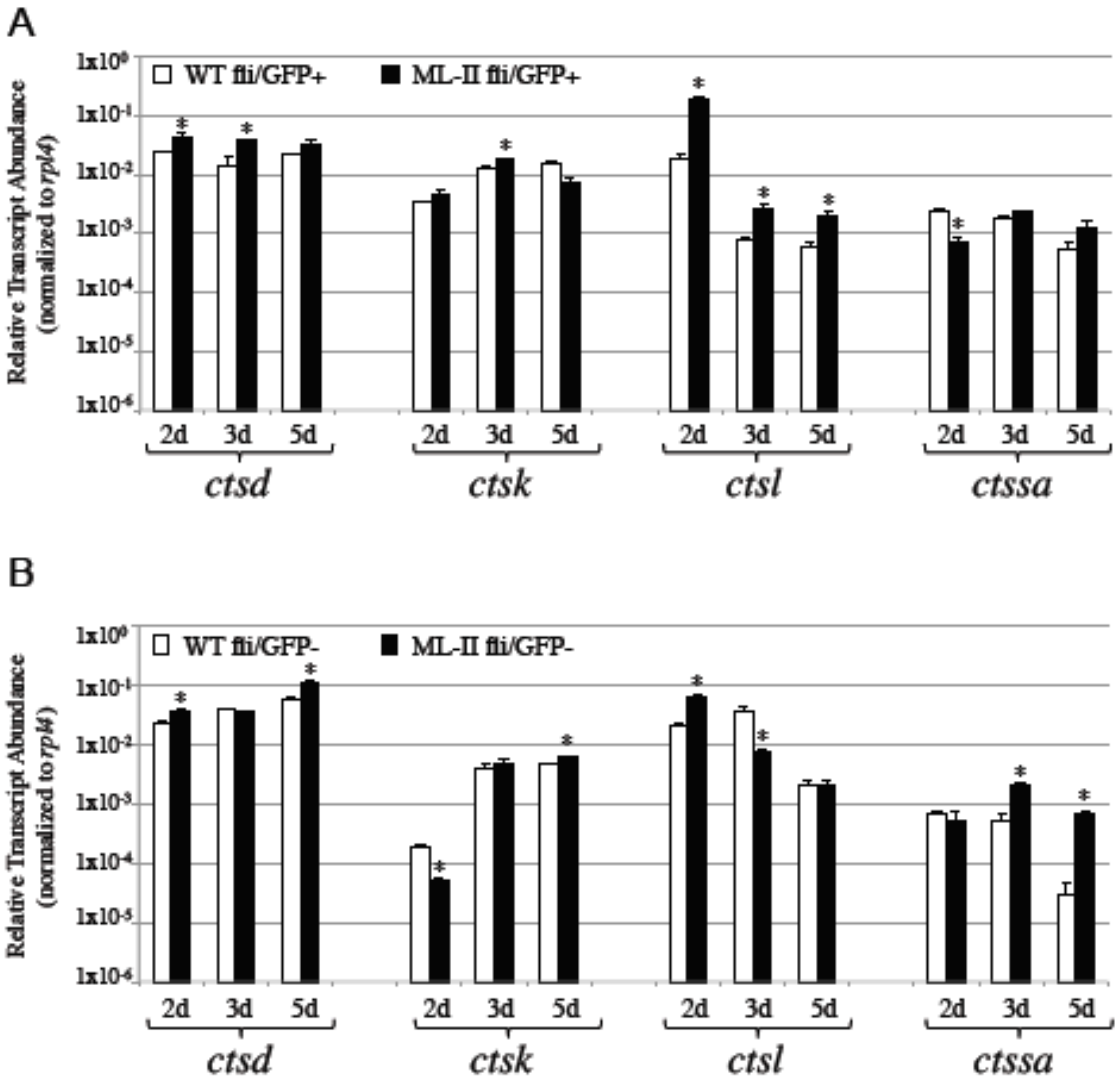

Time course of relative transcript abundance of several cathepsin genes in wild-type (open bars) and ML-II (filled bars) sorted cells for both fli/GFP+ cells (panel A) and fli/GFP- cells (panel B). Data was normalized to a control gene (*rpl4*) and is plotted on a $\log_{10}$ scale. Error bars represent the SEM from four independent biological samples. Asterisks denote a statistically significant difference ($p<0.05$) between the transcript abundance for that gene from WT and ML-II sorted cells.

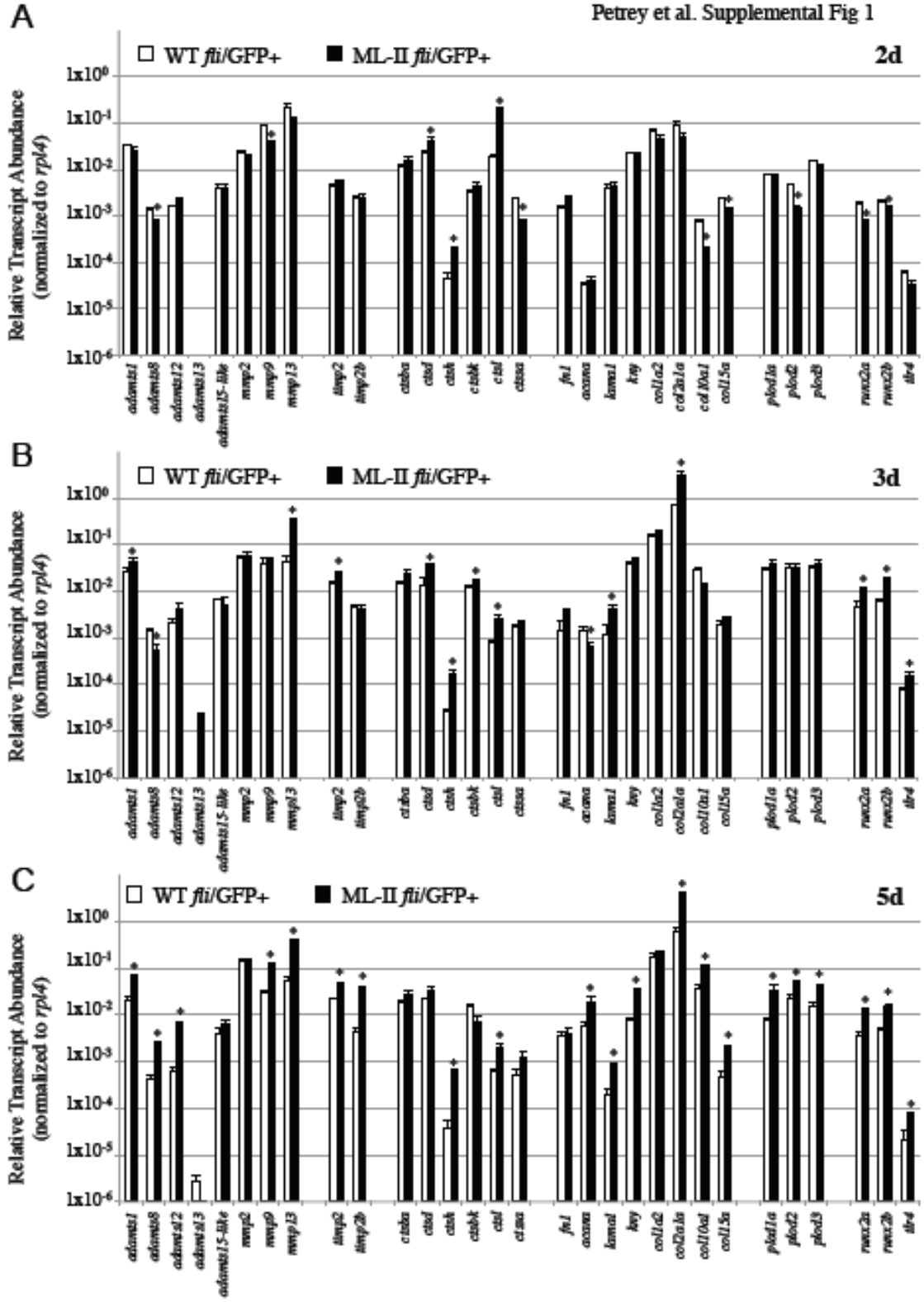
Petrey et al. Supplemental Fig 1
A
B
C
WT fli/GFP+
ML-II fli/GFP+
2d
3d
5d
Relative Transcript Abundance
(normalized to rpl4)
1x10⁰
1x10⁻¹
1x10⁻²
1x10⁻³
1x10⁻⁴
1x10⁻⁵
1x10⁻⁶
adamts1
adamts8
adamts12
adamts13
adamts15-like
mmp2
mmp9
mmp13
timp2
timp2b
ctsba
ctsd
ctsk
ctskb
ctsl
ctss
fn1
acana
kmo1
key
col1a2
col2a1a
col10a1
col15a
plod1a
plod2
plod3
rwtx2a
rwtx2b
tlr4

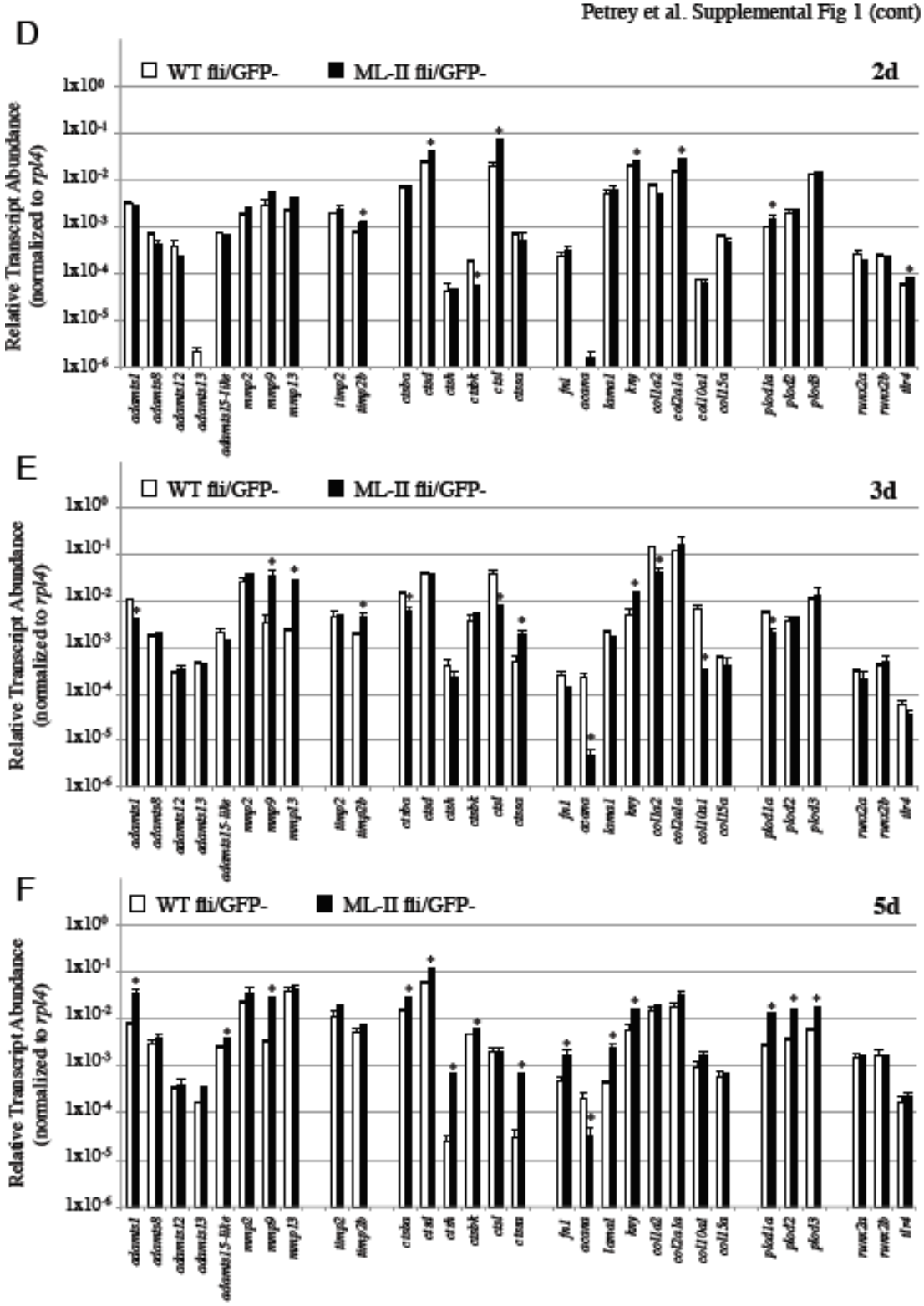

Supplemental Figure 1. Relative transcript abundance for a collection of genes in wild-type(open bars) and ML-II (filled bars) sorted cells for both fli/GFP+ cells (panels A-C) and fli/GFPcells (panel D-F) at 2dpf (top panels, A and D), 3dpf

(center panels, B and E) and 5dpf (bottom panels, C and F). Data was normalized to a control gene (*rpl4*) and is plotted on a log10 scale. Error bars represent the SEM from four independent biological samples. Asterisks denote a statistically significant difference ($p<0.05$) between the transcript abundance for that gene between WT and ML-II sorted cells.

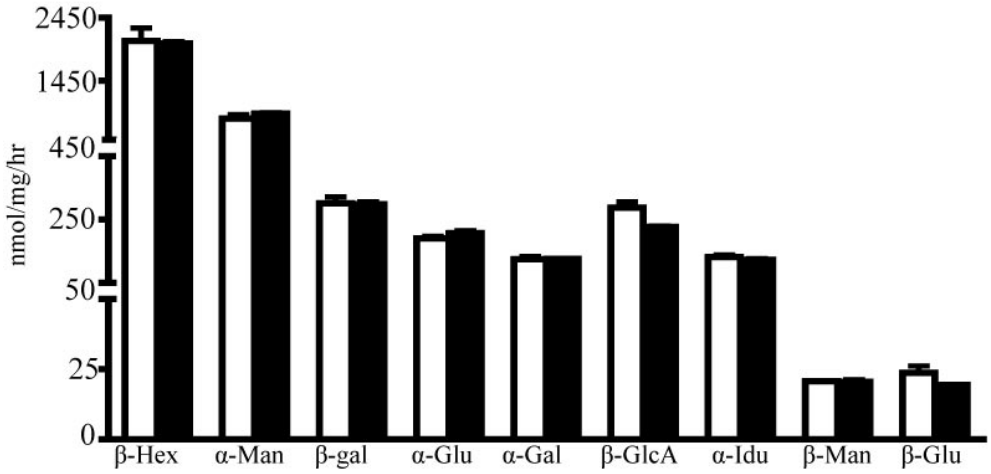

Supplemental Figure 2. Total glycosidase activity is not altered in ML-II embryos. Whole embryo lysates from WT (white bars) and ML-II (black bars) zebrafish at 3dpf were assayed for glycosidase activity.

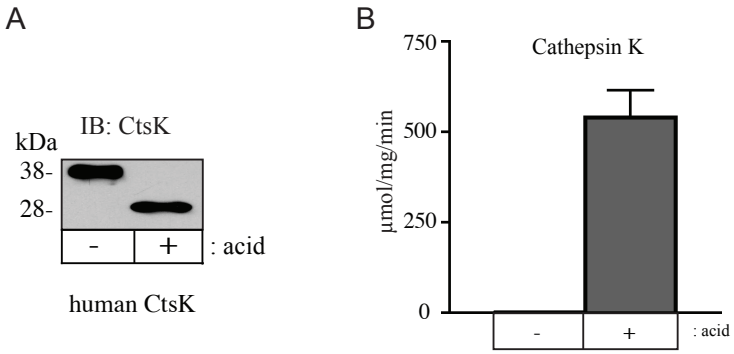

Supplemental Figure 3. Acid activation of recombinant human cathepsin K. Recombinant cathepsin K was treated with acid to induce autocatalytic activation prior to western blot analysis (A) and activity assay (B), n=3.

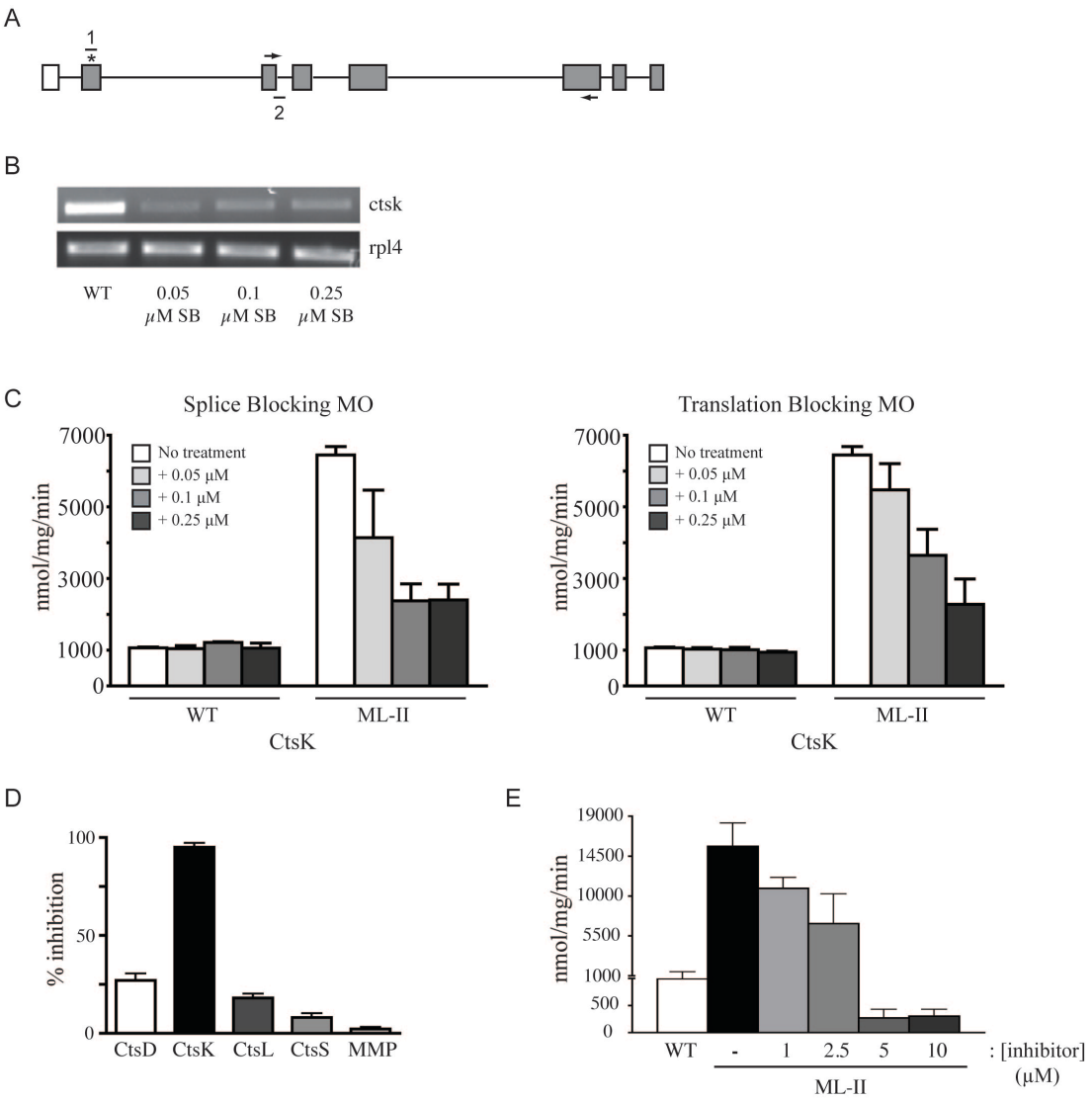

Supplemental Figure 4. Validation of cathepsin K inhibition methodology. A) Scematic representation of of cathepsin K gene. Dashes labeled 1 and 2 represent the translation blocking (TB) and splice blocking (SB) MOs, respectively. (*) represents location of the initiating ATG. Arrows represent the forward and reverse primers used to analyze mRNA expression of SB MO. B) RT-PCR analysis of ctsk expression at 1dpf in WT embryos following introduction of various concentrations of SB MO. RT-PCR analysis of rpl4 performed on each sample served as a normalizing control. C) Analysis of cathepsin K activity in lysates of 3dpf WT and ML-II embryos following introduction of a range of SB and TB MO concentrations. D) Specificity of the cathepsin K inhibitor was determined in vitro using whole embryo lysates. Analysis of cathepsin enzyme activities in the presence of 10μM inhibitor indicates that cathespins D, L, S, and MMP are only minimally affected by this molecule (n=3) E) Dose-dependent inhibition of cathepsin K activity in inhibitor-treated embryo lysates. Based on this analysis, we chose to work with 2.5 and 5 μM for subsequent analyses.

Supplemental Table 1. Selectivity of the cathepsin K inhibitor. *In vitro* assays were performed from whole embryo lysates to assess the selectivity of the cathepsin K inhibitor at a concentration of 10uM. Data shown as percent inhibition. (n=3).

CtsD	CtsK	CtsL	CtsS	MMP
30% ±7	95% ± 4	14% ± 12	4% ± 2	<1%

Supplemental Table 2. Mannose phosphorylation of zebrafish cathepsins. Detergent extracts from adult brain or 3dpf gamma subunit null embryos were fractionated over the CI-MPR column. Bound activity relative to total activity was determined. For embryos, n represents the number of independent assays of 20 fish.

Mannose Phosphorylation of Acid Hydrolases from Zebrafish

	% of activity bound to CI-MPR column	
Lysosomal hydrolase	y/y Brain (n=6)	y/y Embryos (n=4)
Cathepsin D	17.3 ± 5.1	5.1 ± 3.6
Cathepsin K	96.4 ± 3.3	15.1 ± 4.6
Cathepsin L	98.1± 6.8	13.0 ± 2.9
Cathepsin S	64.5 ± 9.2	10.8 ± 13.7

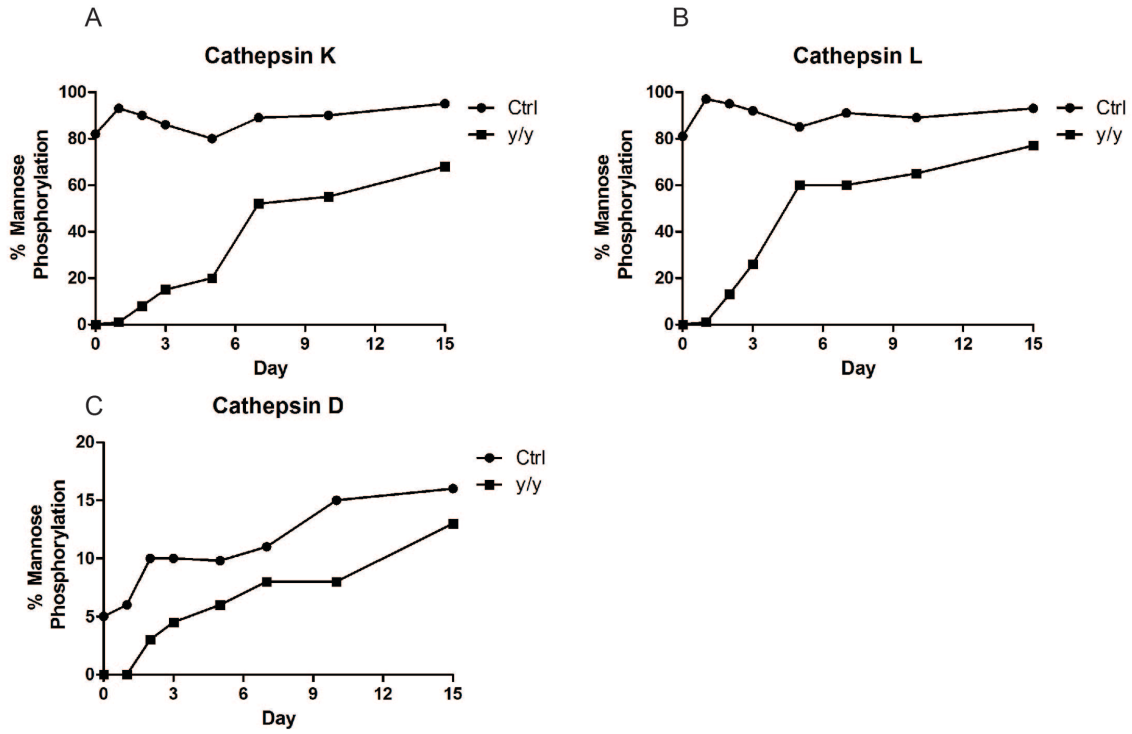

Supplemental Figure 5. Cathepsin mannose phosphorylation in gamma-subunit null embryos. Detergent extracts from zebrafish at the indicated time points were fractionated over the CI-MPR column. Bound activity relative to total activity was determined.

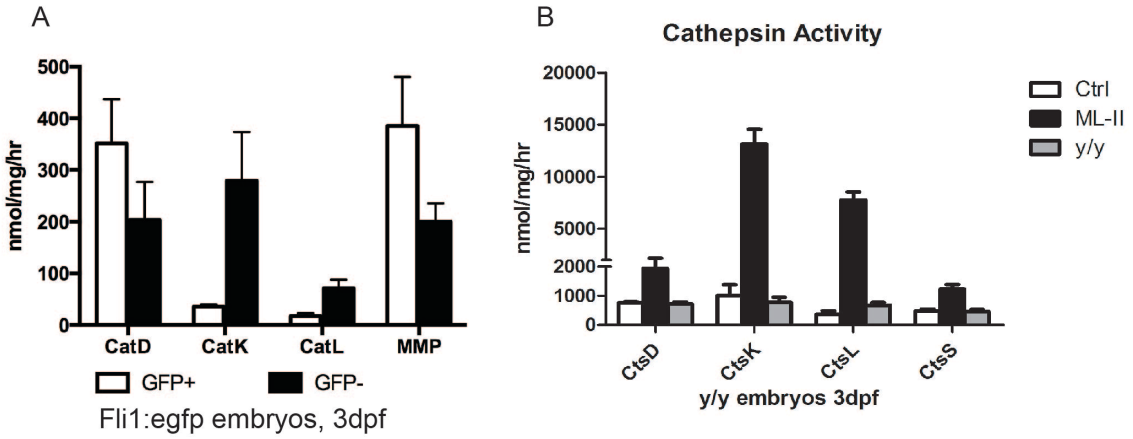

Supplemental Figure 6. Cathepsin Protease Activity from Gamma-subunit null embryos and sorted cells. (A) Gamma-subunit null / *fli1a*:EGFP embryos were dissociated and enriched for chondrocytes by FACS and 3dpf. Cell lysates were assayed for intracellular cathepsin protease activity using specific fluorogenic substrates. Activity measurements were performed on three independent cellular isolations. (B) Cathepsin activity was compared in control, ML-II morphants, and gamma-subunit null embryos at 3dpf.